



## Field Trip Post-EX-1

### Transect across the Eastern Alps

FRANZ NEUBAUER & JOHANN GENSER

(with contributions by BIANCA HEBERER, ANDREAS ETZEL & OLIVER STAUBER)

Department Geography and Geology, University of Salzburg, Hellbrunnerstr. 34, 5020 Salzburg, Austria.  
franz.neubauer@sbg.ac.at; johann.genser@sbg.ac.at

### 1 Tectonic evolution of the Eastern Alps: From Permian rifting to Cretaceous and Cenozoic collisions

FRANZ NEUBAUER & JOHANN GENSER

#### 1.1 Introduction

Facts and models on geology of the Eastern Alps made rapid progress during the last two decades mainly due deep seismic profiling, palaeogeographical, structural, petrological and geochronological investigations (Handy et al., 2010, 2015 and references therein; Schmid et al., 2004). These, together with results of the TRANSALP seismic line (TRANSALP Working Group, 2002, Lüschen et al., 2006; Lippitsch et al., 2003), studies on the crustal structure (Brückl et al., 2010; Bianchi and Bokelmann, 2014) and lithospheric-scale geophysical investigations including the recent Alp-Array (Lippitsch et al., 2003; Hetényi et al., 2018), allow new insights into the present-day structure of the Eastern Alps and surrounding areas (Belinić et al., 2018). These triggered new models, which fundamentally changed ideas on the geological evolution of the Eastern Alps.

Despite although old controversies remain and new controversies arised (for reviews, see e.g. Frank, 1987; Mandl, 2000; Neubauer et al., 2000; Schmid et al., 2004; Handy et al., 2010, 2015). Furthermore, the geological evolution of the Eastern Alps can be only understood when data from the north-eastern extension of the Eastern Alpine units in the Western Carpathians are considered in models, too (e. g., Dallmeyer et al., 1996; Froitzheim et al., 2008; Pomella et al., 2015; Plašienka, 2018). There, passive continental margin successions similar to the Austroalpine units sensu lato of the Eastern Alps are exposed, which are overlain by the blueschist-bearing, partly oceanic Meliata unit.

This review synthesizes the principal structural data of the Eastern Alps in respect to the distribution of the Alpine metamorphic overprint, its timing and the general tectonic framework of its evolution. A further goal is to discuss some specific processes and concepts found in the Eastern Alps for the first time, which were later applied in many other orogens (see, e.g., Neubauer, 2014).

Eastern and Western Alps display a fundamentally different geological structure (see below), geological development and in part a distinct geomorphology (Schmid et al., 2004). The boundary between Western (respectively Swiss Central) Alps and Eastern Alps is a thrust at the base of the Austroalpine unit exposed ca. along the Rhine valley S of Lake Constance (Fig. 1). The most prominent

mountain peaks are along the central axis in the Eastern Alps and the Swiss Central and French/Italian Western Alps. East of the Tauern window area, the topography gradually changes from high elevations in the Hohe Tauern area into the Neogene Pannonian basin with its plains and a very low elevation above sea level.

The present structure and the Late Paleozoic to Recent geological evolution of the Eastern Alps are reviewed mainly in respect to the distribution of Alpidic, Cretaceous and Cenozoic aged metamorphic overprint and the corresponding ductile structure (for details of various views, see Faupl and Wagreich, 2000; Mandl, 2000; Neubauer et al., 2000; Schmid et al., 2004; Froitzheim et al., 2008). Following these data, the Alps as a whole, and the Eastern Alps in particular, are the result of two independent Alpine collisional orogenies: The Cretaceous orogeny formed the present Austroalpine units *sensu lato* (including from footwall to hangingwall the Austroalpine *s. str.* unit, the Meliata unit, and the Upper Juvavic unit). The Eocene-Oligocene orogeny resulted from oblique continent-continent collision and overriding of the stable European continental lithosphere by the combined Austroalpine/Adriatic continental microplate (TRANSALP Working Group, 2002; Schmid et al., 2004; Handy et al., 2015). Consequently, a fundamental difference in the present-day structure of the Eastern and Central/Western Alps resulted (Fig. 1). The Western Alps expose deep structural levels, particularly the Penninic units, which are found in Eastern Alps only in the Lower Engadin, Tauern and Rechnitz windows.

## 1.2 Tectonic units of the Eastern Alps

In the following, we briefly discuss the tectonic units of the Eastern Alps (Fig. 1) and their metamorphic overprint (Fig. 2). These ages are compiled in Frank et al. (1987a), Dallmeyer et al. (1998), Neubauer et al. (1999), Thöni (1999, 2002) and Schuster et al. (2003) and are also graphically summarized in Frey et al. (1999) and Oberhänsli et al. (2004). For tectonic subdivision of Austroalpine units we do not use the new subdivision proposed of Schmid et al. (2004) because of some significant objections, but follow the older terminology introduced by Tollmann (1977 and references therein) as used, e.g., in Neubauer et al. (2000). A simplified comparison of the Austroalpine units between the two terminologies will be given during the excursion. The TRANSALP section extending from NE München to N of Venezia displays the overall crustal-scale structure (Fig. 2) with the Tauern window in the centre of the section.

The Eastern Alps comprise several principal tectonic units. These are discussed from north to south. The Helvetic unit represents a thin-skinned tectonic wedge along the northern margin of the Alpine orogen and is the detached Jurassic to Eocene sedimentary sequence of the passive continental margin of stable Europe.

The Penninic units are mainly exposed in the Tauern window (Kurz et al., 1998; Schmid et al., 2004, 2013). Here, we use a simplified terminology, and the units include from base to top: (1) In the center of the Tauern window, a parautochthonous basement consisting of a pre-Upper Carboniferous basement complex is intruded by Variscan granitoids, the so-called Zentralgneis (Central Gneiss). On top is a primary Permo-Mesozoic cover sequence, the Silbereck Group in this area and the Hochsteggen zone in the western Tauern window. (2) These units are overlain by basement-cover nappes with a Mesozoic cover parts derived from continental margin successions. The Eclogite zone occurs only in the central-southern Tauern window and represents part of one of these nappes. The seemingly parautochthonous unit the basement-cover nappes form the sub-Penninic nappes. (3) The Glockner nappe comprises of ophiolites mainly volcano-sedimentary sequences of the South Penninic oceanic basin (e.g., Höck and Koller, 1989). The overlying Matrei and the Nordrahmen units are considered to

represent a tectonic/sedimentary mélange deposited during the active margin stage (Frisch et al., 1987).

The Lower Cretaceous to Eocene Rhenodanubian Flysch zone along northern margin of the Eastern Alps is of a Penninic palaeogeographic origin and represents largely the sedimentary cover on rarely preserved oceanic crust (Fig. 1). Furthermore, the sub-Penninic nappes exposed in the Tauern window represent a thick-skinned wedge detached from stable Europe, too.

The Austroalpine and Southalpine units are of continental affinity and comprise a pre-Variscan and Variscan basement (usually coined as “Altkristallin”), mostly in a polyphase amphibolite-facies metamorphic grade, and an Upper Carboniferous to Cretaceous, respectively, Palaeogene sedimentary cover (Fig. 1). The Austroalpine nappe complex is exposed to the north of the dextral Periadriatic fault, the Southalpine unit to the south of it (Figs. 1, 2, 3). Both comprise a Variscan basement, which is metamorphosed within anchizonal to granulite-/eclogite-grade conditions during Carboniferous and locally during Permian times (Frey et al., 1999; Oberhänsli et al., 2004), and Upper Carboniferous/Permian to Palaeogene cover successions. The Southalpine unit remained largely unaffected by Alpine metamorphism except some small portions with very-low- and low-grade metamorphism along the Periadriatic fault (e.g., Läufer et al., 1977; Rantitsch, 1997; Hoinkes et al. 1999). The Austroalpine domain is variably affected by Cretaceous (Eo-Alpine) metamorphism ranging from very low-grade to ultra-high pressure conditions (Fig. 3). The Austroalpine domain is considered to represent a Permian to Middle Triassic rift succession, and Middle Triassic passive continental margin in the NW of the Meliata ocean. During the Jurassic, the Austroalpine domain separated from stable Europe by opening of the Penninic ocean in between.

The Meliata unit exposed in the Eastern Alps comprises distal continental margin deposits and recently detected oceanic sedimentary rocks of Middle Triassic to Doggerian age (Mandl and Ondrejíkova, 1991; Kozur, 1991; Mandl, 2000 and references). These include Middle and Late Triassic pelagic carbonates, Late Triassic radiolarites and the Doggerian Florianikogel Formation with shales, volcanogenic greywackes and ashfall tuffs (Kozur and Mostler, 1992). Late Jurassic and Cretaceous tectonic events of the central Northern Calcareous Alps have been related to the closure of the Meliata ocean (e.g., Faupl and Wagreich, 2000, Gawlick et al., 1999, Missoni and Gawlick, 2011 and references therein). The enigmatic very low- to low-grade metamorphic overprint of the structural base of the Northern Calcareous Alps at ca. 149–135 Ma argues for a major tectonic event at that time (Spötl et al., 1998; Vozárova et al., 1999; Schorn et al., 2013). This event likely represents the onset of collision but needs further confirmation (see also Frank and Schlager, 2006).

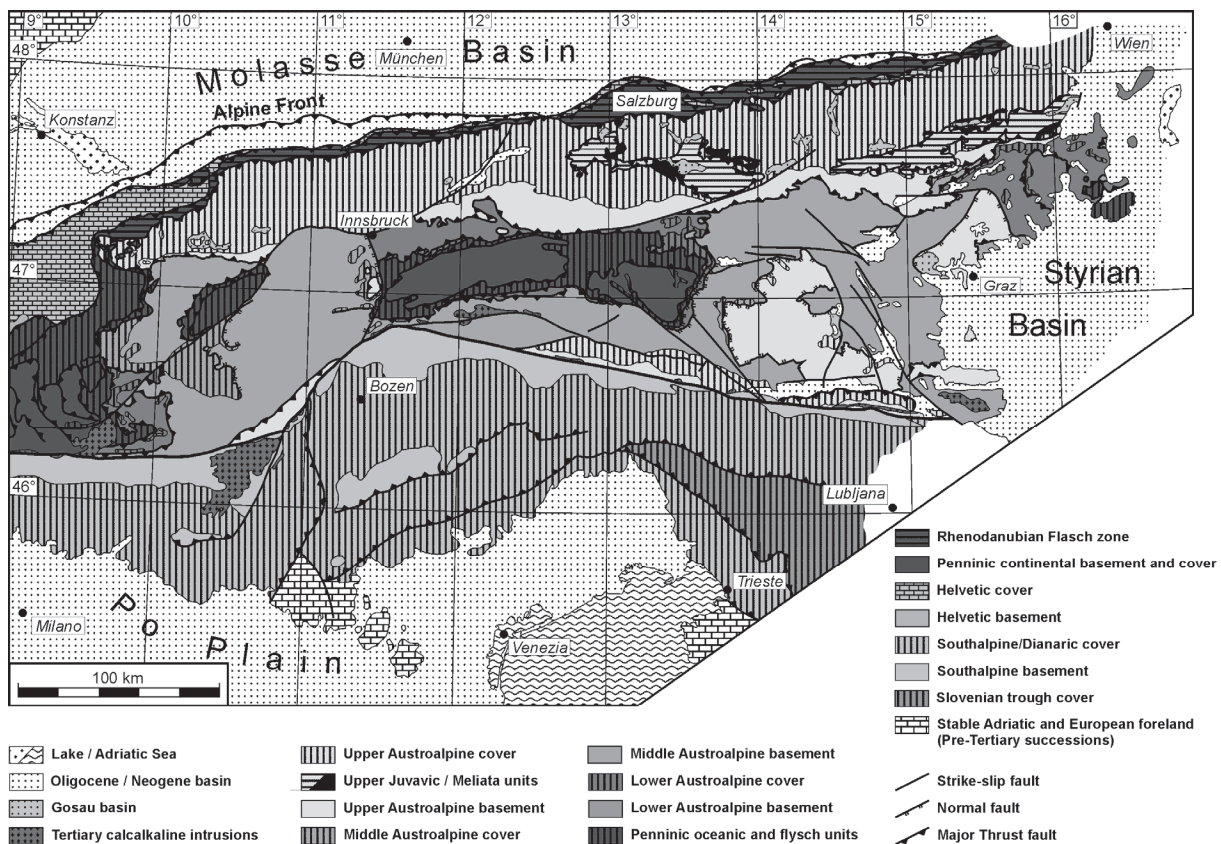


Fig. 1: Simplified geological map of Eastern Alps.

The Austroalpine nappe complex represents a Middle-Late Cretaceous nappe complex, which formed by ductile top-W to WNW shear contemporaneous with amphibolite- to eclogite-grade metamorphism in basement rocks (e.g., Ratschbacher, 1986; Dallmeyer et al., 1998; Hoinkes et al., 1999; Thöni, 1999). The age of peak conditions of metamorphism of Austroalpine units is at 95–90 Ma (Thöni, 2002), and  $^{40}\text{Ar}/^{39}\text{Ar}$  mineral ages prove cooling through the Ar retention temperature of white mica between ca. 120 Ma in uppermost tectonic levels to ca. 80 Ma lowermost units (Dallmeyer et al., 1998; Wiesinger et al., 2006) locally overprinted by rare Eocene ages (ca. 50 Ma; Liu et al., 1999). The general Cretaceous nappe transport direction was towards the WNW ( $D_1$ ) and N ( $D_2$ ), respectively (e.g., Ratschbacher, 1986; Krohe, 1987; Neubauer et al., 2000; Kurz and Fritz, 2003 and references therein). The related thrust structures are overprinted by ESE-directed ductile low-angle normal faults ( $D_3$ ), which were operative during exhumation of previously buried Middle Austroalpine units between ca. 87 and 80 Ma (Neubauer et al., 1995; Koroknai et al., 1999 and references therein). These are associated with orogenic collapse of the over-thickened orogenic wedge and formation of Turonian to Palaeogene collapse basins, the so-called Gosau basins. These unconformably overstep earlier structures of the uppermost nappes (Ratschbacher et al., 1989; Wagreich, 1995; Neubauer et al., 1995; Willingshofer et al., 1999b; Wagreich and Decker, 2001).

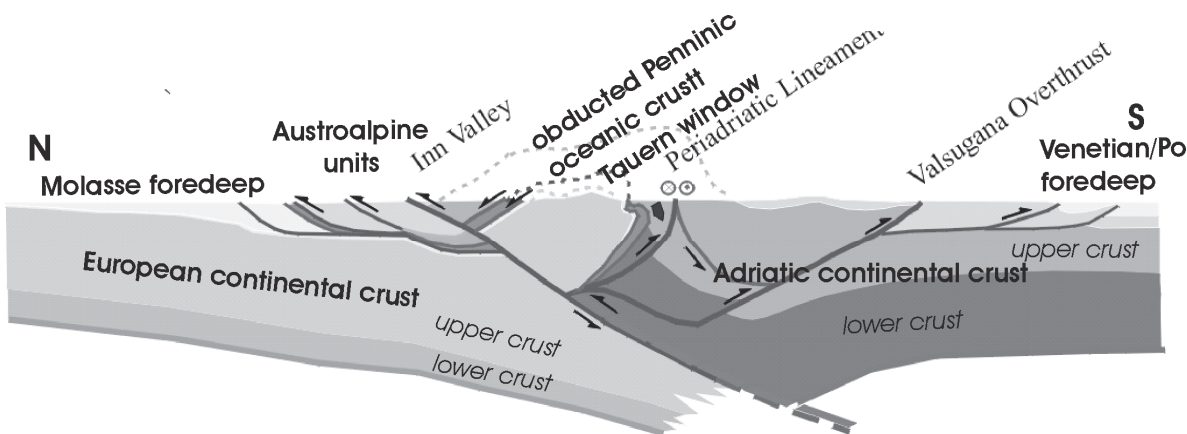


Fig. 2: TRANSALP section showing the overall structure of Eastern Alps (modified from TRANSALP Working Group, 2002).

In contrast, the Southalpine unit is not affected at all by Cretaceous-aged deformation and metamorphism, and is largely unmetamorphosed except some small units with low-grade metamorphism at ca. 50 Ma (own unpublished data). For the tectonic evolution of the eastern Southalpine unit, see Castellarin et al. (2006). Furthermore, there is no Cretaceous unconformity in the sedimentary succession, although the Lombardian and Slovenian Flysch successions (Fig. 3) are considered to monitor Late Cretaceous tectonic processes in the Austroalpine units (Castellarin et al., 2006). The dextral Cenozoic offset of the Periadriatic fault is ca. 150 to 400 km (Schmid et al., 1989; Haas et al., 1995). Structural relationships suggest that the Austroalpine nappe complex represents the orogenic wedge, and the Southalpine unit a retro-wedge.

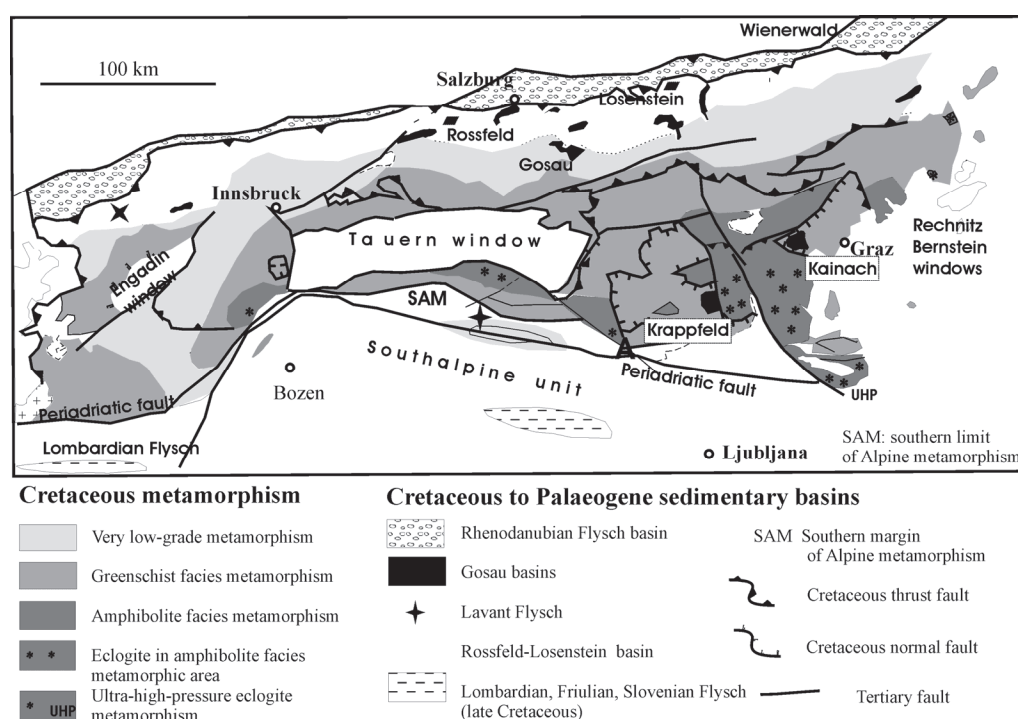


Fig. 3: Distribution of Cretaceous orogenic metamorphism in the Eastern Alps and their relationship to some Cretaceous sedimentary basins. PF – Periadriatic fault, SAM – southern limit of Alpine metamorphism, UHP – ultra-high pressure.

The overriding of the Penninic oceanic and Subpenninic continental units by Austroalpine units occurred during Palaeogene (Liu et al., 2001), and plate collision started with flexure of the European foreland in Late Eocene times. Penninic and Subpenninic units are exposed in the Tauern and other windows. Metamorphism within Penninic and sub-Penninic units peaked at ca. 30 Ma and K-Ar and  $^{40}\text{Ar}/^{39}\text{Ar}$  white mica ages are between 38 and 18 Ma (Frank et al., 1987a; Liu et al., 2001).

Nearly all tectonic units of the Austroalpine nappe complex and the Southalpine unit include a Variscan basement. In the Austroalpine units, the basement is exposed mainly along central sectors of the Eastern Alps (Grauwackenzone and klippens like the Gurktal and Graz nappe complexes) (Fig. 1). The composition and evolution of the Austroalpine basement units is not considered in detail here. However, it must be noted that each Alpine nappe (see Fig. 4) comprises a basement that differs from under- and overlying basement units in composition, age and degree of pre-Alpine tectono-thermal events (e.g., Neubauer et al., 1999, and Schuster et al., 2004, and references). For example, the Upper Austroalpine units comprise fossil-bearing Ordovician to Lower Carboniferous successions only affected by a late Variscan (ca. 300 – 320 Ma) and/or Cretaceous very low- to low-grade metamorphic overprint and white mica ages range between 123 and 95 Ma (Dallmeyer et al., 1998; Schuster and Frank, 1999; Frank and Schlager, 2006; Wiesinger et al., 2006). In contrast, various units of the Middle Austroalpine nappe complex comprise a mostly medium-grade polymetamorphic basement (Schuster et al., 2001; Gaidies et al., 2006; Miller et al., 2005) and age groups of white mica are (ca. 340 – 300 Ma, 270 – 240 Ma, and 88 – 80 Ma (Dallmeyer et al., 1998; Schuster and Frank, 1999; Schuster et al., 2001; Wiesinger et al., 2006). The Lower Austroalpine nappe complex is variably affected within low-grade to rare medium-grade metamorphic conditions at ca. 82 and 72 Ma as  $^{40}\text{Ar}/^{39}\text{Ar}$  white mica ages indicate (Frank et al., 1996; Dallmeyer et al., 1998; Müller et al., 1999; Heidorn et al., 2003). Pre-Alpine  $^{40}\text{Ar}/^{39}\text{Ar}$  white mica ages are often well preserved.

### **1.3 Lithospheric-scale structure**

The common interpretation for the late-stage evolution of Eastern Alps was that the European plate was bent underneath the Eastern Alps. This is expressed as by flexure of the European crust and formation of the ca. 4 km deep North-Alpine Molasse basin. Mantle tomography revealed a polarity change in the central part of Eastern Alps implying subduction of the Adriatic lithosphere (Lippitsch et al., 2003) as well as slab-break-off of the Adriatic lithosphere in the southeast adjacent Dinarides (Wortel and Spakman, 2000). Recent work is both in support (Héteniy et al., 2018; Fig. 4) and in contradiction (Belinić et al., 2018). Ustaszewski et al. (2008) prepared a first palaeogeographic restoration for the case of polarity change and late-stage subduction of the Adriatic plate underneath the Eastern Alps. A geological argument in contraction of Adriatic plate subduction is the missing flexure of the foreland base along the Southalpine front when the available high-quality seismic lines are considered (Fantoni and Franciosi, 2010) are taken into consideration. Two parts of the Adriatic plate, Istria and Monte Euganei, are directly attached to the Southalpine and Dinaric thrust front (Fig. 1).

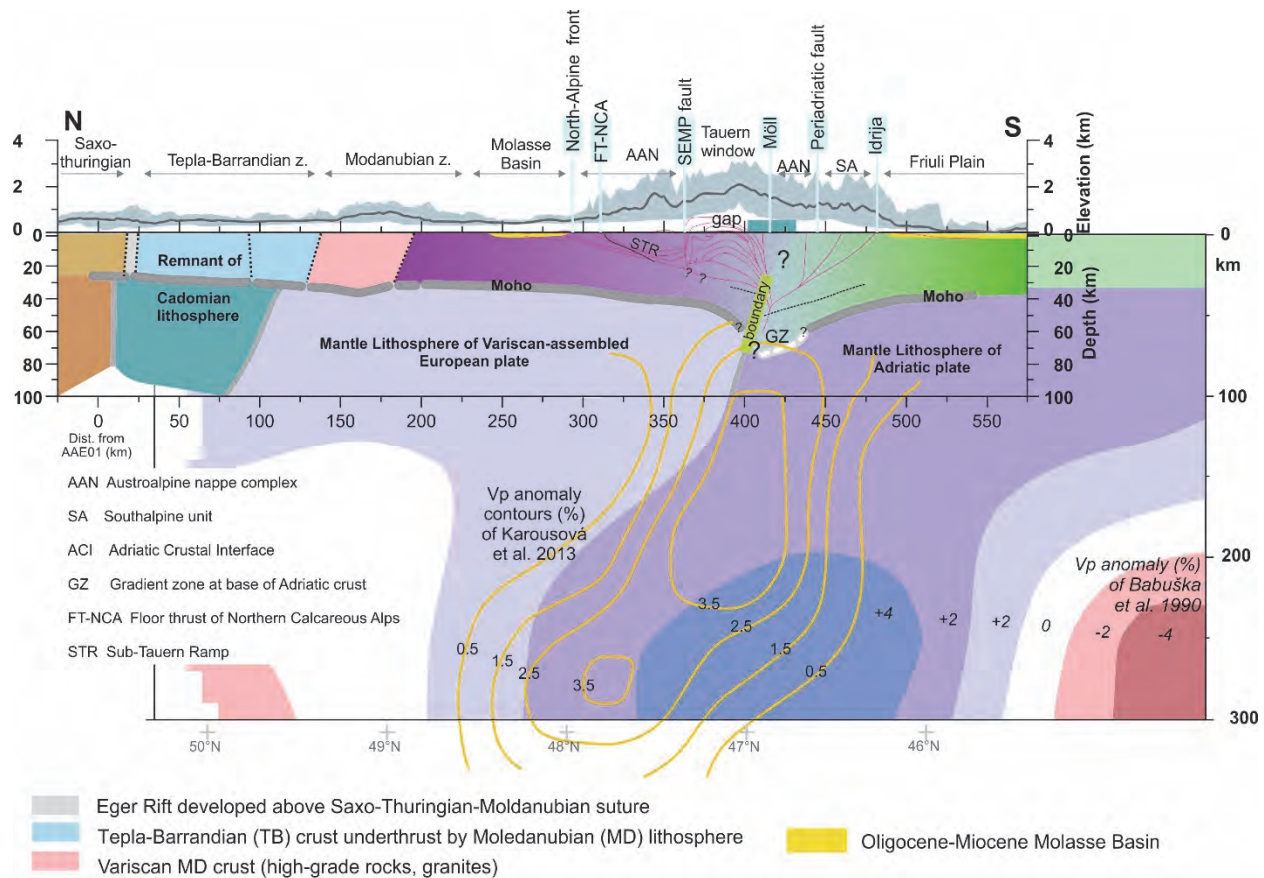


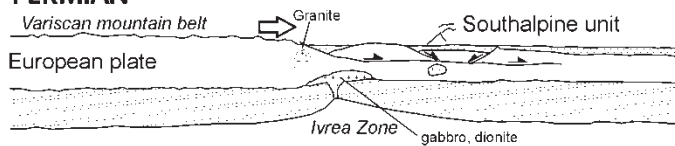
Fig. 4: Lithospheric-scale structure of the Eastern Alps (modified after Héteniy et al., 2018).

#### 1.4 Tectonic evolution

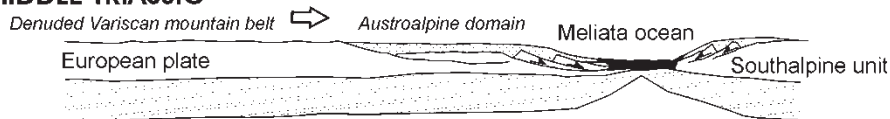
In terms of orogenic high-pressure and regional metamorphism and associated deformation, the Alps are divided into three units: (1) The Austroalpine units s.l., Meliata-Hallstatt units, and Upper Juvavic units which were overprinted by Cretaceous deformation, W- to NW-directed, ductile thrusting (Ratschbacher, 1986; Ratschbacher et al., 1989); (2) the Penninic continental and oceanic units, and the Helvetic units which were partly overprinted by Cenozoic metamorphism and associated N- to W-directed ductile deformation (Kurz et al., 2001 and references); and (3) the Southalpine units, which are largely unaffected by metamorphism except northernmost sectors adjacent to the Periadriatic fault and which were mainly deformed during Cenozoic, c. S-directed thrusting and shortening (e.g. Läufer et al., 1997).

In the following, we discuss principal stages of Permian to Recent tectonic evolution of the Eastern Alps (Fig. 5). Large-scale tectonic restoration can be found in, e.g., Stampfli and Mosar (1999), Schmid et al. (2004) and Handy et al. (2010, 2015).

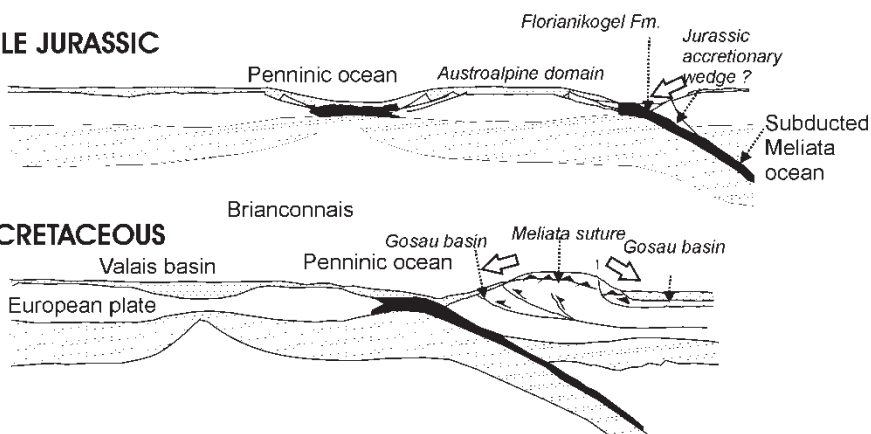
### EARLY PERMIAN



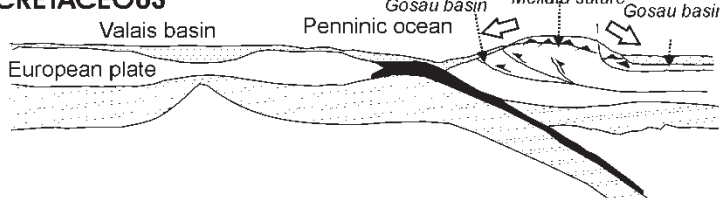
### MIDDLE TRIASSIC



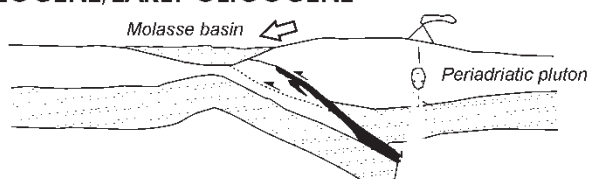
### MIDDLE JURASSIC



### LATE CRETACEOUS



### LATE EOCENE/EARLY OLIGOCENE



### NEOGENE

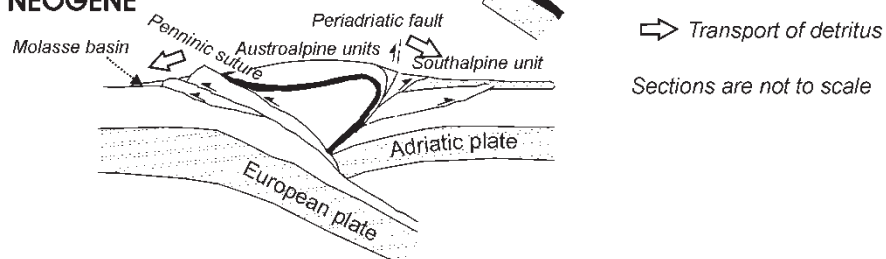


*Fig. 5: Schematic tectonic model of the tectonic evolution of the Eastern Alps for time slices represented in this study. From top to base: **Early Permian** lithospheric-scale extension, heating and subsequent cooling of crustal rocks due to exhumation, surface subsidence and onset of sedimentation. **Middle Triassic** opening of the Meliata ocean. (**Middle**) **Jurassic** opening of the Piemont (Penninic) ocean separating Austroalpine and Penninic continental units with shear zone formation at the continental margin. **Early Late Cretaceous** nappe stacking with deformation of higher nappes of the Lower Austroalpine unit and subsequent formation of the Gosau collapse basins. **Late Eocene** collision between the Austroalpine and Penninic continental units, break-off of the subducted lithosphere and deformation of the lowermost Lower Austroalpine nappe. **Late Oligocene to early Neogene** exhumation of the overthickened Penninic nappe complex by activity along the ductile low-angle normal fault zone separating the Penninic and Austroalpine tectonic units.*

**Permian to early Mid-Triassic rifting:** The Alpine tectonic evolution started with Permian rifting immediately following the Variscan orogeny and after deposition of Late Carboniferous molasse in all future continental domains. Rifting may have resulted by continuous dextral transtensional shear between Gondwana and Laurussia (e.g., Muttoni et al., 1996). Evidence for strong early to late Permian tectonic subsidence and extension is in the eastern Southalpine units where a carbonate platform was established during the Permian, and the Palaeotethys Sea transgressed from SE towards NW, respectively W. Further evidence of divergence and extension of the lithosphere was the emplacement of tholeiitic gabbros, low-pressure metamorphism due to unroofing of metamorphic core complexes, and magmatic underplating during the Permian (Thöni, 1999; Schuster et al., 2001; Schuster and Stüwe, 2008).

**Late Mid to Late Triassic drifting of Meliata Ocean:** However, the main phase of tectonic subsidence in Austroalpine passive margin was during Middle Triassic times (Lein, 1987) and processes of passive margin formation are getting more obvious. A new shelf carbonate platform established between Southalpine/Austroalpine s. str. and Upper Juvavic domains, facing towards the Meliata oceanic basin forming a passive continental margin. Ladinian and Upper Triassic radiolarites are considered to represent the infilling of the Meliata oceanic basin from which the westernmost remnants were found in the easternmost sectors of Northern Calcareous Alps (Fig. 1).

**Latest Triassic to Early Jurassic rifting of the future Penninic Ocean:** A further, independent rift stage during late Triassic and early Jurassic led to the opening of the (South) Penninic, Piemontais-Ligurian ocean due to rifting the Austroalpine domain off from stable Europe. Nearly all Penninic ophiolites of the Eastern Alps were metamorphosed during Cenozoic times. They comprise serpentinites, greenschist and prasinite (consisting of albite, chlorite, epidote, and amphibole), and thick clastic-carbonatic schists, the latter typical for narrow oceanic rifts. Recent U-Pb data of a plagiogranite of the Rechnitz window confirm an age of ca. 140 Ma during earliest Cretaceous. Nearly no gabbro or descendants of sheeted dyke rocks were found. The width of the oceanic seaway is estimated as ca. 500 km (Schmid et al., 2004).

**Mid Jurassic drifting to early Late Cretaceous convergence and plate collision:** On the other hand, the Meliata oceanic basin started to close during the Jurassic, most likely not later than middle Jurassic due to the record of the Lammer unit S of Salzburg (Gawlick et al., 1999; Missoni and Gawlick, 2011) and of the Florianikogel Formation (Neubauer et al., 2000, and references therein). The final closure occurred during the Early Cretaceous with the formation of a deep-sea trench (Roßfeld basin; Faupl and Tollmann, 1978; Schorn et al., 2013). Collision between Austroalpine s. str. units in a footwall position and the Upper Juvavic units in a hangingwall position occurred during early Late Cretaceous with the formation of a nappe pile of basement-cover nappes exposed in the south and cover nappes in northern, external domains (Frank, 1987; Dallmeyer et al., 1996). Nappe stacking likely prograded from SE to NW (e.g., Ratschbacher, 1986; Ring et al., 1989). The eo-Alpine (Cretaceous) metamorphism reached eclogite and UHP eclogite conditions (Jának et al., 2015). Late Cretaceous Gosau basins seal the Meliata suture and nappe stacking structures. The Middle Austroalpine continental eclogite-gneiss units represent the exhuming UHP/HP wedge, which was subducted to depths corresponding to max. ca. 3.0 GPa in southernmost exposures (Jának et al., 2005, 2015) at ca. 95–90 Ma (Thöni and Jagoutz, 1992; Thöni, 1999). In the north, the pressure is ca. 1 GPa. Most pronounced exhumation of the UHP/HP wedge occurred at 90–80 Ma, as cooling ages indicate. Consequently, thrust faults are known in the footwall and a ductile low-angle normal faults in the hangingwall of the eclogite-gneiss unit (Wiesinger et al., 2006).

## LATE CRETACEOUS

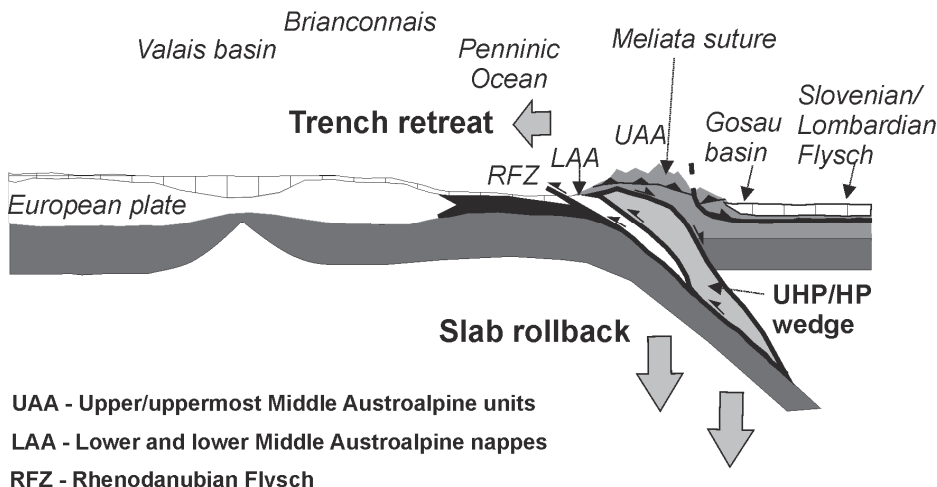


Fig. 6: Generalized (Chemenda-type) model for exhumation of high-/ultra-high-pressure rocks from Middle Austroalpine unit and its relationships to formation of adjacent sedimentary basins.

**Late Cretaceous formation of collapse basins:** Formation of Gosau basins in the Eastern Alps was associated with sinistral wrenching, normal faulting at shallow crustal levels and exhumation of eclogite-bearing crust within Austroalpine units (Neubauer et al., 1995; Froitzheim et al., 1996; Willingshofer et al., 1999a, b; Kurz and Fritz, 2003). Furthermore, Wagreich (1995) suggested tilting of the Austroalpine nappe stack towards NW associated with final shortening, thrusting and doming, in deep levels of the crust (Neubauer et al., 2000). The Lower Austroalpine nappe complex is variably affected within low-grade to rare medium-grade metamorphic conditions at ca. 82 and 72 Ma as  $^{40}\text{Ar}/^{39}\text{Ar}$  white mica ages indicate (Frank et al., 1996; Dallmeyer et al., 1998; Müller et al., 1999; Heidorn et al., 2003). Metamorphism was associated with ductile thrusting at that time. Pre-Alpine  $^{40}\text{Ar}/^{39}\text{Ar}$  white mica ages are often well preserved in Lower Austroalpine units.

The Austroalpine nappe complex is continental basement-cover nappe complex with southward increasing, Cretaceous-age metamorphic overprint, which received its final internal structure largely by middle-late Cretaceous tectonic processes. During this time, subduction of the Penninic (Piemontais-Ligurian) Ocean beneath the Austroalpine units started. In detail, the Lower Austroalpine and the lower part of Middle Austroalpine basement-cover nappes represent the footwall of the UHP/HP wedge and were accreted to the exhuming complex at ca. 80 Ma during a pronounced stage of thrusting. In the hangingwall, a series of ductile low-angle normal faults separates the UHP/HP wedge from uppermost Middle Austroalpine and Upper Austroalpine nappes representing the upper plate. Low angle normal faults were most active between 87–80 Ma as published thermochronologic data indicate (summarized in Willingshofer et al., 1999b; Wiesinger et al., 2006). Normal faulting occurred in a sinistral transtensional setting. In consequence of the transtension, collapse basins (Central Alpine Gosau basins) formed on top of the upper plate. We explain this by disturbance of steady-state subduction by oceanward retreat of the subduction zone (Fig. 6). The tectonic unroofing of the UHP/HP wedge continuously increased to and was most pronounced at the rear end of the wedge, so that up to more than 50 km of overburden was cut out. The overall tempo of exhumation can be confronted with the infill history of flexural and collapse basins. These data show rapid exhumation between ca. 87 – 84 Ma and subsequent down-slowning motion. Subsequent footwall

accretion of Lower Austroalpine nappes at ca. 80–78 Ma formed a duplex, which finally led to updoming of the exhuming UHP/HP wedge.

A Chemenda-type model is applied to explain exhumation of high-pressure rocks (Fig. 6). The Chemenda model (Chemenda et al., 1995) predicts exhumation of previously subducted and continental crust metamorphosed at UHP/HP metamorphic conditions mainly driven by both (1) buoyancy of subducted material, and (2) associated surface erosion of the subducted wedge. Thrust surfaces in the footwall and a major normal fault in the hangingwall confine, therefore, the exhuming UHP/HP metamorphic wedge. Clastic material mainly derived from the surface of the uplifting subductional wedge infill a synorogenic flexural sedimentary basin located on top of the lower plate in front of the UHP/HP wedge. Material mainly derives from the surface of the uplifting previously subducted wedge, which commonly form a mountain range at this stage. A cross-section through an orogen exposes, therefore, the following units: (1) the non-subducted lower plate rocks with a collapse basin at the top, (2) the exhumed, previously subducted wedge with a nappe stack, which is dominated by cover rocks at the leading edge front and exhumed metamorphic, mostly polymetamorphic basement rocks, all metamorphosed at HP/UHP conditions at the rear front and all these units were accreted from the footwall plate, and (3) the upper plate with collapse-type basins at top only in the case when extension-induced subsidence exceeds uplift. This is not the case in setting of steady-state subduction. The subhorizontal attitude of nappes originates from subsequent processes.

**Eocene/Oligocene continent-continent collision:** The Piemontais ocean of the Eastern Alps was closed not earlier than early Eocene because of (1) the presence of pelagic Eocene sediments both in Eastern and Western Alps, and (2) Eocene ages of thrusting in the Penninic/Austroalpine boundary in the northeast and northwest of the Tauern window (Dingeldey et al., 1997; Liu et al., 2001; Heidorn et al., 2003). Obviously, the subduction not only included oceanic crust but also distal Penninic continental crust in Eastern and Western Alps (Kurz et al., 2001, and references therein). Break-off of the subducted lithosphere and associated magmatism are considered to represent important mechanisms of continent-continent collision (von Blanckenburg and Davies, 1995). Upper sectors of the crust were later detached from the downgoing continental lithosphere due to lowering of strength because of temperature increase. Exhumation of these crustal pieces was associated with final thrusting, tectonic unroofing and surface denudation within the uprising mountain chain (e.g., Ratschbacher et al., 1989; Frisch et al., 2000a, 2000b; Fügenschuh et al., 2000).

Final collision was driven by oblique indentation of the Adriatic microplate into the Alpine nappe edifice (e.g., Ratschbacher et al., 1989; Rosenberg et al., 2007, 2018; Wölfle et al., 2011; van Gelder et al., 2017). This resulted in Late Oligocene/Early Miocene sinistral wrenching, and subsequent eastward extrusion of blocks in the Eastern Alps, and westward motion and W-directed indentation of the Adriatic microplate forming the West-Alpine arc (e.g., Ratschbacher et al., 1989, 1991a). Due to effects of ca. S-directed back-thrusting along the Periadriatic fault and within the Southalpine units, upper crustal levels of the down-going Penninic and European continental lithosphere were delaminated and accumulated within a double-vergent orogenic wedge. Exhumation of metamorphic crust, as exposed e.g. within the Tauern window, is achieved, therefore, by the combined effects of shortening (Lammerer and Weger, 1998), and gravity-driven tectonic unroofing in upper levels of the crust and raft tectonics away from the Tauern window towards the Pannonian basin (Keil and Neubauer, 2015).

**Extrusion tectonics:** Neogene tectonics of Eastern Alps is governed by indentation of the stiff Adria microplate (e.g., Willingshofer and Cloetingh, 2003) into the Alpine orogenic wedge, and associated eastward lateral extrusion of eastern part of Eastern Alps along sinistral (Inn Valley, Salzach-Enns and Mur-Mürz fault systems) and dextral strike-slip faults (Periadriatic fault; Fig. 7; Ratschbacher et al., 1989, 1991a). Extrusion tectonics is also responsible for high heat flow in Austroalpine units during Early Miocene (Sachsenhofer, 2001). Within an overstep between the Salzach-Enns and DAV faults, the Tauern window uprisen in a sort of pull-apart dome (Gensler and Neubauer, 1989; Neubauer et al., 1999; Scharf et al., 2013). This model is highly debated, however explains contemporaneous activation of N-S trending Brenner and Katschberg normal faults (Fig. 7). In principle, extrusion tectonics is still in operation as earthquakes along the sinistral Inn Valley, Salzach-Enns, and Mur-Mürz faults and dextral Save fault and GPS data indicate (Grenerczy & Kenyeres, 2006; Caporali et al., 2013). This is explained by the ongoing indentation of the Venetian Platform at the northern tip of the Adriatic microplate. Further geodetic measurements display pronounced surface uplift of the Hohe Tauern area (Cheloni et al., 2014 and references).

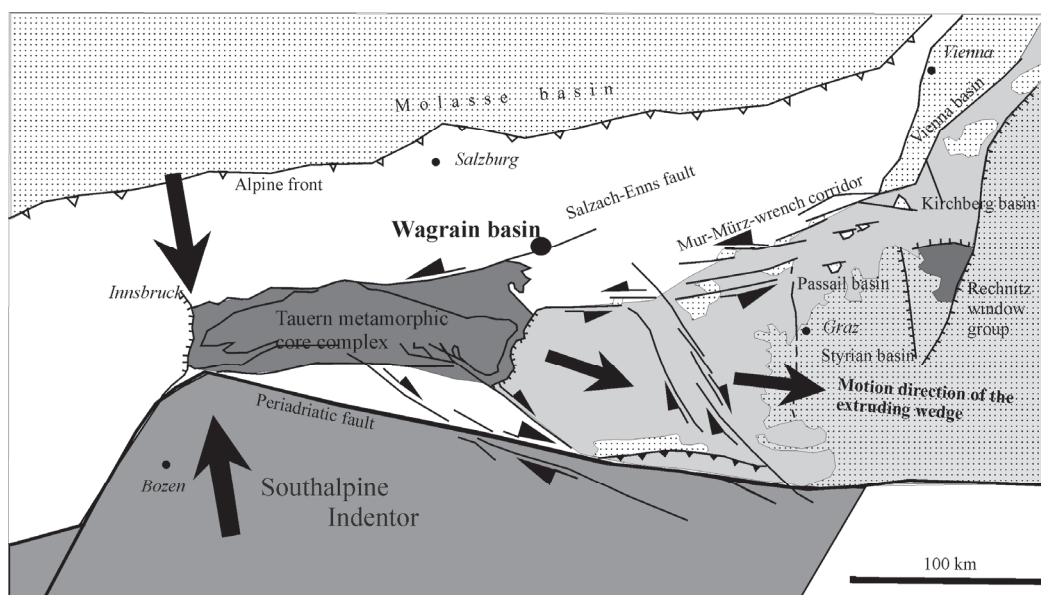


Fig. 7: Extrusion tectonics.

**Pliocene to Quaternary deformation:** The subsidence of westernmost sectors within the Pannonian basin is related to extrusion (e.g., Sachsenhofer et al., 1997). Furthermore, surface uplift east of the Tauern window is moderate (Hejl, 1997; Frisch et al., 2000b). The process of extrusion is still ongoing as the distribution of earthquakes indicate (Reinecker and Lenhardt, 1999).

Based on deformational characteristics and paleomagnetism of Alps, the Adriatic microplate is interpreted to have moved first to the NW (ca. Oligocene) and later to the N (mostly Miocene). In the eastern sectors, the stiff South-Alpine block in front of the Adriatic microplate indented into the weak Alpine orogen and contributed to crustal thickening, exhumation of previously subducted Penninic units, and to lateral extrusion of central sectors of the Eastern Alps. This scenario indicates a dextral Late Miocene-Pliocene transpressional setting in the Dinarides and back-thrusting along the front of Southern Alps. As GPS data and seismicity suggest, the northward motion is still ongoing, although slowed down, and is diminishing towards north (to ca. 2.4 mm/a) and is east-directed (ca. 1 mm/a) in the Eastern Alps. In this scenario, several features remain unexplained: (1) the age and mode of formation of the Friuli Orocline, a feature showing the change from ENE-strike to SE-trend of Dinarides

in front of the Venetian Platform; (2) the apparent ca. 20–25 degree Late Miocene-Pliocene counterclockwise block rotation of combined Eastern Alps, Adria, and northeastern Dinarides with a pole of rotation located to the SW of present Italian peninsula (Márton et al., 2003; Ortner et al., 2006; Robl and Stüwe, 2005); and (3) the strong Pleistocene sediment accumulation (1 mm/a) of northern Adria (around Venice) in front of the Friuli Orocline (Stefani, 2002). The strong subsidence of Northern Adria is opposite to surface uplift to the N of Alps and Pannonian basin and could be explained by flexural loading or by slab pull in front of a slab tear as slab break-off at the transition southeastern Alps to Dinarides has been suggested by Lippitsch et al. (2003) or as a distal effect flexuring of Appennines.

Quaternary and Recent deformation structures of Central Eastern Alps are studied in Pleistocene conglomerates in various, in partly still ongoing projects. These data indicate maximum NNW-SSE horizontal stresses and shortening and ca. E-W extension in accordance with above mentioned northward indentation.

The tectonic signal of surface uplift is superposed by the signal of post-glacial unloading and is estimated at ca. 1.5 mm/a, which is obviously related to the distribution of the last, Würm ice shield. For Holocene, series of elevated river terraces indicate stepwise surface uplift with increasing surface elevation from external Alps towards the Hohe Tauern with a minimum of 60 meters of terrace elevation in the centre. The present-day rivers incise into bedrocks, sometimes blanketed by moraines, so that the apparent Holocene uplift is ca. 6 mm/yr close to the Hohe Tauern, more than in external sectors of Eastern Alps where the Holocene river terraces are at much lower elevation. Cyclic Pleistocene surface uplift is potentially monitored by a number of other geomorphologic effects including: (1) river terraces (“Niederterrassen”) external to the area covered by the Alpine ice shield, (2) bedrock terraces along valleys in the centre of the Eastern Alps, (3) gorges along rivers, which could have been formed during rapid surface uplift due to rapid post-glacial river incision, and (4) elevated Pleistocene karst caves relative close to the present-day river levels.

### **1.5 Morphology formation**

Significant work on formation of the morphology of Eastern Alps was done initially by the Tübingen working group (e.g., Frisch et al., 2000a, b). The group recognized the morphological difference between Hohe Tauern/Niedere Tauern with a young morphology and the Austroalpine domain with an old morphology, which formed since Oligocene and includes now uplifted peneplanation surfaces (Frisch et al., 2001). Much work has been done by using low-temperature geochronology explaining the differences of exhumation and surface uplift between different areas (Luth and Willingshofer, 2008 and references therein; Wölfler et al., 2011; Heberer et al., 2017). This type is representative for the eastern part of the Eastern Alps. Robl et al. (2008a, b) and Bartosch et al. (2017) modelled the morphology development by interaction of shortening and erosion and could explain the formation of longitudinal fault-controlled valleys by lateral extrusion. The incision of rivers into older Miocene landscapes is young and surface uplift is dated at ca. 6 – 3 Ma before present (Wagner et al., 2011; Legrain et al., 2014).

## 2 Northern Calcareous Alps and Radstadt Mountains

**Aim:** The aim of this part of the excursion is:

- (1) introduce into some important aspects of the rift and two-stage passive margin successions exposed in the Northern Calcareous Alps,
- (2) to examine some aspects of the cover successions of the Lower Austroalpine nappe complex and of its LateCretaceous deformation,
- (3) to demonstrate the footwall propagation of thrusting during formation of the Austroalpine nappe complex between ca. 110 and 50 Ma, as a result closure of the Meliata Ocean and subsequent Penninic Ocean, and
- (4) to check the significance of the Salzach-Enns-Mariazell-Puchberg (SEMP) fault and the related Miocene Wagrain basin on the northern edge of Miocene lateral extrusion wedge.

### 2.1 Introduction

The Northern Calcareous Alps are part of the Upper Austroalpine nappe complex and represent a ca. 600 km long and ca. 40 km wide cover nappe succession dominated by Middle to Upper Triassic dolomites and limestones (Fig. 1). The succession starts with thick uppermost Carboniferous and Permian terrestrial siliciclastic deposits, which are locally overlain by evaporites (Haselgebirge Fm.) with salt and sulfates, which particularly important and widespread in the surroundings of Salzburg (salt = Salz in German, e.g., Salzburg, Salzkammergut). The Permian siliciclastic strata are interpreted to represent a rift, with halfgraben formation with up to 1.5 km thick sediments (Fig. 8). Recently, an inverted Permian normal fault was identified (see below). In earliest Triassic, a gradual transition from siliciclastic rocks to marine carbonates occurred, which form the thick carbonates on a passive continental margin opening towards the evolving Meliata Ocean (Lein, 1987; Kozur, 1991; Mandl, 2000). A classical lithostratigraphic section is shown for the Tennengebirge massif (Fig. 9). Here, we detected an also a Middle-Upper Triassic northward tilted block (Figs. 10, 11). This is now explained as raft tectonics and a corresponding model is shown in Figure 11. Thick Upper Triassic reef and lagoonal deposits are overlying these units.

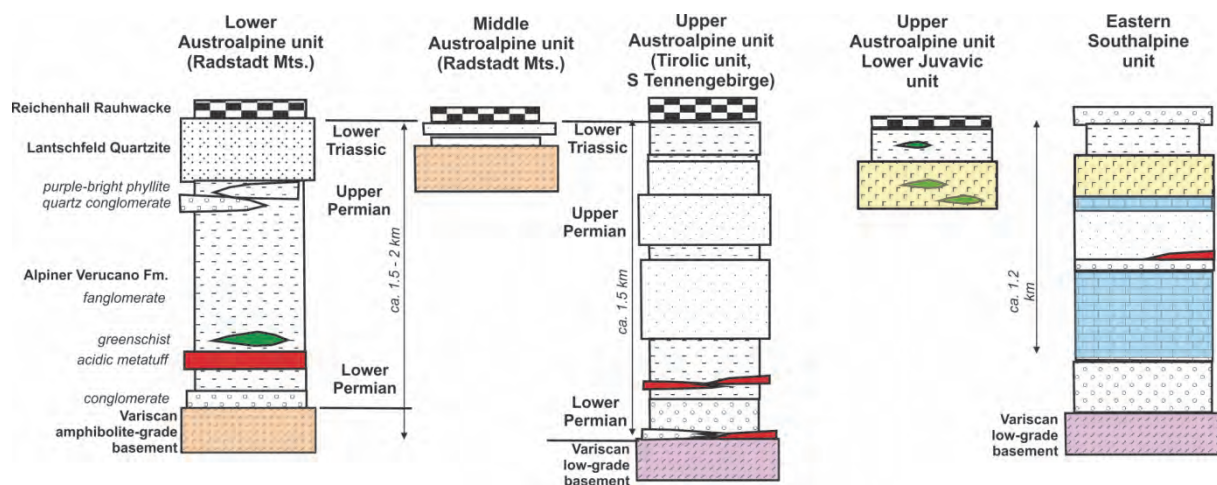


Fig. 8: Basal formations of the Upper Paleozoic cover successions of the Austroalpine and Southalpine units.

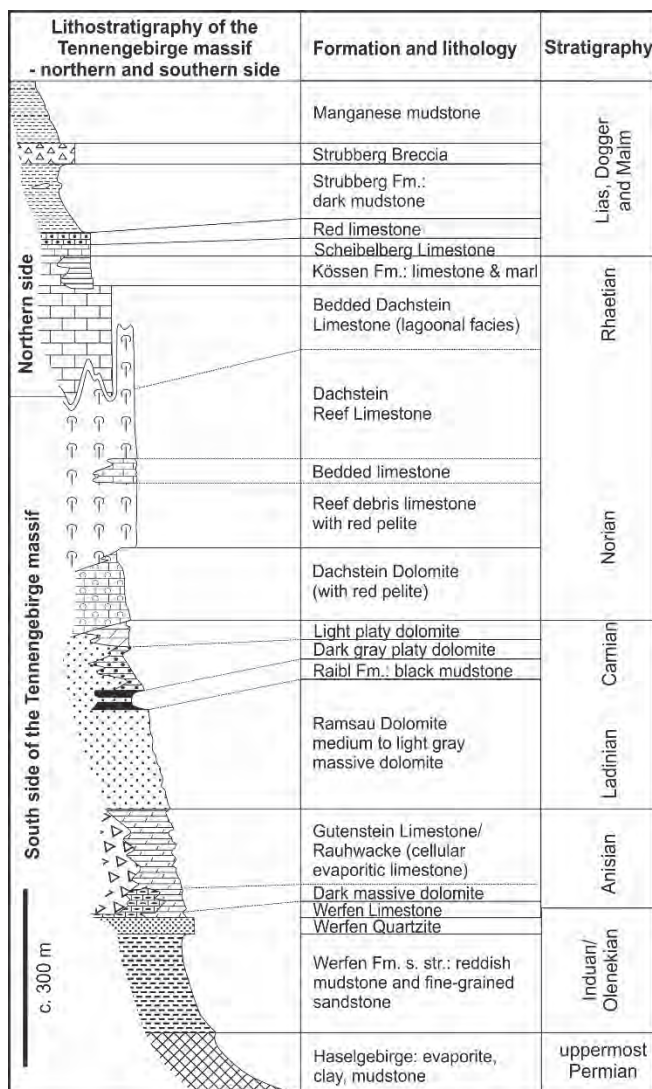


Fig. 9: Lithostratigraphic section of the Tennengebirge block of Northern Calcareous Alps (modified after an unpublished sketch of Gottfried Tichy).

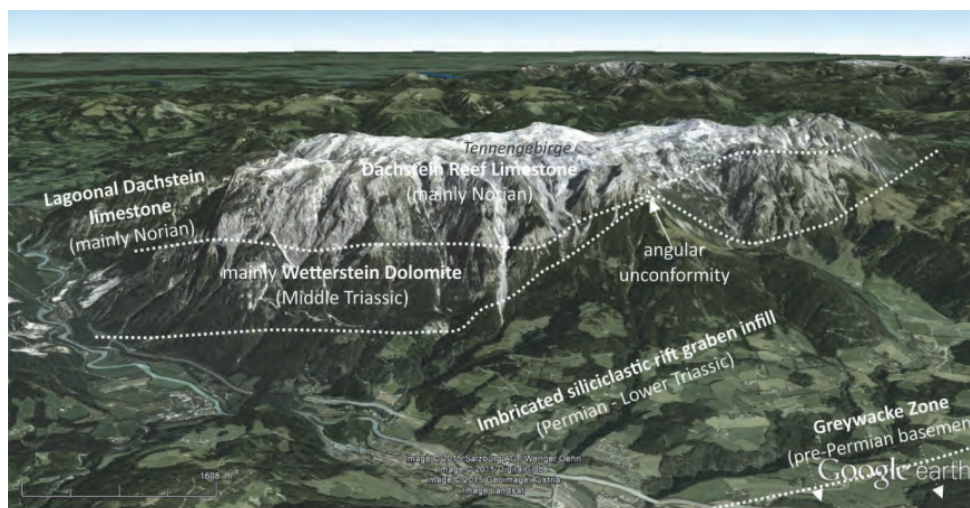
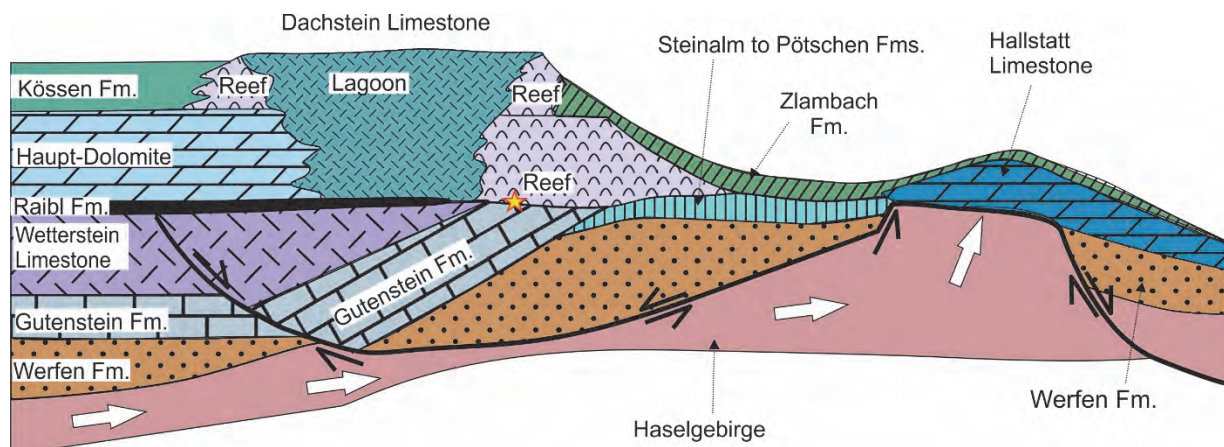


Fig. 10: Google Earth view of the Tennengebirge massif interpreted as Middle-Upper Triassic tilted block (base: [www.googleearth.com](http://www.googleearth.com)).

During latest Triassic to Early Jurassic, the shallow water deposits suddenly disappeared and were replaced by reddish pelagic limestones (e.g., by the Adnet Limestone, an ammonitico rosso-type limestone). These features have been interpreted to result from ongoing subsidence related to the extension during rifting of the future Penninic Ocean. Later, radiolarites were deposited as well as the well bedded Oberalm Limestone exposed to the southeast of Salzburg. The subsidence of the Upper Jurassic successions is interpreted to relate to the ongoing closure of the oceanic Meliata rift (Missoni and Gawlick, 2011). Following a marly interval (Schrambach Fm.), these are then overlain by the Lower to lowermost Upper Cretaceous Rossfeld Group, a trench fill mixed of siliciclastic and carbonates due to the closure of the Meliata Ocean (e.g., Faupl and Tollmann, 1978; Krische et al., 2014; Krische and Gawlick, 2015). These latter units are part of the Tirolic nappes, which are overridden by the Juvavic units (Juvavum: Roman word for Salzburg). The tectonics are discussed to result from Late Jurassic gravity gliding (Missoni and Gawlick, 2011) or Early to earliest Late Cretaceous nappe tectonics (Schorn et al., 2013 and references therein). The palaeogeographic development is shown in Faupl and Wagreich, 2000). The Cretaceous and Eocene nappe structures and brittle deformation are discussed in Linzer et al. (1995, 1997).

The St. Martin-Werfen Imbricate zone is exposed south of the Tennengebirge and represents a zone of structural imbricates composed of Permian to Lower Triassic siliciclastic formations and Middle Triassic carbonates. Only a few structural studies did deal with that zone (e.g., Rossner, 1977) and top-s vs. top-N imbrication was discussed.



*Fig. 11: Tectonic model of the passive margin formation involving raft tectonics on uppermost Permian Haselgebirge evaporites (from Neubauer et al., 2017; palaeogeographic section is based on Mandl, 2000 and references therein).*

Upper Cretaceous to Eocene Gosau basins are collapse basin on top of the Cretaceous-aged Upper Austroalpine nappe edifice. The succession of these Gosau basins are divided into basal terrestrial and shallow water deposits gradually changing into marly and turbiditic deep-water deposits.

The Lower Austroalpine nappe complex of the northern Radstadt Mountains is characterized by largely inverted nappes (with mainly Permian to Jurassic successions) including the prominent Quartzphyllite nappe (see also Rossner, 1976). The sections include very thick Permian to Lower Triassic siliciclastic strata, which are overlain by a thick Middle to Upper Triassic dolomites (Rossner, 1979) and Jurassic marls, breccias and radiolarites (Häusler, 1988).

A structural map is shown in Figure 12 and the tectonostratigraphy in Figure 13. These Lower Austroalpine nappes are thrusted over Penninic tectonic units of the NE edge of Tauern window during Eocene as dating of ductile fabrics of the Hochfeind nappe suggests (c. 50–54 Ma; Liu et al., 2001; Fig. 13). Successions of the Quartzphyllite nappe show a dominant foliation and a ca. WNW-trending stretching lineation formed during deformation stage D<sub>1</sub> during nappe transport towards WNW during Late Cretaceous (<sup>40</sup>Ar/<sup>39</sup>Ar white mica: c. 78–80 Ma). Ductile shear zones in overlying basement units and isoclinal km-scaled folds with subhorizontal axial surfaces and local internal thrust splays in the Quartzphyllite nappe are associated with D<sub>1</sub> deformation. D<sub>1</sub> fabrics are overprinted by D<sub>2</sub> ductile fabrics at the structural base of the Quartzphyllite nappe to the underlying Penninic units. In the interior of the Quartzphyllite nappe, the foliation S<sub>1</sub> is overprinted by kilometer-meter-scaled open N-vergent, ENE to E plunging D<sub>3</sub> folds with amplitudes of ca. 1 – 2 km. These folds also affect the D<sub>2</sub> thrust boundary of Penninic to Lower Austroalpine nappe complex (Fig. 14) and postdate, therefore, plate collision. In outcrops, a non-penetrative axial plane foliation S<sub>3</sub> formed by pressure solution or cataclastic deformation, and no recrystallization of these fabrics occurred. The D<sub>3</sub> folding postdates, therefore, D<sub>2</sub> thrusting dated at ca. 50–54 Ma and indicates a previously unrecognized stage of shortening of Lower Austroalpine units. This folding stage with a minimum shortening estimate of c. 30 percent is interpreted to be associated with internal dome formation within the Tauern window. Regional considerations allow date D<sub>3</sub> N-S shortening to latest Eocene to earliest Miocene. D<sub>3</sub> shortening is overprinted by D<sub>4</sub> activation of the SEMP strike-slip fault and finally by Early Miocene ESE-directed D<sub>4</sub> ductile normal faulting (Katschberg fault) and contemporaneous activation of the Mur-Mürz fault.

The new data are similar to D<sub>3</sub> N-S shortening structures occurring over the whole N-S section in the Eastern and Southern Alps. These structures include internal thrusts within Northern Calcareous Alps (NCA), the footwall accretion and deformation of Penninic units along the northern floor thrust of Eastern Alps.

Taking all the evidence from this section together, the Eastern Alps expose the plate boundary between the combined Europe-derived lower plate continental units and obducted Mesozoic Penninic ocean basin fill and the overlying continental Austroalpine nappe complex in the dome-shaped Tauern window. A structural study in Radstadt Mountains associated with reinterpretation of Ar-Ar geochronology of ductile low-grade metamorphic fabrics and the interpretation of a N-S cross-section of Eastern Alps allow recognize the following major processes: (1) A regular footwall progradation of thrusting from ca. 110 Ma to ca. 50 Ma is partly contemporaneous with orogen-parallel extension (Late Cretaceous and Miocene) in uppermost units (Fig. 14). (2) Latest Eocene and earliest Miocene post-collisional plate boundary folding and shortening formed in the rheologically weak center of the orogen. (3) The interplay of Miocene outward thrust propagation and strike-slip faults is potentially controlled by inherited rift structures in the subducted plate.

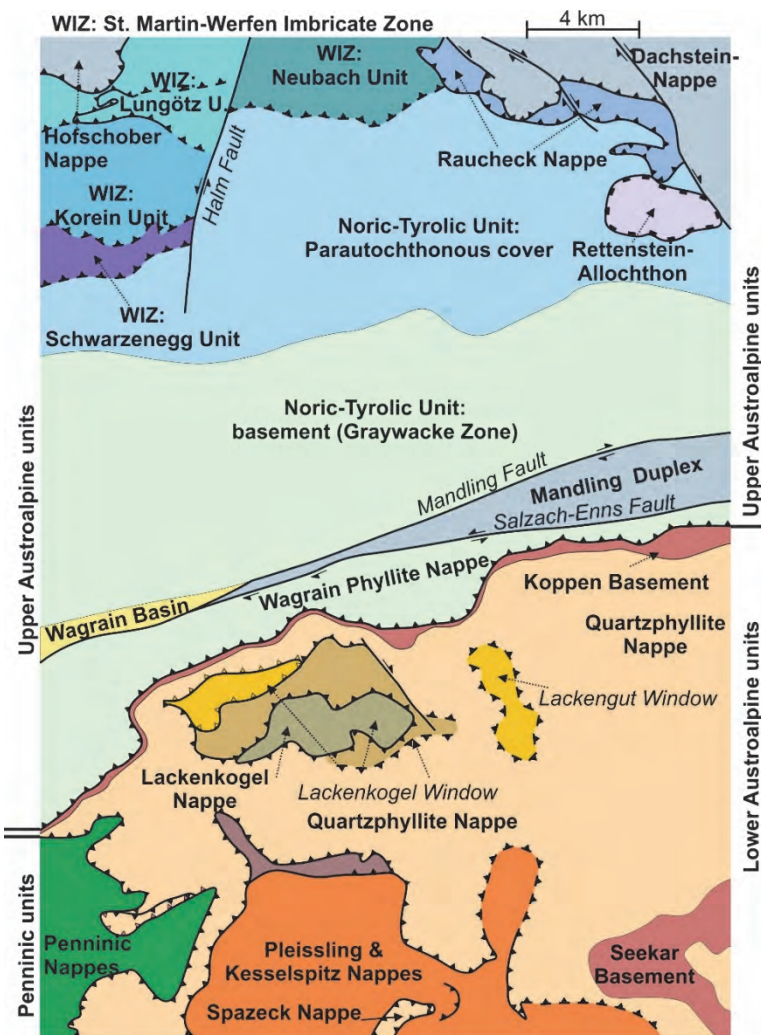


Fig. 12: Tectonic map of the area between St. Martin-Werfen Imbricate zone and uppermost Penninic units.

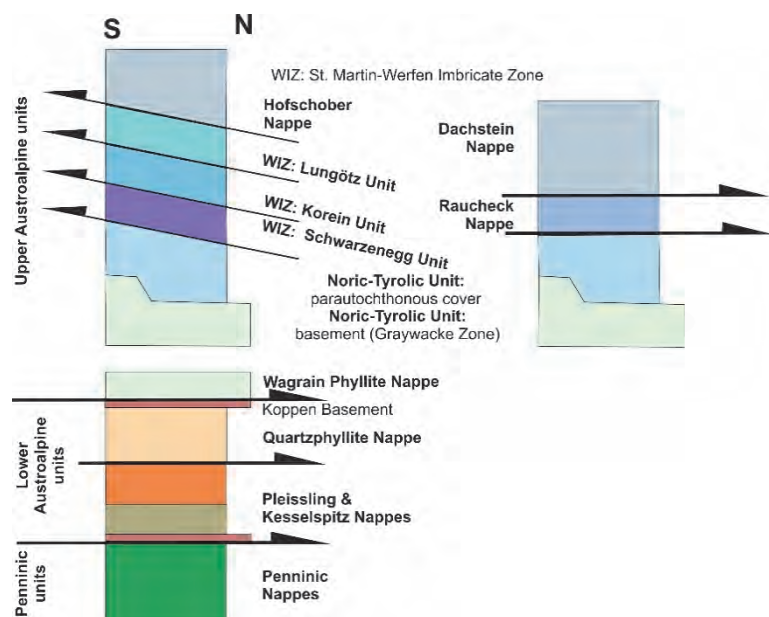


Fig. 13: Tectonostratigraphy of the area between the St. Martin-Werfen Imbricate zone and uppermost Penninic units.

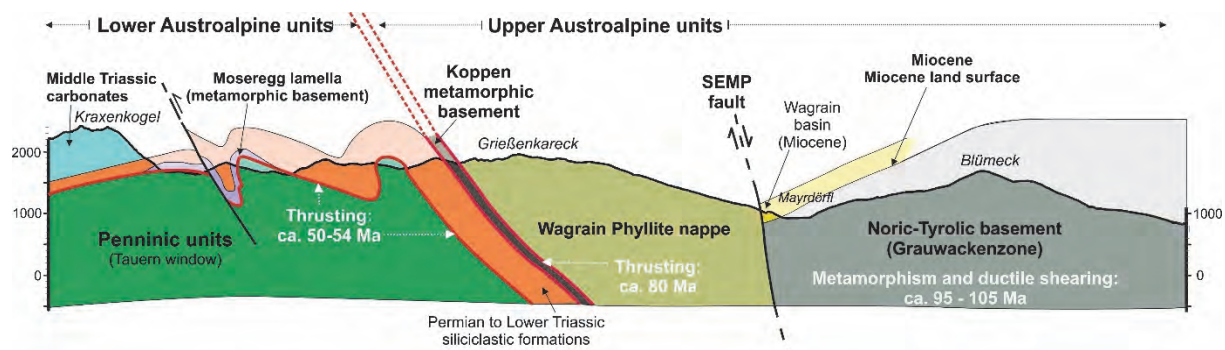


Fig. 14: Simplified cross-section showing the structure of Lower Austroalpine units.

## 2.2 Stops

### Stop 1-1: Adnet quarries Lienbacher quarry: Liassic Adnet Limestone

Location: N47° 41' 47.7" E13° 08' 17.6"; ÖK 50, sheet 94 Hallein; the quarries are located to the NE of the village Adnet. ÖK 50: older version of the Austrian topographic map, scale 1 : 50,000.

In the surroundings of Adnet-Langmoos the Adnet-limestone is cut in numerous quarries, some are active and others are abandoned and overgrown. Detailed descriptions can be found in Böhm (1992) and Dorner et al. (2009). The Adnet Limestone is a red lutitic nodular limestone. The ferro-manganese crusts and the halmyrolysis (submarine weathering) indicate the strongly condensed sequence (Fig. 15). There are only 30 meters compared with about 300 meters of the Glasenbach gorge section in the north. Within the condensed horizons, ammonites are frequent, but it is very hard to get them out. The fossils are not well preserved. Within the threshold facies, *Psiloceras planorbis* (Sowerby) is missing, but not so in Glasenbach gorge. The sequence starts here with *Schlotheimia angulata* (Schlotheim). Neptunian dykes filled with bioclastic detritus occasionally occur. The Adnet Limestone is also strongly deformed with stylolites and abundant signs of pressure solution.

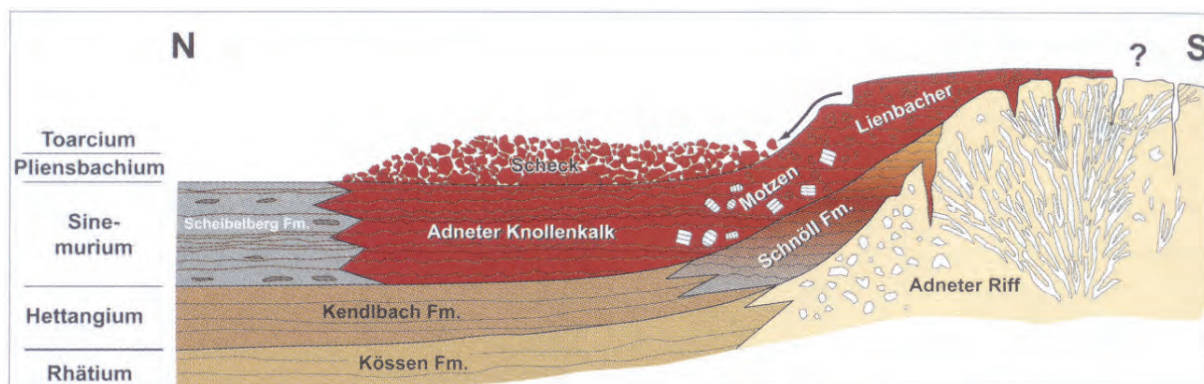


Fig. 15: Various lithotypes of the Adnet Limestone and its relationships to underlying formations (from Dorner et al., 2009).

**Stop 1-2: Pass Lueg, Upper Trias: Dachstein Limestone**

Location: N47° 34' 30.1" E13° 11' 46.5"; ÖK 50, sheet 94 Hallein; road cut to the South of Pass Lueg along the Federal Road.

The road cut exposes bedded Dachstein Limestone with the famous loferite cycle. The exposure, an ice-polished surface, is rich in megalodonts (*Conchodus infraliasicus* STOPPANI) and shows complete Norian loferite cycles (Plöchinger, 1983).

**Stop 1-3: Middle and Upper Triassic carbonate platforms; viewpoint**

Location: N47° 31' 58.9" E13° 10' 07.6"; ÖK 50, sheet 94 Hallein; parking place on the western side on the federal road between Pass Lueg and Sulzau

A N-S cross-section through western Tennengebirge is shown in Fig. 16. The panoramic view to the steep western slope of the Tennengebirge massif (shows the thick succession of Lower to Upper Triassic carbonate platform with Ladinian Wetterstein Limestone and Upper Triassic bedded Dachstein Limestone formed by the loferite cycles in an lagoonal depositional environment. No strata of the Carnian Raibl Fm. occur. The whole section with always shallow water deposits is well preserved and displays a thickness of ca. 2 km of Middle-Upper Triassic units (Figs 16, 17) implying rapid subsidence interpreted to represent the tectonic subsidence during opening of the Meliata Ocean.

**Stop 1-4: Obermoos W Filzmoos: Overview on structural/stratigraphic base of Northern Calcareous Alps**

Location: N47° 26' 04.5" E13° 29' 46.6"; ÖK 50, sheet 126 Radstadt; forest ca. 400 m NW the village Obermoos W Filzmoos.

The roadcut along a forest road exposes a succession of low-grade metamorphic greyish sandstones and quartz-conglomerates of the Filzmoos conglomerate. This unit is interpreted to represent an intramontane molasse basin deposited on top the Ordovician to Devonian Grauwackenzone basement (Figs 18, 19). No unconformity was found in that region. The metaclastic succession is foliated, and traces of axial surface foliation can be found recording the Cretaceous deformation during nappe stacking associated with coeval metamorphism.  $^{40}\text{Ar}/^{39}\text{Ar}$  white mica ages from nearby outcrops are at ca. 100 Ma although some older ages up to 120 Ma were recorded, too Frank and Schlager, 2006) potentially due to inherited detrital grains.

During Late Eocene, the NCA were transported towards N and loaded onto the European lithosphere. Based on the top-S imbricates south of the Tennengebirge (Fig. 12), the St. Martin-Werfen imbricate zone, the Northern Calcareous Alps represent a large-scale pop-up (Fig. 20).

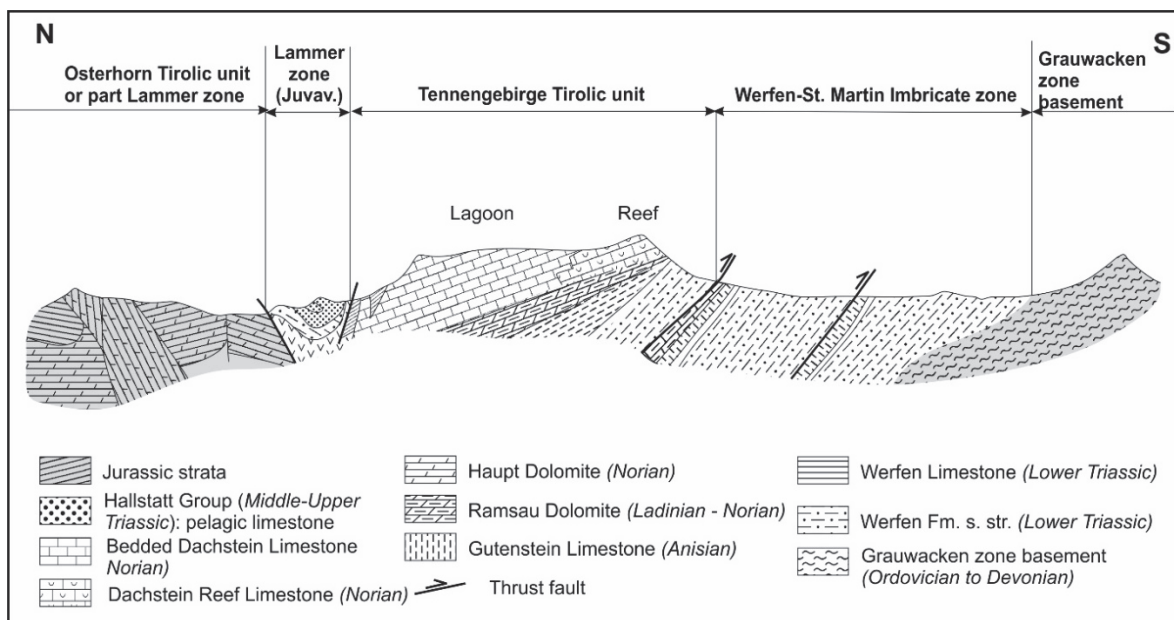
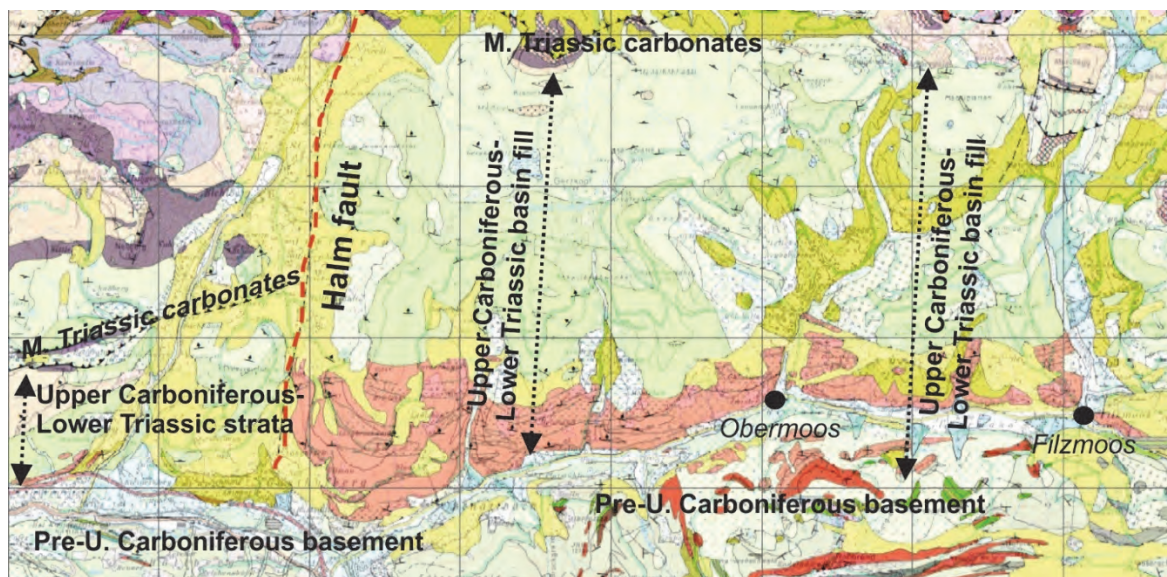


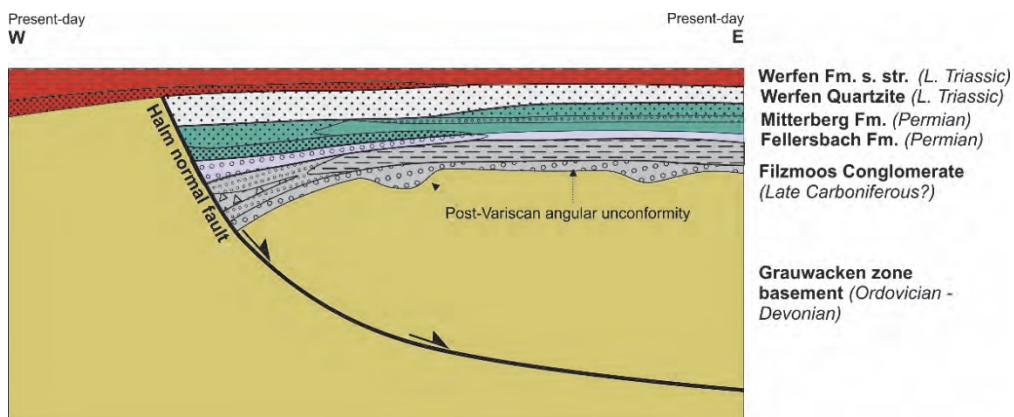
Fig. 16: Cross-section across the Tennengebirge block (modified from Schramm and Tichy, unpublished sketch).



Fig. 17: Google Earth image of the Tennengebirge massif with the Wetterstein Dolomite at the base and Bedded Dachstein Limestone at top and northern margin (from Google Earth Pro). The whole Middle to Upper Triassic shallow water succession is more than 2 km thick indicating rapid subsidence during passive margin formation. Note also the transition from Dachstein reefs in the south to lagoonal well bedded Dachstein Limestone in the north, as well as the Early Miocene Dachstein peneplanation surface on top.



*Fig. 18: Geological map of the Filzmoos region exposing a thick succession of Upper Carboniferous to Lower Triassic siliciclastic strata in contrast to area to the west of the Halm fault. The Halm fault is now a strike-slip tear fault separating the thick infill of a halfgraben from a thin succession west of it.*



*Fig. 19: Tectonic model of the Upper Carboniferous (?) to Permian successions interpreted as a Permian halfgraben.*

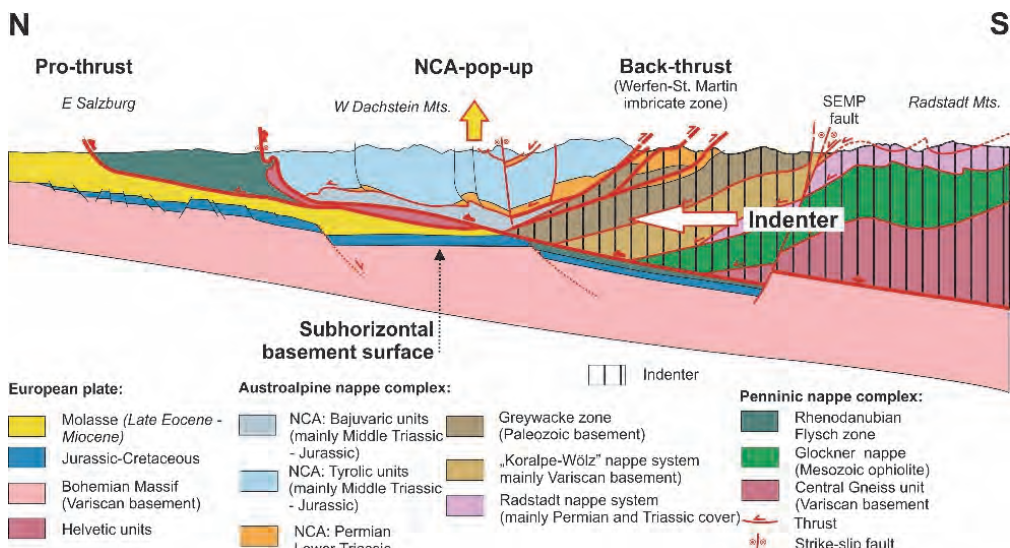


*Fig. 20: Cross-section across the northern part of Eastern Alps.*

**Stop 1-5: E of Wagrain: uppermost part of the Miocene Wagrain basin fill and SEMP fault**

Location: N47° 20' 50.8" E13° 20' 05.1" ; ÖK 50, sheet 125 Bischofshofen; artificial water reservoir at middle cable car station SE Weberland hill east of Wagrain

The outcrop exposes the uppermost part of the Wagrain basin fill of the coaly sandstone lithofacies (Neubauer, 2016). The preserved Wagrain basin (Fig. 21) is ca. 200 m thick, with an angular unconformity over phyllites of the Grauwackenzone basement at its base. The SEMP fault stretches in the south and can be traced only by morphology due to intense weathering of the cataastically deformed rocks.

In this exposure, grey-brown sandstones grade into 6–8 m thick dark greyish to locally black, coaly sandstones (Fig. 22). These sandstone beds are internally massive and ca. 10–60 cm thick. Single-grain  $^{40}\text{Ar}/^{39}\text{Ar}$  dating of detrital white mica yields an age peak between  $85.9 \pm 3.6$  and  $109.2 \pm 4.9$  with a majority around 100 Ma (Fig. 23). One grain is younger ( $77.5 \pm 3.3$  Ma) and a few grains are slightly older ( $119.0 \pm 5.9$  Ma;  $148.2 \pm 11.1$  Ma) and one grain is dated at  $382.2 \pm 7.5$  Ma. The dominating Cretaceous-age population indicates a nearly exclusive origin of the dated detrital white mica from higher greenschist facies to medium-grade metamorphic rocks largely overprinted by eo-Alpine metamorphism. Based on this age populations and apatite fission track ages, Neubauer (2016) proposed that the Bösenstein area is the likely source because it already cooled during the Eocene through ca. 100 °C-isotherm, as apatite fission track ages indicate (Hejl, 1997). The high white mica and garnet contents could have their origin in the spatially widespread Wölz Micaschist complex with its abundant garnet micaschists. This implies a sinistral displacement of ca. 40 km along the SEMP fault after deposition of these strata of the Wagrain basin (Fig. 24).

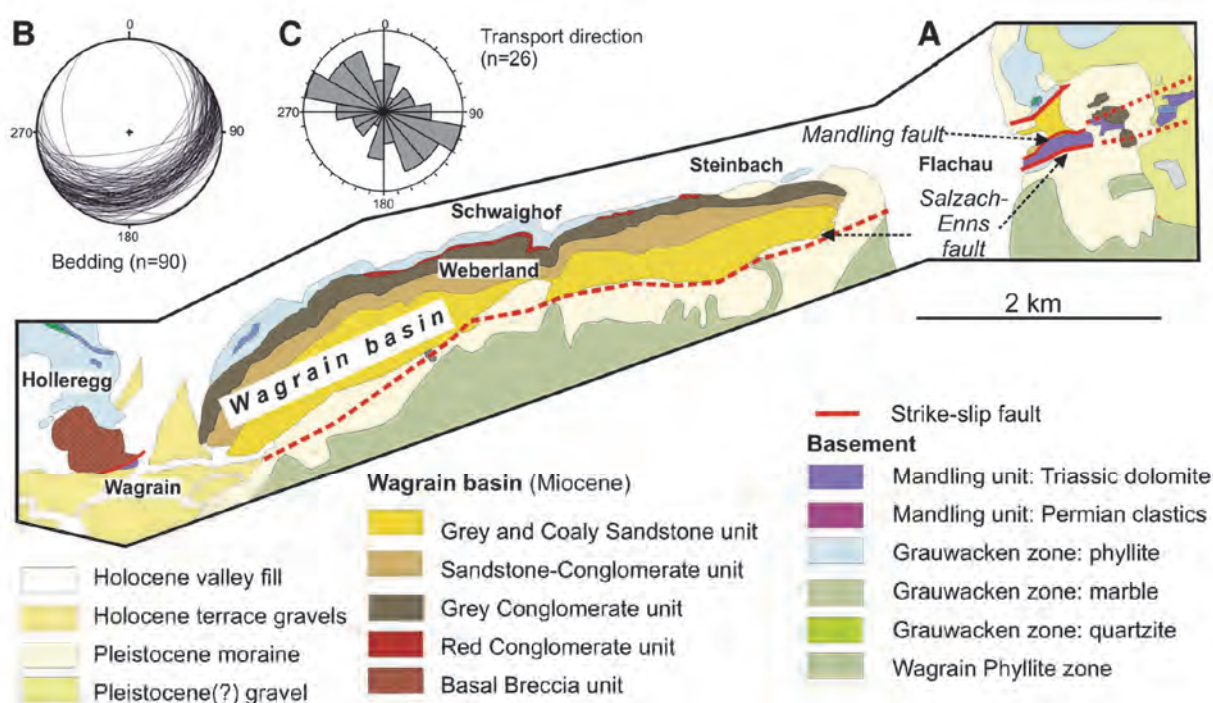


Fig. 21: Geological map of the Wagrain basin (from Neubauer, 2016).

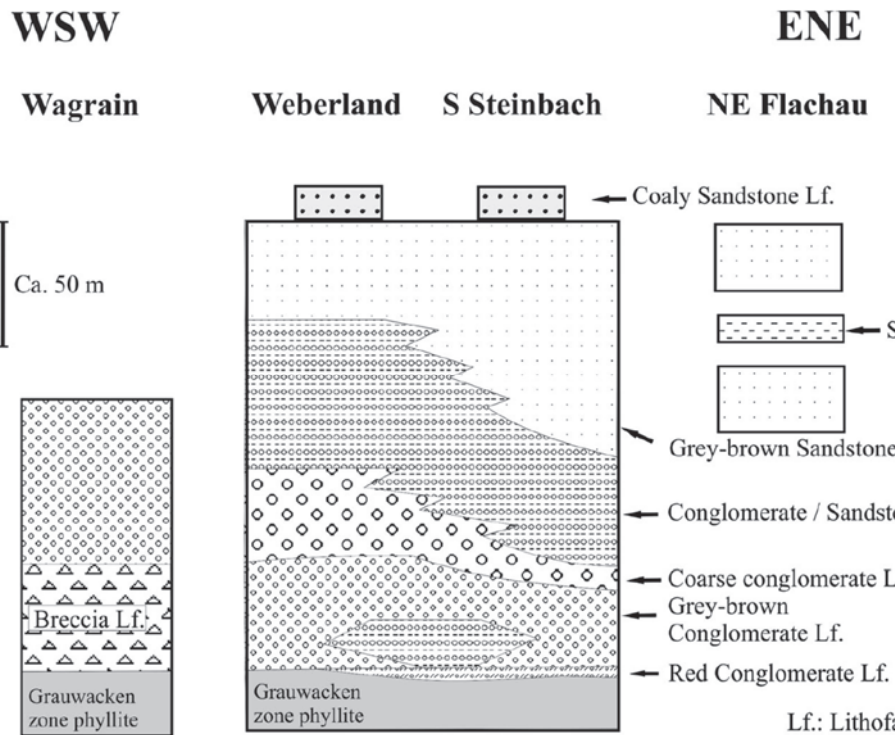


Fig. 22: Lithostratigraphic sections showing the distribution of various lithofacies types (from Neubauer, 2016).

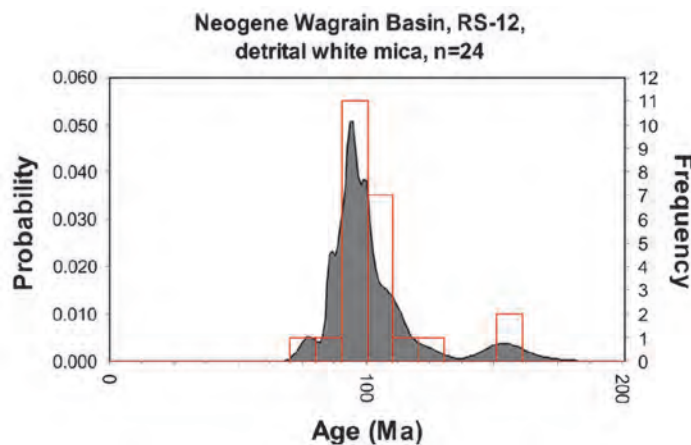


Fig. 23: Ar-Ar ages of detrital single grains of the coaly sandstone lithofacies (from Neubauer, 2016).

#### Stop 1-6: Radstadt: Upper Ordovician porphyroid of Grauwackenzone

Location: N47° 23' 01.2" E13° 27' 40.9"; ÖK 50, sheet 126, Radstadt; base of tower in the southwestern corner of the medieval city wall

The small outcrop exposes the Middle-Upper Ordovician Blasseneck Porphyroid, a distinct widespread element of the Grauwackenzone basement. The rock well exposes the porphyric texture of the precursor volcanic rock. This is overprinted by Cretaceous greenschist facies-grade metamorphism and top WNW-directed ductile deformation similar as in Upper Carboniferous to Triassic cover successions.

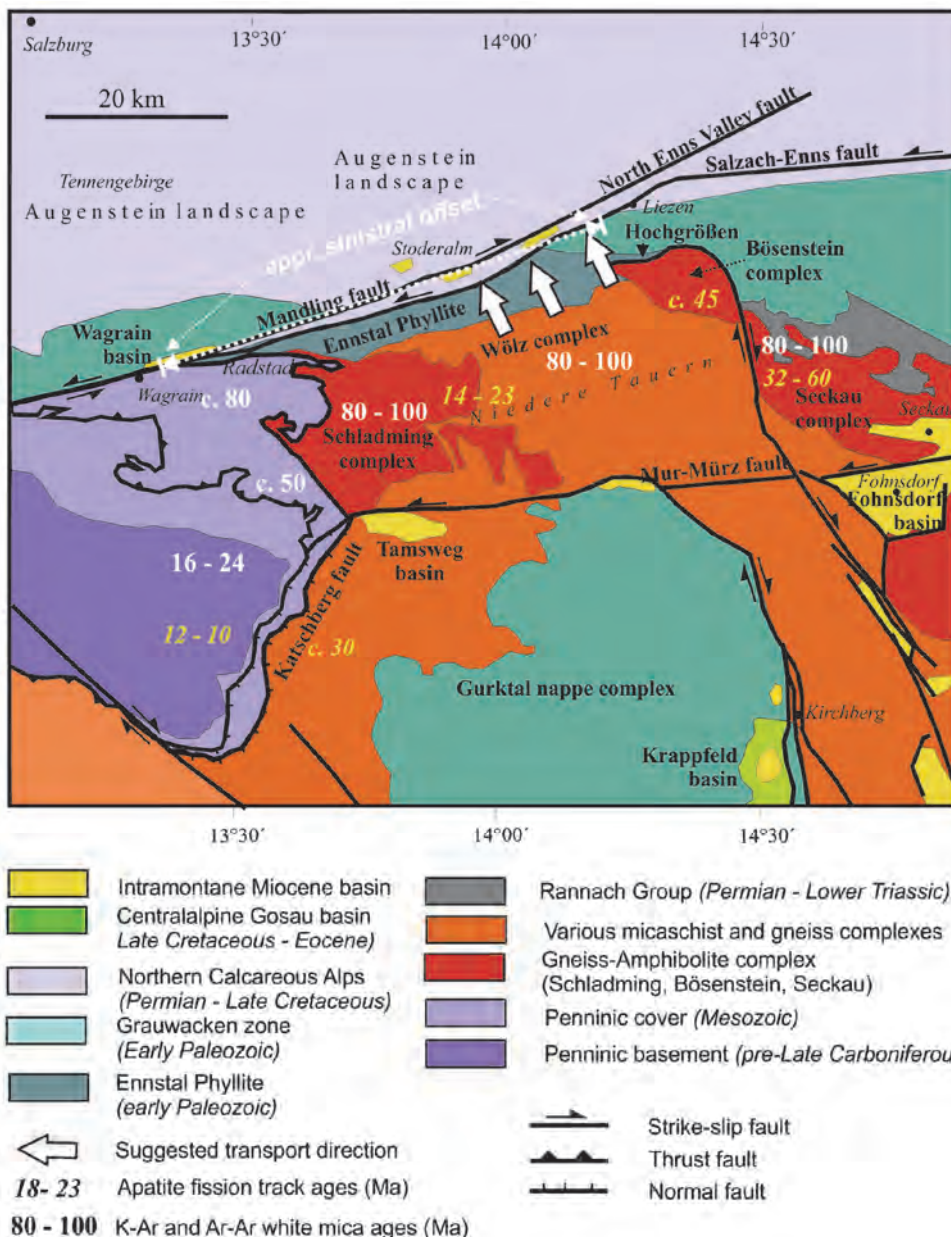


Fig. 24: Model of potential provenance in the eastern Niedere Tauern and Bösenstein areas for the Wagrain basin fill (from Neubauer, 2016).

#### Stop 1-7: Gnadenalm: “Black” middle Triassic facies of the Pleising nappe

Location: N47° 16' 13.2" E13° 30' 00.2"; ÖK 50, sheet 126, Radstadt; south of Gnadenalm meadow

These exposures along the road 'to Obertauern and the access road to the Gnadenalm expose unusual, dark-colored and bedded dolomite. These dolomites are interpreted as lagoonal deposits (Rossner, 1979). The dark-greyish to black color is unusual for the Middle Triassic successions. Although representing lagoonal deposits, a partly anoxic facies ("black "Anisian/Ladinian" according to older papers of Tollmann, 1977) can be assumed. The area is also rich intraformational monomictic breccia so that fault-controlled escarpment breccia formation is assumed along margins of deepening, increasingly anoxic basins.

**Stop 1-8: Obertauern road, W Obertauern: Overview on partly inverted nappes of central Radstadt Mts.**

Location: N47° 15' 07.9" E13° 31' 38.2"; ÖK 50, sheet 126, Radstad; parking place at access to Johannisfall.

The viewpoint with a view to the west allows explain a peculiar feature of this part of Radstadt Mountains. The upper nappe, the Quartzphyllite nappe, is inverted and comprises the Permian Alpine Verrucano Fm. at top and underlying Lantschfeld Quartzite (Fig. 25). North of this viewpoint, the amphibolite-grade metamorphic Seekar crystalline basement with Variscan relics is the likely basement of the Quartzphyllite nappe. The Quartzphyllite nappe is underlain by the Pleising nappe with thick Middle Triassic to Carnian carbonate deposits which also include dark phyllites and fine-grained metasandstones of Raibl Formation. The ductilely deformed limestones are within greenschist facies metamorphism and  $^{40}\text{Ar}/^{39}\text{Ar}$  white mica ages indicate ages of ca. 78 – 80 Ma (Late Cretaceous). Consequently, the nappe structure is considered to be of Late Cretaceous age (ca. 78 – 80 Ma).

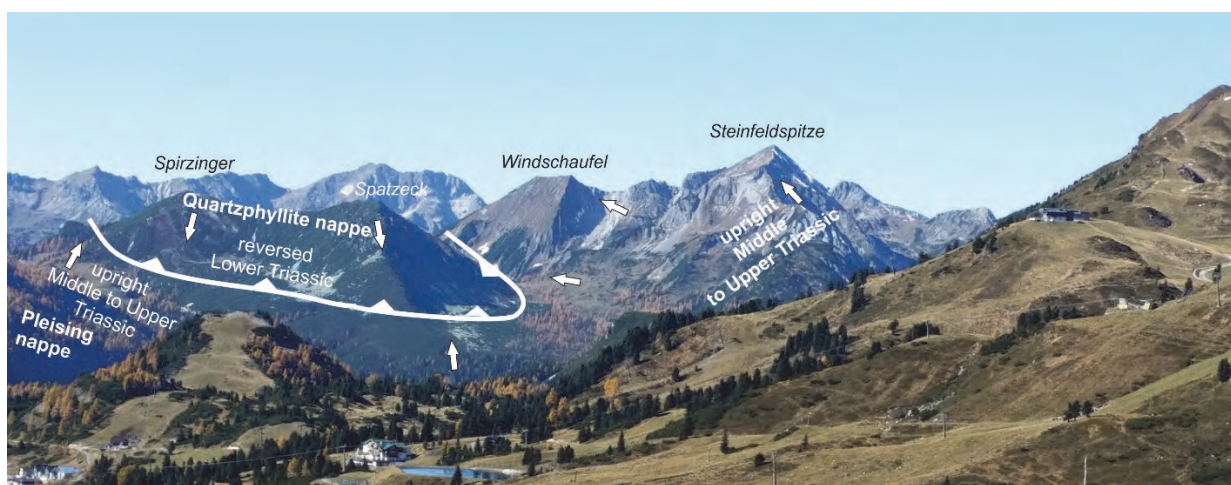


Fig. 25: View towards the Spatzeck and Spirzinger showing the inverted Quartzphyllite nappe.

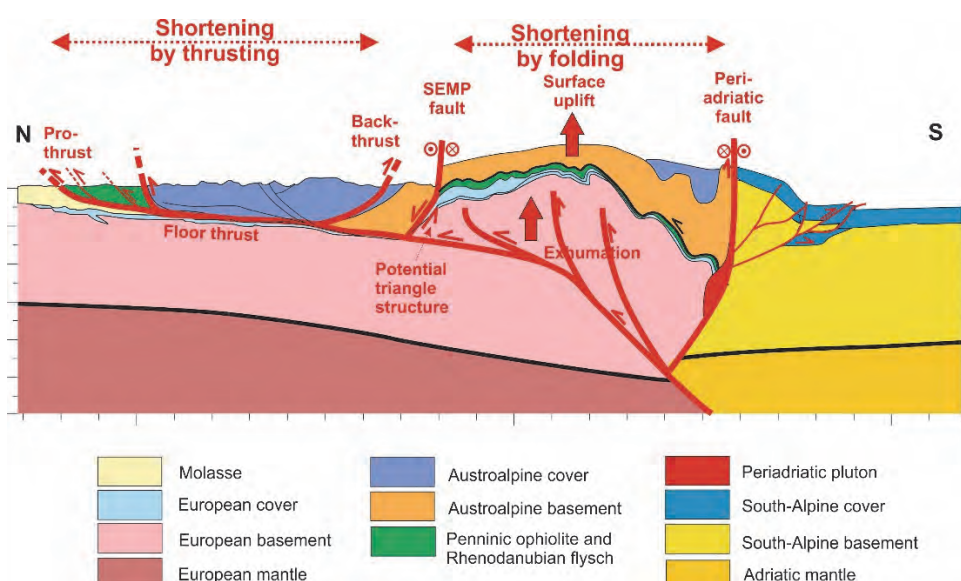


Fig. 26: Tectonic model for the Late Paleogene to Miocene tectonic processes of Eastern Alps in the section across the Eastern Tauern window.

This feature allows discussion of the overall late-stage structure in a N-S cross-section across the Eastern Alps (Fig. 26). We interpret the shortening features by folding as contemporaneous with thrust shortening and fore- and back-thrust of the NCA pop-up (Fig. 26).

### **Stop 1-9: Obertauern: Paleogene metamorphism in Jurassic successions**

Location: N47° 14' 35.5" E13° 34' 00.6"; ÖK 50, sheet 156, Muhr; SE of Obertauern village

This exposure reveals phyllites, marbles, metasandstones, calcareous phyllites of Jurassic age. Single grain  $^{40}\text{Ar}/^{39}\text{Ar}$  ages of detrital white mica reveal an early Eocene age (ca. 50 Ma). This indicate that this part was already affected by heating by the underlying Penninic units and represents the age of thrusting of Lower Austroalpine units over Penninic units as initially postulated, in the area further south, by Liu et al. (2001). This implies a footwall propagation of thrusting within Austroalpine units.

## **3 The eastern Tauern window: deformation phases and age data of the Austro-Alpine – Penninic plate boundary**

JOHANN GENSER

### **3.1 Introduction**

One of the main questions regarding the tectonic evolution of the Eastern Alps is the relation between nappe stacking and metamorphism in the Austro-Alpine unit to the subduction of the Penninic units beneath, as new data challenge important assumptions of present (plate)tectonic models (Hawkesworth et al., 1975; Frisch, 1979; Tollmann, 1987; Frank, 1987; Behrmann, 1990; Scharf et al., 2013; Schmid et al., 2013; Rosenberg et al., 2018). These models relate the early to middle Cretaceous nappe stacking and Barrovian type metamorphism in the Austro-Alpine unit to the subduction of the South Penninic ocean beneath or to the final collision with the Middle Penninic basement complex, exposed in the Tauern Window. Recognition of a Cretaceous high-P metamorphism (Thöni and Jagoutz, 1992) in the Austro-Alpine unit in the last years points to a Cretaceous subduction of the AA and hence a lower plate position for this unit during that time span, rather. The two mega-units also show very different timings of the metamorphic evolution, but very similar metamorphic paths (eclogite facies followed by amphibolite facies). In the Austro-Alpine, the temperature peak occurred in the early Late Cretaceous, cooling below c. 300 °C was completed in the late Cretaceous already. In the Penninic units, the thermal peak falls into the late Palaeogene, cooling into the Miocene (Frank et al., 1987a, b) (Fig. 27).

The following is a presentation and discussion of mainly structural and thermochronological data from the Eastern Tauern window, where in the area of the Malta and Lieser valleys, a continuous profile from the deepest tectonic units of the eastern Tauern window up to the Middle Austro-Alpine units is exposed (Fig. 28). It is situated ideally, therefore, to study the relationships between the two mega-units. The area of the eastern TW includes three tectonic mega-units, the Austro-Alpine upper plate, the Glockner Nappe and the basement units of the Venediger Nappe (Fig. 28). The Austro-Alpine unit consists of three individual nappes in the area that were stacked during the Cretaceous and subsequently thrusted onto the Penninic unit. The Penninic unit comprises the remnants of the South Penninic oceanic crust, the Glockner Nappe, and Middle Penninic units comprising a basement complex and an overlying Permo-Mesozoic cover unit. Between the Glockner Nappe and the

parautochthonous basement are several nappes that were derived from the Middle Penninic continental complex (Kurz et al., 1998; Schmid et al., 2013).

### Alpine metamorphism Tauern Window

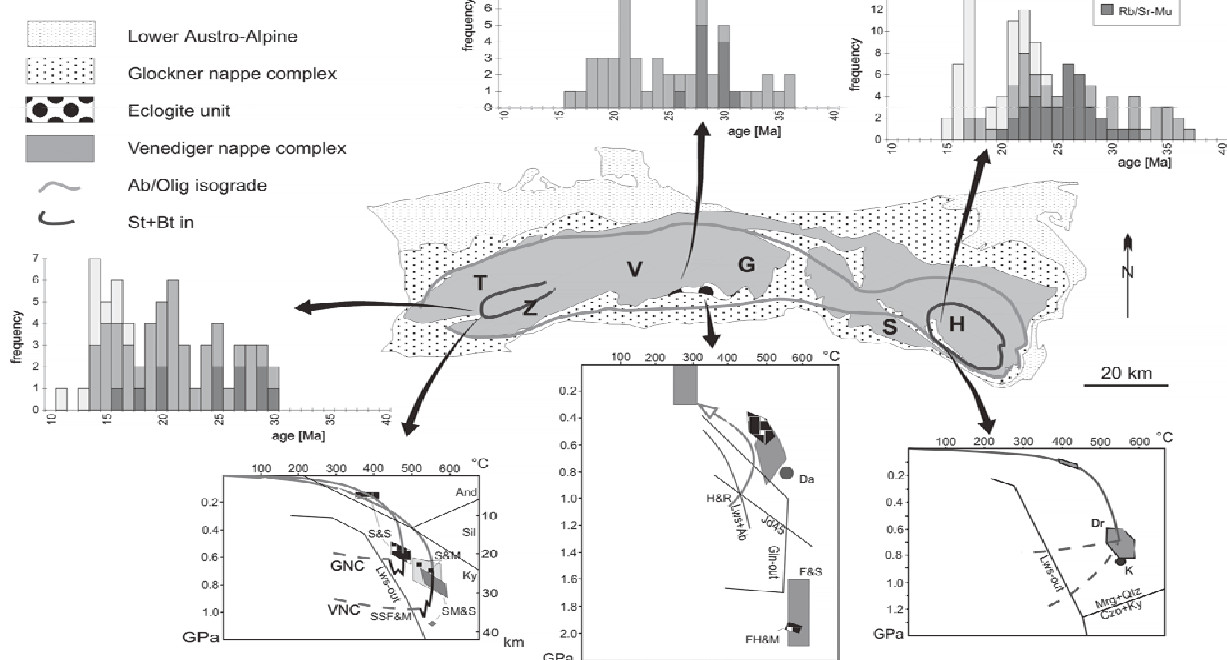


*Fig. 27: Alpine metamorphism in the Tauern window with p-T paths and radiometric age data (from Genser et al., 1996; see references therein).*

### 3.2. Tectonic setting and structural evolution of Penninic units

From bottom to top we can distinguish the following tectonic units (Fig. 28), which can be correlated over the entire Tauern window (Kurz et al., 1998; Schmid et al., 2004, 2013). Here, the previous terminology is used:

1. Parautochthonous basement consisting of a pre-Permian basement complex intruded by Variscan granitoids, the Zentralgneis (Central gneisses). On top is a primary Permo-Mesozoic cover sequence, the Silbereck Group in this area.
2. The Eclogite zone, that occurs only in the middle part of the Tauern window.
3. Nappes that consist of basement and cover parts that were derived from continental margin sequences of the Middle Penninic terrane.
4. The Glockner nappe, comprising ophiolites and mainly volcano-sedimentary sequences of the South Penninic oceanic basin.
5. The Matrei and the Nordrahmen units, melange units deposited during the active margin stage.

This study describes the area around Malta and Lieser valley. Beside early work (e.g. Cliff et al., 1971) and mapping (Exner, 1980b, 1983b), further recent data concerning the eastern Tauern window can be found: petrological studies in Kruhl (1993), Scharf et al. (2013), structural and geochronological data and geodynamic interpretations in Bertrand et al. (2015, 2017), Favaro et al. (2015), Neubauer and

Genser (1990), Ratschbacher et al. (1989), Scharf et al. (2016), Schmid et al. (2013) and Rosenberg et al. (2007, 2015, 2018).

In detail, the basement essentially consists of migmatitic paragneisses and minor micaschists and amphibolites (e.g., Frisch et al., 1993). The Variscan granitoids represent intrusions ranging from tonalites to granites, with the main members (Holub and Marschallinger, 1989; Marschallinger and Holub, 1991; Finger et al., 1993): a high-K, calc-alkaline I-type series with syenite, Malta tonalite, Hochalm porphyrygranite, Kölnbrein leucogranite, and two-mica granite and the Na-rich Göß granodiorites to granites. These Variscan granites occur in several cores, divided by metasedimentary basement units. In the eastern Tauern Window (TW), these are the Göß, Hochalm, Hölltor, Sieglitz and Sonnblick cores.

These basement units are overlain by the post-Variscan, Permo-Mesozoic sedimentary sequence of the Silbereck Group. It comprises basal quartzites, overlain by marbles, cagneuls, dolomites and finally calcschists, phyllites to micaschists and minor greenschists. Thrusted onto this parautochthonous unit are the Mureck and the Storz Nappe that comprises mainly Variscan metamorphic paragneisses, amphibolites and micaschists (Vavra, 1989; Vavra and Frisch, 1989; Frisch et al., 1993) and minor granites that intruded during the Variscan (Vavra and Hansen, 1991). The overlying Murtörl unit consists of black albite-phyllites, chloritoid-bearing chlorite-micaschists and graphitic quartzites that are probably of post-Variscan age (because of missing intrusions) and the primary cover of the Storz Group (Kurz et al., 1998).

The Schrovin Nappe comprises orthogneisses and mainly Permo-Mesozoic sediments, quartzites, calcite and dolomite marbles and calcschists. It must be derived from a continental shelf sequence, too (Exner, 1990).

The Glockner Nappe is delineated by some ophiolitic remnants (serpentinites, MOR-basalts) at its base (Höck and Miller, 1987). It mainly consists of the so called Bündner schists, calcschists, grading into marbles and phyllites, and greenschists, deposits of a deep oceanic basin. In this area, the relationship of the basement rocks of the Storz Nappe to the overlying sequence of black phyllites, a Permotriassic shelf sequence and the deep-sea sediments of the Glockner facies is obscured by the strong tectonic overprint, expressed in the parallelism of all the lithological boundaries and also in the strong thinning of the units. All the post-Variscan series are therefore often subsumed in the Peripheral Schieferhülle.

Detailed descriptions of the rock successions and lithologies can be found in the papers by Exner (1971, 1980b, 1982, 1983, 1984, 1989, 1990).

The oldest brittle to semiductile deformation structures in the Penninic units are overprinted by the main, ductile deformation. Indications of earlier deformations under cooler conditions are imbrications of different rock units and parallel trails of graphitic material, preserved in porphyroblasts (mainly albite), pointing to pressure solution as an early deformation mechanism.

The earliest kinematically interpretable deformation structures are a mylonitic foliation parallel to the lithological boundaries with only few intrafolial isoclinal folds (transposition) and a related N-S trending stretching lineation (Fig. 29). Kinematic indicators, as asymmetric porphyroclasts in granitoids and asymmetric quartz textures, the latter preserved in Triassic quartzites of the Peripheral Schieferhülle, indicate tectonic transport top to the N.

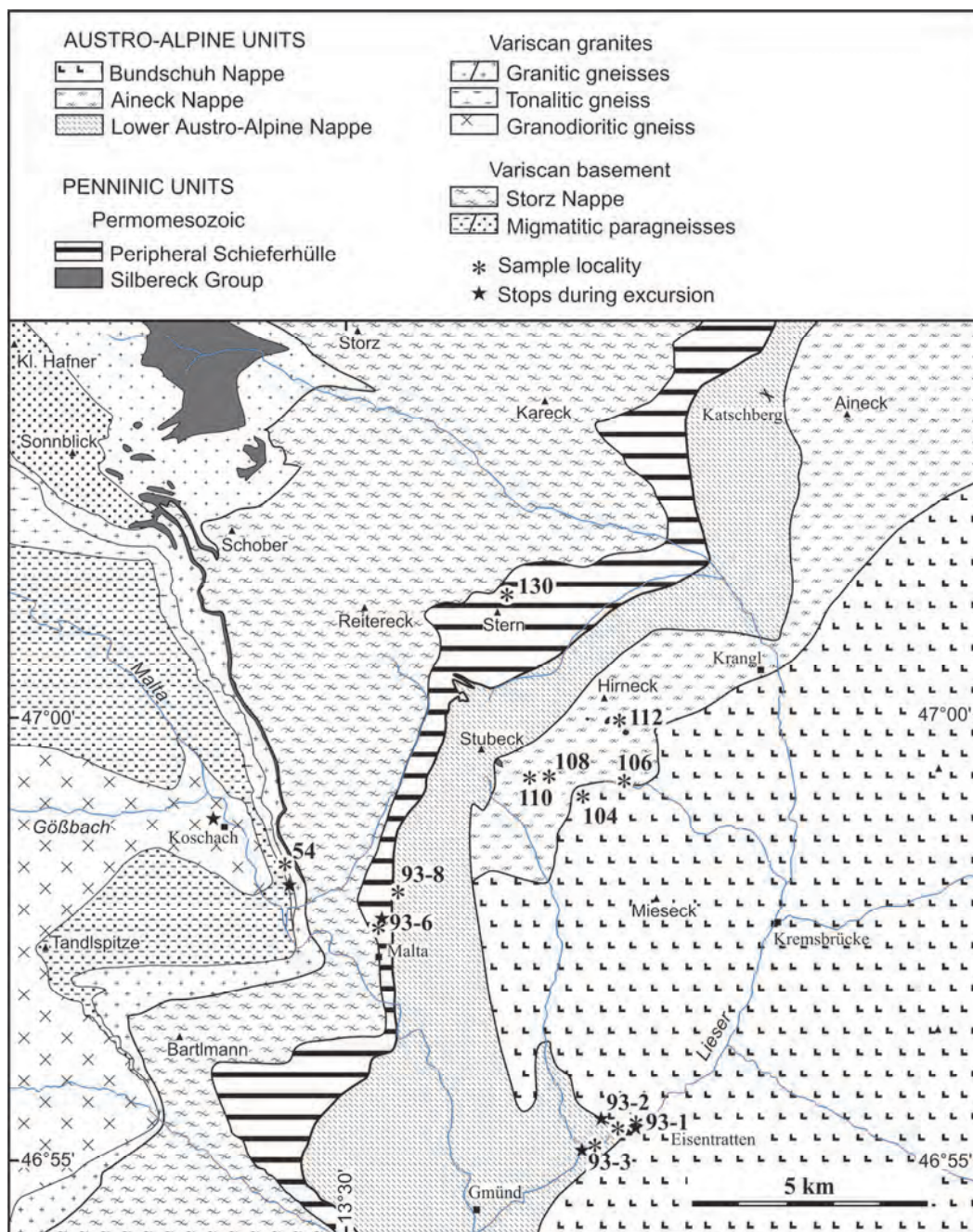


Fig. 28: Geological map of the area of the eastern Tauern window, Lieser and Malta valleys. The numbers relate to samples with new petrological, microstructural and geochronological data.

This N-S trending stretching lineation can be traced from the Peripheral Schieferhülle down to the base of the Silbereck-Fm., affecting the uppermost part of the basement locally (Fig. 29). A mylonitic foliation with N-S trending stretching lineations can be found throughout the Storz nappe, especially well developed in granitic rocks and amphibolites. In paragneisses and micaschists an older (pre-Alpine?) foliation is folded isoclinally and transposed by this foliation. The structures related to this deformation are best preserved in Triassic rocks of the Peripheral Schieferhülle in northern parts of the investigated area (around Stern). Quartzites, dolomites and intercalated calcite marbles display a strong mylonitic foliation with a pronounced N-S trending stretching lineation. Earlier planar structures, as graphitic trails, are folded isoclinally, but also the mylonitic foliation can show a progressive isoclinal refolding with fold axes parallel to the stretching lineation. During this

deformation quartz, calcite, and dolomite recrystallised dynamically. In the Peripheral Schieferhülle this deformation occurred until peak metamorphic conditions were reached, as dolomite was deformed by crystal-plastic mechanisms. Dolomite marbles and quartzites kept their synkinematic deformation features, only calcite shows evidence for a subsequent static recrystallization (Genser, 1992).

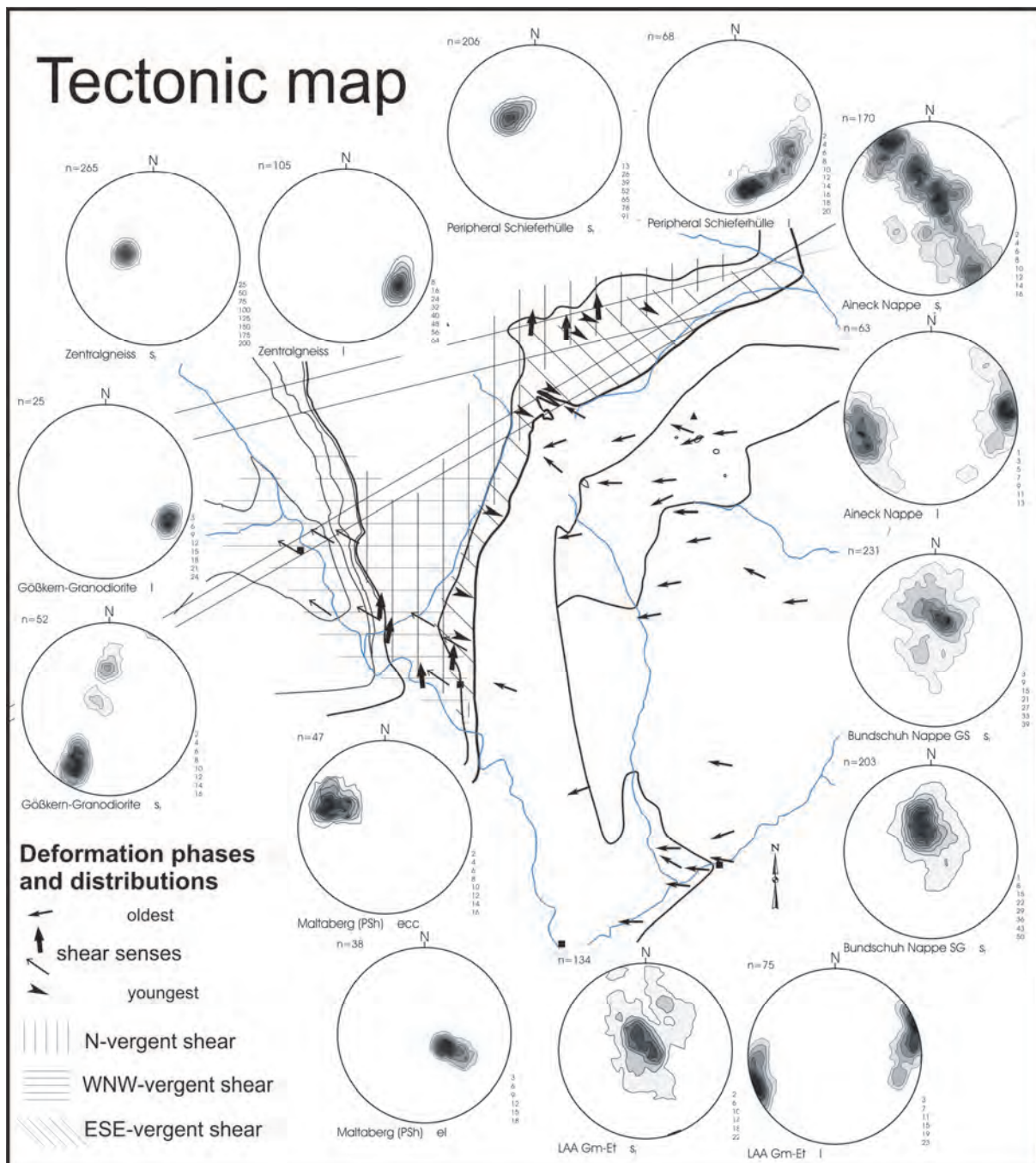


Fig. 29: Tectonic map showing the spread of deformation structures, shear senses, and plots (equal area, lower hemisphere) of foliations and lineations.  $s_f$  and  $l$  are the penetrative foliations and stretching lineations,  $ecc$  and  $el$  extensional crenulation cleavage and related extensional lineation, respectively.

In deeper Penninic units, this deformation preceded the temperature peak, but occurred at higher pressure conditions than those of the metamorphic peak. This deformation started within the stability field of albite, even at tectonic levels that later on reached the oligoclase field during metamorphic peak conditions. Granitic gneisses affected by this deformation display the growth of white mica, with celadonite-rich cores and celadonite-poor rims, pointing to a pressure decrease during this deformation.

The next deformation phase affects almost all of the Penninic units in the investigated area and represents the main deformation phase in the mass of the Variscan granitoids. Only parts of the deeper Peripheral Schieferhüllle and also parts of the deeper basement complex remain spared. It develops a mylonitic foliation with a very consistent WNW-ESE trending stretching lineation (Fig. 29). Numerous sense-of-shear criteria, as asymmetric porphyroclasts ( $\delta$ - and  $\sigma$ -clasts), shear bands, C/S structures and quartz textures unequivocally prove shear of top-to-the WNW.

In the higher Penninic parts, especially in the Storz-Nappe, this deformation is expressed in discrete, W-dipping shear bands with WNW-ESE trending striations, without obliterating the penetrative N-S trending stretching lineation. But quartz textures, mainly oblique cross to single girdle c-axes distributions, indicating WNW-directed shearing, prove a penetrative deformation during this phase in these parts, too. In deeper parts, this deformation phase is the first penetrative event, except in country rocks of the Variscan granitoids that display pre-Alpine deformation structures (sometimes even several phases of superposed folding sealed by Variscan intrusions). Along the northern side of the Malta valley the foliation dips to the E to SE, the stretching lineations to the ESE, in the deepest exposed levels the stretching lineation keeps this very consistent plunge to the ESE, but the foliations display a great circle distribution around this lineation (Fig. 29). Across the Malta valley the foliations in the granodiorites of the Göß core dip gently to the ESE on the northern side of the valley, steeply to the NNE in the middle (Koschach) and moderately to the S on the southern side. In the central part no foliation can be defined, the rocks display apparently uniaxial extension. In the area of steep foliations pronounced stretching lineations also point to deformation in the constrictional field, but some shear criteria, as asymmetric porphyroclasts, asymmetric quartz textures, and asymmetric distributions of extensional and compressional quadrants of aplitic veins point to general non-coaxial deformation with a right-lateral sense of shear. In the granitoids of the Göß core, discordant aplitic and pegmatitic veins show a strong deformation too, although not very obvious macroscopically. It is expressed in a strong recrystallization of feldspars and quartz, mostly occurring in elongated aggregates, and strong lattice preferred orientations of quartz.

During this deformation all major rock forming minerals recrystallised dynamically. It continued until peak metamorphic conditions were reached in deeper tectonic levels. Feldspars recrystallised dynamically, with inversely zoned recrystallised grains of oligoclase, pointing to deformation at at least uppermost greenschist facies conditions.

The last main deformation event led to the exhumation of the Penninic unit. The main shearing was concentrated within a low-angle fault zone in the top of the Glockner Nappe, displacing the AA nappe stack to the ESE (Gensler and Neubauer, 1989; Elsner, 1991). Structures range from mylonitic shear zones with penetrative deformation, especially in calcschists, to the development of a discrete extensional crenulation cleavage, often as multiple sets. Other structures are extension veins and boudinage of competent rock layers. Numerous shear criteria prove shearing top-to-the-ESE. This deformation started at elevated temperatures (crystal-plastic deformation of quartz), but continued

until cool, brittle conditions under the same kinematic frame (Kurz et al., 1994, 1996). In deeper parts, flat-lying, conjugate shear zones are related to this event. Prominent examples are fine grained, cm-thick shear zones in granitoids of the Göß core, that cross-cut the main foliation. In these shear zones, feldspars, quartz, and biotite recrystallised dynamically, quartz-c-axes textures show a maximum parallel to the Y-axis. Deformation here also started near peak metamorphic conditions, but can then be followed to cool, brittle conditions within the same kinematic frame.

### 3.3. Tectonic setting and structural evolution of Austro-Alpine units

In the area of investigation (Fig. 28), the Austro-Alpine (AA) unit can be divided into three nappes: from the top to the bottom, the (1) Bundschuh Nappe, the (2) Aineck or Radenthein Nappe, and (3) the LAA Nappe (Theiner, 1987). These nappes are distinguished by distinct pre-Alpine and Alpine metamorphic conditions.

The Bundschuh Nappe comprises mainly paragneisses, micaschists and granitic gneisses and shows a two-stage metamorphic evolution. The Bundschuh Nappe shows widespread Variscan amphibolite facies metamorphism, with garnet and staurolite (Exner, 1980a). The Alpine metamorphism reached lower amphibolite facies conditions, leading to the growth of a second, Alpine garnet generation, often as rims around pre-Alpine garnet cores (Schimana, 1986; Theiner, 1987) (Fig. 30). Thermobarometry on the Alpine paragenesis yielded c. 600°C and 10 kbar for the Alpine metamorphic peak.

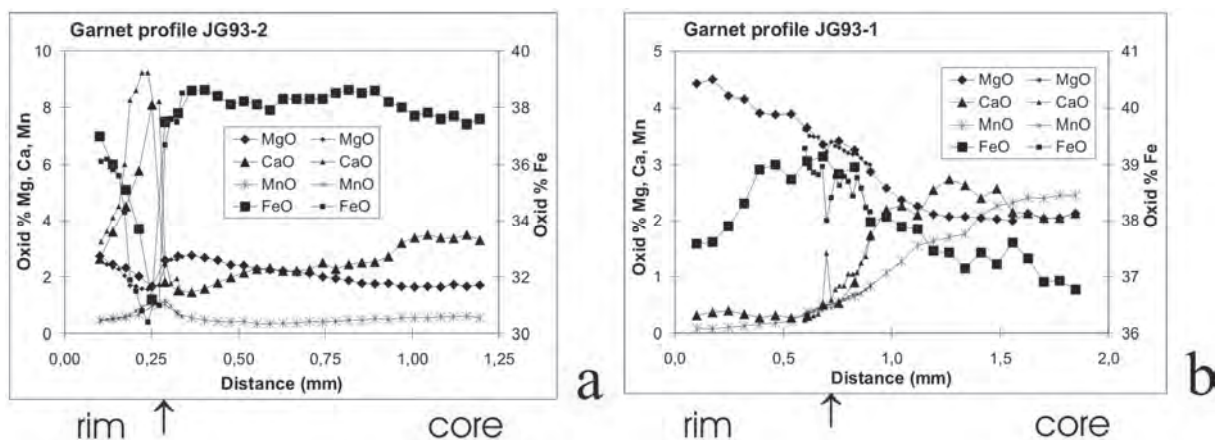


*Fig. 30: a, b) Two-phase garnets from micaschists of the Bundschuh nappe. Alpine rims are separated from Variscan cores by a strong increase in Ca and a decrease in Fe. Mg and Mn show only minor variations (boundary is indicated by arrow). Sample JG93-1 contains no plagioclase, so the break is less pronounced. Locations are shown in Fig. 28.*

The underlying Aineck Nappe includes garnet-micaschists, paragneisses, and amphibolites and shows only one peak metamorphic assemblage of upper greenschist facies conditions. Garnets typically show continuous zonations and the same suite of inclusion minerals from the core to the rim (Theiner, 1987) (Fig. 30). Thermobarometry gave conditions for the metamorphic peak of approximately 540°C and 9 kbar. The Radenthein unit that underlies the Bundschuh Nappe in the south, displays also only a single stage metamorphism, but shows somewhat higher temperatures (amphibolite facies conditions) (Schimana, 1986).

The LAA Nappe along the eastern margin of the Tauern window is only a remnant of the prominent development at the north-eastern corner in the Radstädter Tauern. There, the Lower Austro-Alpine unit consists of several nappes, build up of pre-Alpine basement slices (para- and orthogneisses, often retrogressed) and thick Permo-Mesozoic cover units of a terrestrial to shallow marine evolution (e.g., Tollmann, 1977; Becker, 1993). In this area, the only remaining nappe displays an inverted tectonic and metamorphic position with pre-Alpine relics of upper greenschist facies minerals, as e.g. garnet, in tectonic higher parts, and only lower greenschist facies conditions in deeper parts. This setting is also evidenced by a remnant Permo-Mesozoic cover sequence at the base of the unit, which is inverted too (Exner, 1971; 1982).

The main deformation event in the Bundschuh Nappe, related to thrusting, occurred prior to the metamorphic peak. This deformation is characterised by an E–W-trending stretching lineation and the transposition of a pre-Alpine planar fabric (Fig. 29). Pre-Alpine garnets are broken and pulled apart, the individual pieces overgrown by a rim of Alpine garnet. Micas show only weak alignments in the Alpine foliation, quartz has recrystallised statically as well (random lattice preferred orientations). The main deformation must have taken place in the ductile domain, however, i.e. at least within greenschist facies conditions. The thermal peak must have outlasted the thrust-related deformation, however, and annealed earlier deformation fabrics.

In the Aineck Nappe, the main deformation, again with an E–W-trending stretching lineation (Fig. 29), is pre- to syn-metamorphic. Micas are aligned in the foliation, garnets show helicitic inclusion trails and quartz various degrees of lattice preferred orientations. The main foliation is folded into upright folds around NE–SW-trending axes, with white mica of the first generation folded around fold hinges. This fabric is overprinted by a static recrystallization under lower greenschist facies conditions, with the growth of white mica, chlorite, albite, and rare stilpnomelane randomly across the older fabric. The main deformation must thus have occurred under upper greenschist facies conditions, followed by a phase of cooling and folding of the main foliation. The static overprint happened under lower greenschist facies conditions, most likely driven by fluid infiltration.

The nappe contact between the Bundschuh Nappe and the Aineck Nappe is cut by the basal thrust that carried the two units on top of the LAA Nappe (Fig. 28). Thrusting must thus post-date the internal imbrication within the MAA units.

The LAA Nappe shows the same E–W-trending stretching lineation as the Bundschuh Nappe and the Aineck Nappe (Fig. 29), but the main deformation occurred under lower greenschist facies conditions. Quartz was deformed by low-temperature plasticity and shows lattice preferred orientations typical for cool deformation conditions. Pre-Alpine garnets are mostly chloritised and deformed into elongated ellipsoids. White micas are frequently rotated into the main Alpine foliation, but also occur in microlithons, tracing an older foliation.

### 3.4 Ar/Ar mineral data

Single grain  $^{40}\text{Ar}/^{39}\text{Ar}$  laser probe (step-wise heating) dating was carried out on white mica, biotite, and amphibole across the Penninic–Austro-Alpine suture at the eastern margin of the Tauern Window in order to constrain the timing of the main Alpine deformation events that led to the juxtaposition of the regarded units. Selected age data for white mica are presented in Fig. 31.

The Bundschuh Nappe, mainly deformed prior to the metamorphic peak of lower amphibolite facies conditions, yielded an integrated age of  $107.5 \pm 1.3$  Ma for muscovite, giving a minimum age for the

main deformation. The next deeper unit (Aineck Nappe), deformed close to the metamorphic peak of slightly lower temperatures, gave an integrated age of  $83.5 \pm 2.3$  Ma for white mica of the peak metamorphic assemblage. White mica of a second generation, grown due to a static, fluid-driven metamorphic overprint, gave ages of  $80.8 \pm 6.1$  Ma. The static metamorphic overprint of lower greenschist facies conditions in the Aineck Nappe should be constrained in time by the age of the second generation of muscovite, as the temperature of this event is below or at about the closure temperature of muscovite. The cooling age of Mu I (110) of c. 85 Ma gives a lower age limit for the penetrative deformation in the Aineck Nappe, related to the W-directed nappe stacking process. From these data a short time interval between cooling from the metamorphic peak (Mu I, sample 110) and the static metamorphic overprint (Mu II, sample 106) can be deduced, as the ages are the same within the  $2\sigma$ -error limits. A common cause for cooling from the peak metamorphic conditions, for shortening, expressed in the folding of the penetrative foliation at already cooler conditions, and for the subsequent static metamorphic overprint by fluid infiltration can be the thrusting of the Aineck Nappe onto a cool, fluid-rich unit. This could be the LAA unit, derived from the continental margin, on the one hand and the oceanic South Penninic unit on the other hand. The LAA contains mainly low-grade metamorphic pre-Alpine basement rocks and a Mesozoic, carbonate shelf cover sequence that should be rather depleted in fluids in comparison with the shaly-marly deep sea sequence of the South Penninic unit. Also the retrogressive overprint of the LAA with chloritization of garnet needs external fluid sources. These fluids, infiltrating the base of the MAA, are therefore most likely derived from the South Penninic unit, and give a possible age constraint on the subduction of the South Penninic ocean beneath the AA continental margin.

The deepest, Lower AA Nappe, yielded Variscan white mica ages ( $242.9 \pm 2.2$  and  $239.6 \pm 1.1$  Ma) from tectonically high levels and strongly disturbed ages of c. 100 Ma from the base. Alpine metamorphic conditions were obviously too low to reset the Ar-system of white mica completely, consistent with the observed deformation conditions and metamorphic assemblages. From the presented data no direct time constraint on the deformation of this unit can be given, but if no marked inverted thermal gradient existed during deformation, the Alpine deformation must be younger than the 85 Ma of Mu I of the overlying Aineck Nappe (sample 110). Thermal models indicate that in shallow to medium crustal levels, that are appropriate for the burial of the LAA in this area, no inverted thermal gradients occur at reasonable thrusting rates (Genser et al., 1996). Additionally, the age sequence with cooling of the higher nappe well before cooling of deeper levels indicates that no inverted geothermal gradient existed during nappe stacking within the exposed crustal levels. The observed inverted metamorphic gradient in the AA edifice must therefore be attributed to the late to post-metamorphic transport of those nappes over deeper ones.

For the LAA Nappe in this area, no pressure data are available that could constrain its burial depths. Its position at the base of the AA nappe complex, however, points to burial depths that are in the same order as for the overlying units. This would imply reduced geothermal gradients during underthrusting of the LAA, a scenario that could be met in an oceanic subduction zone environment. Beginning subduction of the SP oceanic lithosphere, together with the leading edge of the AA continental margin that is deformed into the LAA nappe complex, and fluid infiltration of the base of the MAA, fit into this scenario (Kurz et al., 1996). Tectonic inversion of the continental margin, as presently exposed, at the beginning of oceanic subduction conforms, too. We thus correlate the underthrusting of the LAA with the beginning of subduction of the SP ocean rather than with the end, as proposed by Slapansky and

Frank (1987), who connected it with the collision of the AA and the MP units. It is constrained in time by the second generation of muscovite in the Aineck Nappe at about 80-85 Ma.

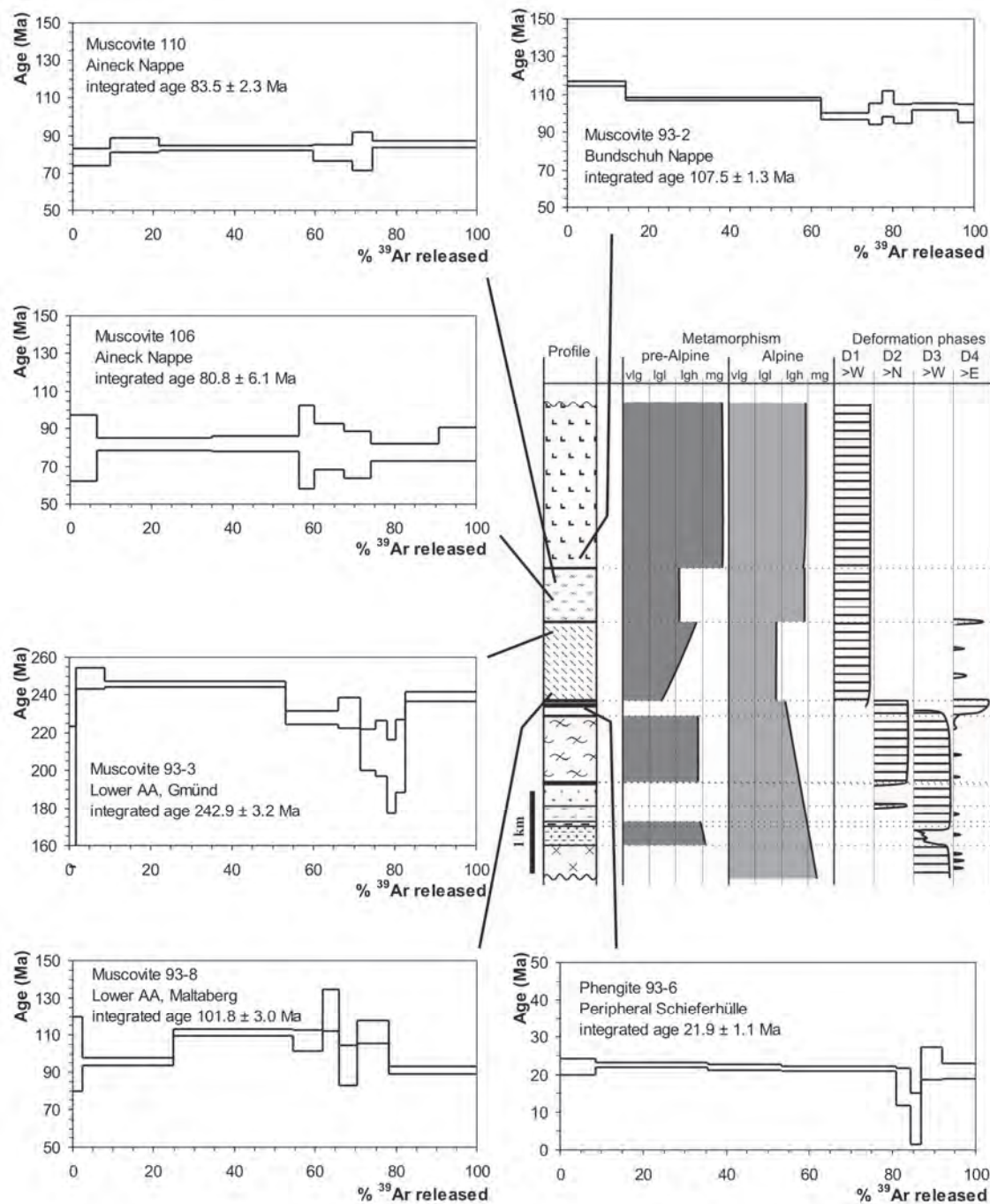


Fig. 31:  $^{40}\text{Ar}/^{39}\text{Ar}$  age diagrams of single grains of white mica and profile of the tectonic units at the eastern margin of the Tauern window. Distributions of pre-Alpine and Alpine metamorphic conditions (vlg: very low grade, lgl, lgh: low grade, mg: medium grade) and parts affected by the main deformation phases are given. For location of samples see also Fig. 28.

A white mica from tectonically high parts of the Penninic unit, showing a normal metamorphic gradient of greenschist facies conditions, yielded an age of  $21.9 \pm 1.1$  Ma. The flat age spectra record the cooling of the Peripheral Schieferhülle through c.  $400^\circ$  C. The second penetrative deformation event in the Penninic units, the WNW-directed shearing that occurred on the heating path and at thermal peak conditions, that were higher than the closure temperature of phengite, must thus precede these ages. This deformation event should thus be Late Oligocene (Cohen et al., 2013) in age. The cooling age of 22 Ma gives the onset or an upper age constraint for the ESE-directed shearing, as structural features (e.g. low-temperature plasticity of quartz, calcite twinning) indicate that this deformation started at lower greenschist facies conditions at these tectonic levels, hence at or below the closure temperature of this system. The resulting differential uplift of the Penninic unit should continue to c. 16.5 Ma, the cooling ages of biotite (Rb/Sr) across the centre of the Hochalm Dome (Cliff et al., 1985).

### 3.5. Discussion

Structural, metamorphic and age data demonstrate distinct Alpine evolutions for the Austro-Alpine and Penninic units. Thrusting in the Austro-Alpine units is generally towards the W, following by folding around E-W to NE-SW trending axes. This thrusting occurred over an extended time-span. The Alpine thrusting in the highest unit (pre-metamorphic) and the subsequent cooling from the highest greenschist to lower amphibolite facies to about  $400^\circ$  C predates 100 Ma. In the next lower unit, thrusting could have persisted until ca. 85 Ma. Nappe stacking must have propagated from the hangingwall to the footwall, therefore, incorporating successively more external and deeper units.

The attainment of higher peak temperatures in higher nappes of the Austro-Alpine unit and the subsequent thrusting onto progressively cooler units of the same mega-unit points to a continuous accretion of parts of the footwall to the hangingwall in the stacking process. Thus thrusting could be explained by an intra-Austro-Alpine subduction. This progressive accretion can also explain the observed inverted metamorphic gradient, without need to invoke inverted temperature gradients.

The beginning of subduction of the oceanic Penninic lithosphere could be dated by the second generation of white mica at the base of the Austro-Alpine unit, that grew due to fluid infiltration. The ages of 80 – 85 Ma indicate a possible interference between intra-Austro-Alpine thrusting and commencing subduction of the Penninic ocean beneath.

In the Penninic units, three distinct deformation stages can be distinguished, that can be found in a very consistent manner over the entire Tauern window (Kurz et al., 1996). The oldest deformation is a shearing top-to-the N to NE, and is found especially the South Penninic Glockner nappe and the underlying gneiss nappes. This event is followed by a shearing top-to-the WNW that affected most of the units, particularly the deeper parautochthonous Zentralgneis unit. The main deformation in the higher Penninic parts, related to their subduction and intra-Penninic stacking is pre- to synmetamorphic. Hence the oldest ages from that unit of about 30 – 32 Ma, already cooling ages, give a minimum age for N-directed shearing, the oldest, ductile deformation. The ages of about 22 Ma place a lower age limit on the WNW-directed shearing, occurring at about peak metamorphic conditions, and an upper age constraint on the subsequent ESE-directed, extensional shearing. K/Ar ages from 22 to 17 Ma for white mica are common along the central dome of the eastern Tauern window, biotite Rb/Sr ages are very uniform at about 15.5 - 17 Ma (Cliff et al., 1985). These ages point to rapid exhumation of the Penninic units from depths of 25 to 20 km to near to the surface in this time span (Cliff et al., 1985). This rapid exhumation was enabled by the tectonic unroofing of the Tauern window along the low-angle normal faults along the Penninic–Austro-Alpine interface. Laterally, the window is

bound by sinistral strike-slip faults, indicating that extension subparallel to the orogen took place in a wrench regime (Genser and Neubauer, 1989; Kurz and Neubauer, 1996).

Thermal modelling of the metamorphism in and around the Tauern window by Genser et al. (1996) also substantiates an independent Alpine evolution of the Penninic and Austro-Alpine units, respectively. A model, where subduction of the South Penninic ocean commenced after the main nappe stacking in the Austro-Alpine unit (Fig. 32), give P-T-t paths, that are in accordance with petrological and thermochronological data (Fig. 27). Models that relate compression and metamorphism in the Austro-Alpine to subduction of the South Penninic ocean and its subsequent collision with the Middle Penninic continental block are grossly inconsistent with these constraining data. A sketch of our preferred model of the relative and absolute timing of the major events is given in Figure 32.

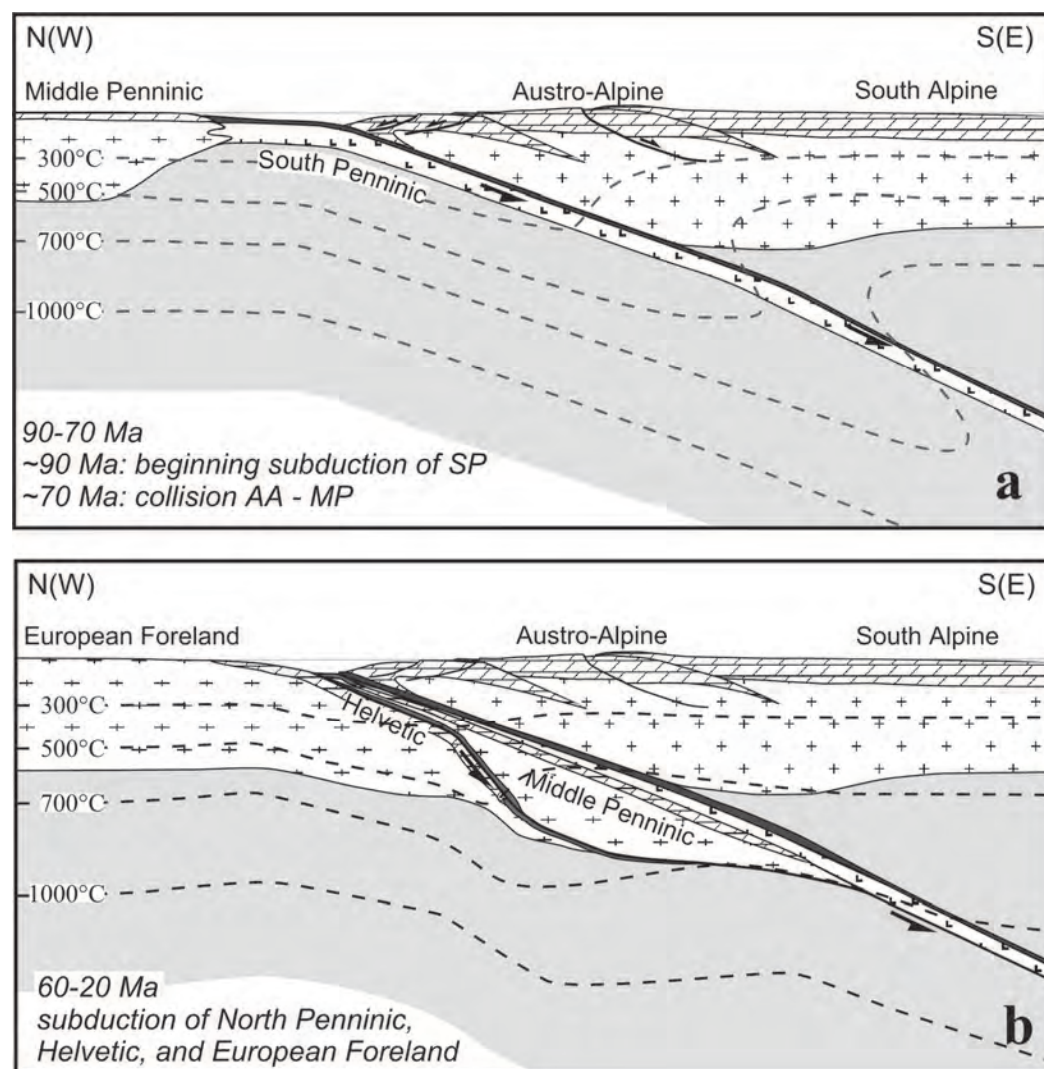


Fig. 32: Thermo-tectonic model for the subduction of the Penninic and Helvetic units beneath the Austro-Alpine hangingwall plate (from Genser et al., 1996).

### 3.6 Stops

#### **Stop 2-1: Greenschists and calcschists of the Glockner nappe.**

Location: N47° 08' 17.2" E13° 32' 06.6"; ÖK 50, sheet 156 Muhr; national road at highway bridge at Kraglau, c. 1.2 km SE of Zederhaus village.

Greenschists and calcschists of the Glockner nappe, which represent metamorphic volcanics (mainly basic tuffs) and sediments (mainly marls), respectively, which were deposited on an oceanic basement.

#### **Stop 2-2: Graphitic phyllites with dolomite clasts of the Nordrahmenzone**

Location: N47° 10' 27.7" E13° 26' 56.6"; ÖK 50, sheet 156 Muhr; national road at highway bridge c. 1 km SE of highway tunnel.

Biotite phyllites with cm thick layers of graphitic quartzites and massive clasts of unfoliated dolomite, several metres to deca-metres thick. This unit belongs to the Matrei zone (Nordrahmenzone) and is interpreted to represent the trench fill during subduction of the Penninic ocean (Frisch et al., 1987).

#### **Stop 2-3: Ductile to brittle low-angle normal faulting to the ESE in the Peripheral Schieferhüllle.**

Location: N46°57'34.4"N, E13°30'18.7" to N46°57'33.5"N, E13°30'32.0"; ÖK 50, sheet 182 Spittal an der Drau; road cut from second turn at elevation 1010 m upwards on the road Malta – Maltaberg. From Malta village by car (difficult access by big bus) or on foot (ca. 25 minutes to walk).

This roadcut exposes a succession from the uppermost Storz Group (Vavra & Frisch, 1989), a pre-Variscan basement unit, here mainly amphibolites and plagioclase gneisses, overlain by the post-Variscan sequence of the Peripheral Schieferhüllle. The latter sequence starts, approximately 70 m after the crossing path, with black albite porphyroblast schists. Then follow whiteschists, strongly retrogressed orthogneisses, and quartzites of probably Permo-Triassic age, and finally calcschists with intercalated greenschists and metapelites, the so called Bündner Schiefer, Jurassic-Cretaceous deep-sea metasediments and -volcanics. A detailed description of this section can be found in Exner (1980b), of structures in Genser and Neubauer (1989). Alpine metamorphic parageneses comprise:

Quartz-albite-phengite-phlogopite-calcite-ilmenite (quartzites)

Albite-quartz-phengite-biotite-chlorite-calcite-ilmenite (semipelites)

Calcite-quartz-albite-muscovite-rutile-chlorite (calcschists)

Amphiboles-chlorite-albite-epidote-quartz-titanite-biotite-calcite (greenschists)

Two structural events can be distinguished in these outcrops:

1) A penetrative foliation with an only weakly developed stretching lineation. The foliation dips moderately to the ESE, the lineation trends NNE-SSW. These structures can best be seen in the rocks of the Storz Group, in higher units they are strongly overprinted by the second deformation. In deeper parts of the Storz unit and in more northerly parts of the Peripheral Schieferhüllle, where these structures are often well preserved, a tectonic transport of top-to-the N can be derived. This deformation occurred close to metamorphic peak conditions.

2) The second deformation led to a further flattening of the older foliation and an extension in an ESE-WNW-direction. The deformation is noncoaxial, expressed in ESE-dipping shear bands, which often occur in multiple sets with different dip angles. A conjugated, WNW-dipping set of shear bands is only weakly developed and restricted to strongly deformed domains. Lineations on the shear bands plunge

to the ESE and WNW, respectively. In calcschists zones with a new mylonitic foliation, angular to the older foliation, develop. This structures, as well as asymmetric calcite-c-axes textures, prove a dominant normal shear of the hanging-wall to the ESE. Other structures related to this extension are extension veins and boudins, mainly in competent quartzites. Small-scale, asymmetric folds that are overturned to the ESE are related to this shearing, too.

This deformation commenced after metamorphic peak conditions, as evidenced by greenschist facies minerals (chlorite, epidote) in shear zones in amphibolites and continued to cool conditions up to the formation of brittle normal faults. The main part of this deformation is ductile, however.

This deformational event, a low-angle normal faulting, led to the unroofing of the metamorphic dome of the Tauern Window by displacement of the Austro-Alpine upper crust to the ESE.  $^{40}\text{Ar}/^{39}\text{Ar}$  dating of a single phengite grain from the quartzites yielded a plateau age of  $21.9 \pm 1.1$  Ma. This age should give the age of cooling below ca. 375 °C and hence an upper limit for the low-angle normal faulting. This event must be placed in the lower Miocene, hence. This is also corroborated by data from Cliff et al. (1985), which indicate nearly isothermal decompression and a following rapid cooling of the Penninic units in the time span between 20 and 16 Ma.

#### **Stop 2-4: Granodiorite of the Göß core**

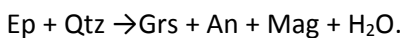
Location: N46°58'45.3", E13°27'44.5"; ÖK 50, sheet 182 Spittal an der Drau; quarry Koschach.

Gmünd-Malta-Koschach (bridge across the Malta river)

In the Göß valley the structurally lowest units of the eastern Tauern Window (and also the Eastern Alps) are exposed (Göß core). It consists mainly of different orthogneisses, ranging from granites to tonalites that represent deformed Variscan granites (intrusion ages of ca. 320 Ma according to Cliff and Cohen, 1980). These orthogneisses are separated from the orthogneisses of the Hochalm core by a paragenetic series. In the Koschach quarry, a strongly lineated, light grey granodioritic augengneiss that is crosscut by several generations of pegmatites to aplites, is exposed.

The magmatic paragenesis of the granodiorite comprises plagioclase, K-feldspar (Karlsbad twinning), quartz, biotite, titanite, allanite, epidote, zircon, and apatite. Geochemically, the rocks resemble Na-rich, high K calc-alkaline I-type granitoids, in part featuring almost trondhjemite affinity (Marschallinger and Holub, 1991). Trace elements show VAG characteristics with selective enrichment of LIL elements and low Rb/Zr.

The Alpine metamorphic paragenesis includes oligoclase, K-feldspar, quartz, biotite, clinozoisite(epidote), garnet, magnetite and sphene. Oligoclase displays inverse zoning (c. An<sub>15</sub> in center to An<sub>25</sub> at rim), K-feldspar is marginally replaced by myrmekite. Garnet formed due to the general reaction



In this outcrop, one can distinguish 3 main deformational events:

1) The main deformation is responsible for the formation of the penetrative foliation and the pronounced lineation of the orthogneisses. Pegmatite veins are sometimes folded due to this deformation, older aplitic veins mostly not, pointing to low viscosity contrasts during deformation. The strain distribution is generally very homogenous. The dominant stretching lineation indicates constrictional deformation geometry, corroborated by quartz-c-axes distributions (type I crossed girdles). In the Koschach quarry, the foliation dips steeply to the NNE (30/70), on the southern side of

the Malta valley to the S (180/40), on the northern side to the ESE. The poles to the foliation hence display a great circle distribution around the stretching lineation (120/20), which is very consistent over the whole area. This distribution we interpret also to have formed in the constrictional deformation field, and not due to later folding. Shear criteria that are mostly only weakly expressed and quartz-c-axes distributions indicate a non-coaxial deformation path with a dextral shear component. This deformation occurred at elevated temperatures up to the Alpine metamorphic peak, with dynamic recrystallization of plagioclase, K-feldspar and quartz.

This deformation event must be placed in Oligocene times, based on radiometric dating of the metamorphic peak at about 20 Ma in deep tectonic levels of the eastern Tauern Window by Cliff et al. (1985).

2) Conjugate, ductile shear zones that are a few mm to cm wide, cut discordantly across the penetrative foliation. These shear zones dip to the ESE and WNW, and show a normal sense of shear to the ESE and WNW, respectively. This deformation led to a subvertical shortening and ESE-WNW-directed extension, therefore. In the shear zones, plagioclase, quartz, and biotite recrystallised, green amphiboles and calcite, respectively, formed. This indicates an activity of these structures at still elevated temperatures (upper greenschist to lower amphibolite facies conditions). This ESE-WNW extension is related to the uplift of the Penninic units.

3) Steeply dipping, ESE-WNW-trending faults (parallel to the main foliation) that show a normal sense of shear of the northern hangingwall indicate an extension in NNE-SSW direction, too. They were active from near peak metamorphic conditions (asymmetric folding of biotite schists and aplites, with static recrystallization of biotite after this deformation) to cool conditions (slickensides, cacirites, fault gouges).

## 4 The Nock area: tectonic evolution of the Gurktal Extensional Allochthon, Eastern Alps

FRANZ NEUBAUER, JOHANN GENSER & OLIVER STAUBER

**Aim:** The main aims of examining the north-western boundary of the Gurktal nappe complex overlying there the Mesozoic cover units (and the underlying Bundschuh basement are:

- (1) to look for the arguments for the Cretaceous nappe structure and, therefore, for the controversy on tectonic reconstruction of Middle vs. Upper Austroalpine units,
- (2) and to examine the subsequent Late Cretaceous extensional tectonics, which is ignored in many recent reconstructions.

### 4.1 Introduction

The nature and extent of Alpine thrusting of the Gurktal nappe complex, which is part of the Upper Austroalpine nappe complex, represents one of the most controversial topics of geology of Eastern Alps (Clar, 1965 and Frank, 1987 vs. Tollmann, 1975, 1987).

### 4.2 Austroalpine units east of the Tauern window

East of the Penninic Tauern window, all major Austroalpine units are exposed in the classical Bundschuh area where Holdhaus (1921) argued for an intra-Austroalpine nappe structure based on the discovery of Late Triassic fossils (Fig. 33). Here, the Austroalpine units comprise, from footwall to hangingwall (Tollmann, 1977; von Gosen, 1989a; Koroknai et al., 1999; Schuster and Frank, 1999):

(1) the Radenthein micaschist complex (RMC), a basement complex constituting the Radenthein nappe; (2) the Bundschuh nappe including the Bundschuh complex (BC), a gneissic, pre-Permian basement unit, and a Permian to Mesozoic cover sequence (Pistotnik, 1973/74; here coined as Stangalm Group); the Radenthein and Bundschuh nappes are classically interpreted to represent part of the Middle Austroalpine units in the sense originally defined by Tollmann (1977 and references therein); (3) the Murau nappe with a phyllitic Paleozoic basement; and (4) the Stolzalpe nappe also with a phyllitic Paleozoic basement (e.g., Neubauer and Pistotnik, 1984), and Late Carboniferous to Triassic cover sequences (Kristan-Tollmann & Tollmann, 1964; Pistotnik, 1973/74; Krainer, 1987, 1989).

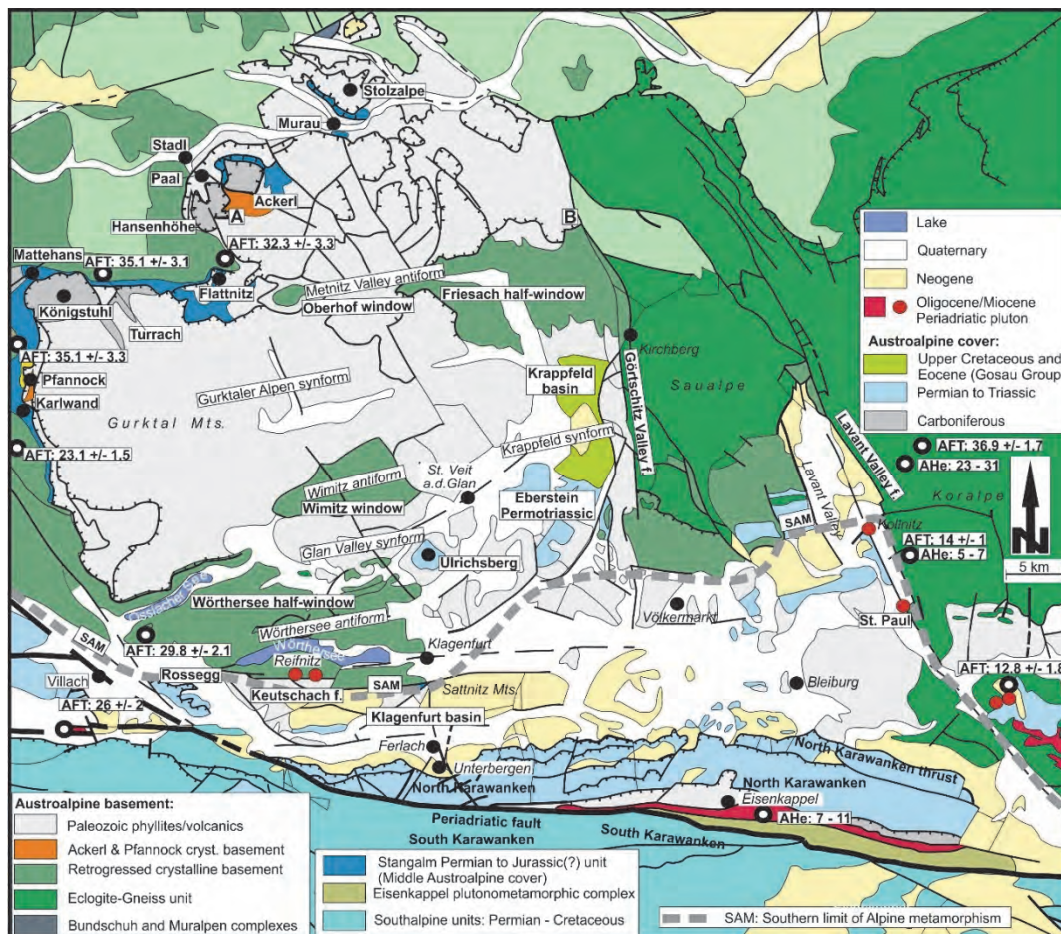


Fig. 33: Simplified geological overview map the Gurktal nappe complex and neighbour units. Late-stage structures and thermochronologic ages are shown, too. AFT – apatite fission track ages, AHe – (U-Th)/He ages. Note also gently late-stage folding of the whole region. Modified after Neubauer et al. (2018), where also data sources can be found.

Furthermore, a post-Variscan angular unconformity below the Lower Triassic Stangalm Quartzites (Pistotnik, 1976) proves the preservation of style and orientation of Variscan structures in the Bundschuh basement unit (see below). Lithostratigraphic peculiarities of the Stangalm Group in comparison to Upper Austroalpine strata include (Figs. 34, 35): only a thin siliciclastic Permian, if any, and thin Lower Triassic quartzites (Pistotnik, 1976; Krainer, 1984), black phyllites, black calc-schists and related synsedimentary ore mineralizations of Anisian age, relatively thin Middle and Upper Triassic dolomites separated by Carnian siliciclastic beds - the latter show extreme thickness variations interpreted to result from synsedimentary normal faulting - and Jurassic cherty limestones and thin Upper Jurassic cherts (Pistotnik, 1973/74; Fig. 34). In contrast, the cover units intercalated between

the Murau and Stolzalpe nappes range from Permian Alpine Verrucano Fm., Buntsandstein-type quartzites, Anisian rauhwacke to Anisian black marble/black calcareous schists.

The Murau and Stolzalpe nappes are part of the Gurktal nappe complex (Upper Austroalpine nappe complex or Central Upper Austroalpine according to Frank, 1987 and Schmid et al., 2004) and are separated from each other by intercalated Triassic successions along northern margins of the Gurktal nappe complex. Both Murau and Stolzalpe nappes comprise a Ordovician to Devonian volcanic-sedimentary successions (Neubauer and Pistotnik, 1984; Giese, 1988). Along the western margin of the Gurktal nappe complex, the Pfannock unit represents a separate tectonic unit (Pistotnik, 1996). It comprises the Pfannock orthogneiss as the basement, and an Upper Carboniferous to Upper Triassic cover succession, which is virtually non-metamorphic (von Gosen et al., 1987; Rantitsch and Russegger, 2000). Among the cover formations, the Anisian Pfannock Fm. represents the transition between clastic Upper Carboniferous and overlying thin Permian and Lower Triassic siliciclastics and Middle-Upper Triassic carbonates (Pistotnik, 1996), which paleogeographically correlated with the Drauzug by Frank (1987). Th section is completrd by Hauptdolomite and Kössen Fm. (with the fossil locality of Holdhaus, 1921). The succession is similar to such in the Northern Calcareous Alps.

### Cover of Middle Austroalpine unit: Stangalm Group

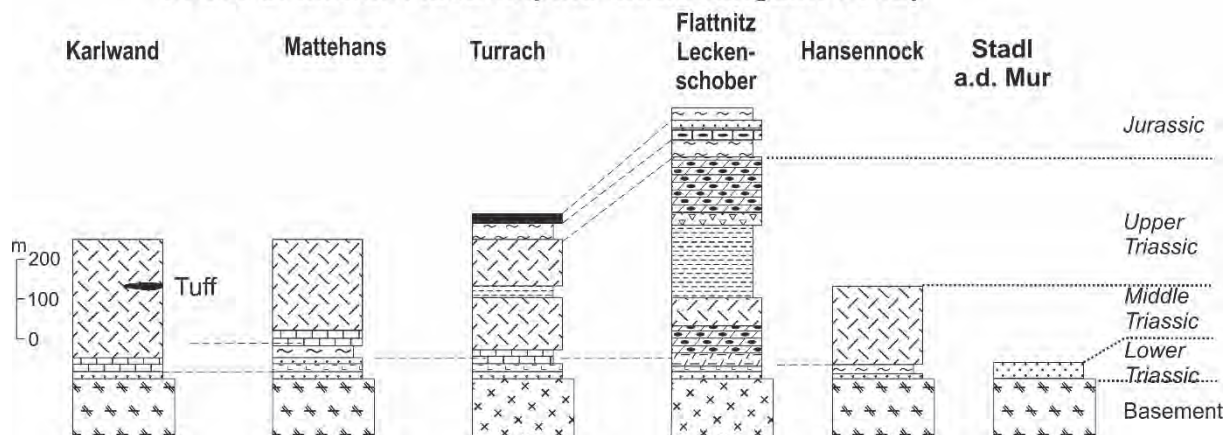
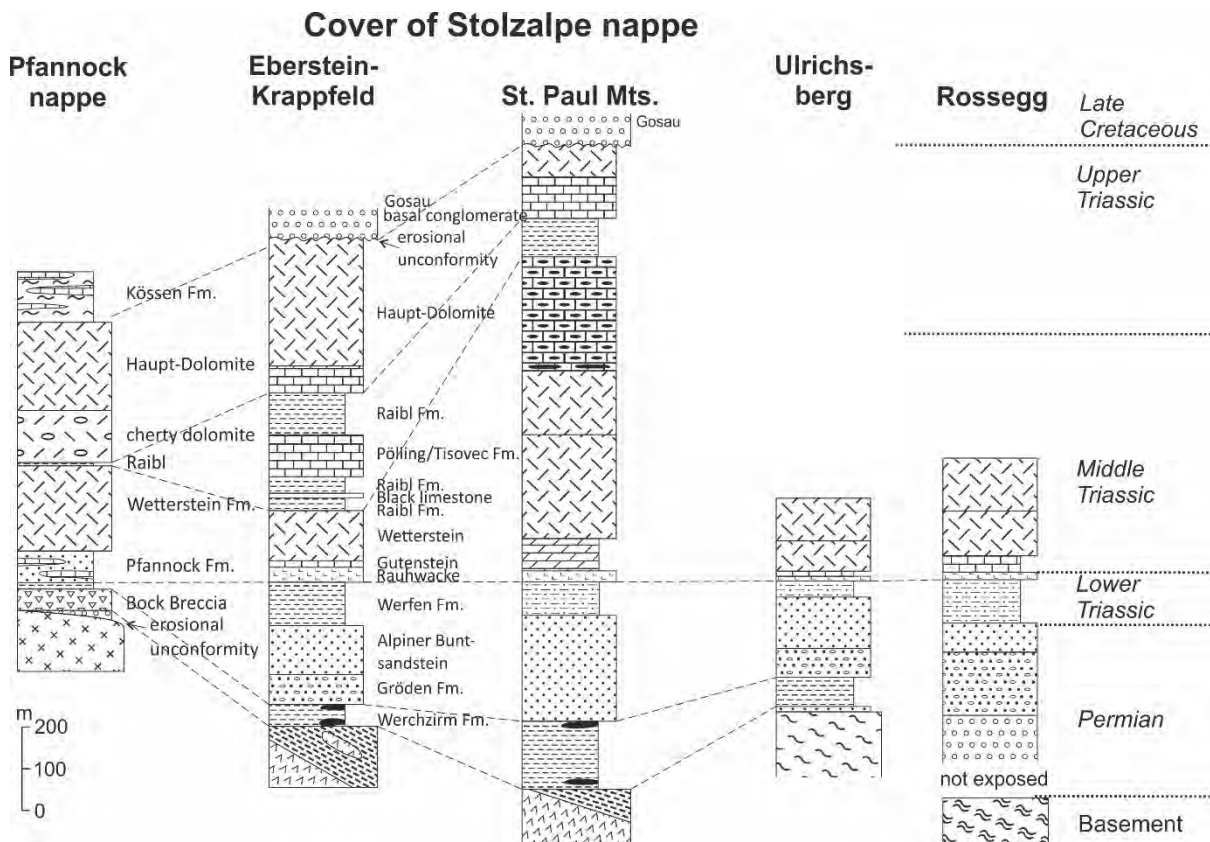


Fig. 34. The Mesozoic cover, the Stangalm Group on the Middle Austroalpine basement.

The unmetamorphic to very low-grade metamorphic cover on the overlying Stolzalpe nappe starts with the post-Variscan intramontane molasse-type uppermost Carboniferous Stangnock and thin Permian Werchzirm Formations (Fritz et al., 1990; Krainer, 1987), which is separated from other portions of the Stolzalpe nappe.

The present superposition of the Gurktal nappe complex over Middle Austroalpine units is interpreted to result from Cretaceous nappe stacking within ductile deformational conditions (Tollmann, 1977; Neubauer, 1987; Ratschbacher and Neubauer, 1989; von Gosen, 1989a; Kurz and Fritz, 2003) although there is still a wide disagreement on the nature and extent of displacement (e.g., Clar, 1965; Tollmann, 1975; Frank, 1987; Frimmel, 1986; 1988). Based on scarce shear sense criteria, a top to the W (WNW) displacement of hangingwall units was proposed (Neubauer, 1987; Ratschbacher and Neubauer, 1989; Ratschbacher et al., 1989; von Gosen, 1989a). Furthermore, many structural data favour an overprint by a second ductile phase with a general top to the ESE displacement (Neubauer, 1987), which was interpreted to represent subsequent Late Cretaceous east-directed motion due to extension

(Ratschbacher and Neubauer, 1989; Ratschbacher et al., 1989; Koroknai et al., 1999). The second event was also interpreted to be responsible for a break in Cretaceous peak metamorphic conditions between the Middle Austroalpine units and the Gurktal nappe complex (Ratschbacher et al., 1991a; Koroknai et al., 1999) and our new geochronological data clearly underline this interpretation.



*Fig. 35: The autochthonous Permian to Mesozoic cover on Pfannock nappe and Stolzalpe nappe. In comparison to the Stangalm Group, thick Permian strata predate the carbonatic Mesozoic units. Tectonically separated Upper Carboniferous to Permian successions of northwestern Stolzalpe nappe are not shown (for sources, see text).*

Based on older microfabric observations (Exner, 1980a) and garnet-biotite geothermometry, Theiner (1987) found a polymetamorphic evolution with a Variscan metamorphic overprint on the Bundschuh complex at ca. 600 – 640°C and, in nearby localities, Alpine temperatures ranging from 500 to 520°C. The age of the Bundschuh orthogneiss is Ordovician according to U-Pb zircon ages ( $462.5 \pm 6.5$  Ma; Genser Liu, unpubl. data). Previous Rb-Sr whole rock investigations resulted in sets of subparallel isochrons with model ages between 371 and 397 Ma and high initial  $^{87}\text{Sr}/^{86}\text{Sr}$  ratios between 0.721 and 0.739 (Frimmel, 1988). Geochemistry and petrography indicate a syn-collisional origin of the granites (Frimmel, 1988).

Previous geochronological data constraining the age of the metamorphic event(s) of the investigated tectonic units were published by Frimmel (1986), Schimana (1986), Hawkesworth (1976) and Schuster and Frank (1999). The minimum age of metamorphism in the Radenthein nappe is about 88–84 Ma according to Rb/Sr small-scale whole rock and mineral isochrones. K/Ar data record an Alpine age in the Radenthein and Bundschuh (Priedröf) nappes mostly in the range of 70–110 Ma. From the Wölz

micaschist underlying the Bundschuh orthogneiss, Schuster and Frank (1999) report several Sm-Nd garnet ages ranging from  $84 \pm 6$  Ma to  $100.6 \pm 6.3$  Ma. Furthermore, they report white mica and biotite K-Ar ages ranging from  $82 \pm 2$  to  $88 \pm 3$  Ma and Rb-Sr biotite ages of  $73.9 \pm 0.7$  to  $77.9 \pm 0.8$  Ma, representing cooling through appropriate closure temperatures. Rb-Sr white mica ages of the Bundschuh orthogneiss from the Innerkrems area range between  $305 \pm 12$  and  $119 \pm 1$  Ma (Theiner, 1987). The muscovite K/Ar age from the Stangalm Mesozoic cover rocks is about 70 Ma (Schimana, 1986). Rb/Sr muscovite ages from the Bundschuh orthogneiss indicate an early Variscan metamorphic event (350–354 Ma) within these rocks. The Bundschuh orthogneiss was deformed intensely during Cretaceous metamorphism and Rb/Sr mineral ages (muscovite, feldspar) were variably reset to 119 to 91 Ma (Frimmel, 1986). This was confirmed by Sm-Nd garnet data with ages at ca. 80 Ma (Schuster and Frank, 1999). Altogether, according to these data, the Radenthein and Bundschuh tectonic units were strongly affected by Cretaceous metamorphism, while pre-Alpine metamorphism is restricted to the Bundschuh basement unit.

We interpret the very thin siliciclastic successions at the base of the Stangalm Group to represent deposition on a rift shoulder - this feature contrasts with many other Austroalpine Permian to Mesozoic cover successions. We interpret the Triassic strata of the Stangalm Group to reflect extension of the rifting stage, which also enhanced synsedimentary Early Anisian iron mineralizations potentially related to normal faults as well as a second stage of extension during Early Carnian.

The Upper Carboniferous to Triassic cover successions of the GNC are dissimilar to those of the Drauzug unit, which exposed to the SW of the GNC, and resemble those of the westernmost Northern Calcareous Alps. The new data makes it necessary to reconsider currently popular paleogeographic and tectonic models of the Austroalpine domain. The term Drauzug-Gurktal nappe system should be dismissed because: (1) the Drauzug unit does not represent a nappe in contrast to the GNC, (2) the palaeogeographic dissimilarities of Permian and Triassic successions, and (3) eastern palaeogeographic extension of the Drauzug unit in the North Karawanken thrust sheet overlying there the southern margin of the GNC.

#### 4.3 Stops

##### **Stop 2-5: Middle Austro-Alpine basement with Priedröf micaschist/paragneiss and Bundschuh orthogneiss; Alpine metamorphic overprint.**

**Location:** N46° 57' 46.8" E13° 43' 41.4"; ÖK 50, sheet 50, sheet 183, Radenthein; road exposure along the Nockalm road in the Heiligenbach valley, ca. 400 metres South of the custom-house at Innerkrems.

Both the Priedröf micaschist/quartzitic paragneisses (footwall) and the Bundschuh orthogneisses (hangingwall) are exposed along the Nockalm road and along the opposite wall of the valley. The Priedröf micaschist/paragneiss essentially contain quartz, feldspar, biotite, muscovite, garnet and rare pseudomorphs after staurolite. The Bundschuh orthogneiss is composed of K-feldspar porphyroclasts, quartz, plagioclase and light-greenish white mica.

Theiner (1987) found a polymetamorphic evolution with a Variscan metamorphic overprint in nearby localities with ca. 600 – 640 °C and Alpine temperatures ranging from 500 to 520 °C based on garnet-biotite geothermometry. The age of the Bundschuh orthogneiss is uncertain. Rb-Sr whole rock investigations resulted in sets of subparallel isochrons with model ages between 371 and 397 Ma and high Sr<sub>0</sub> ratios between 0.721 and 0.739 (Frimmel, 1988). White mica of the Bundschuh orthogneiss from the Innerkrems area range between  $305 \pm 12$  and  $119 \pm 1$  Ma (Theiner, 1987). Geochemical and

petrography indicate a syn-collisional granites (Frimmel, 1988). The first age is interpreted to be close to the time of Variscan metamorphism, the second age as result of Cretaceous resetting of the Rb-Sr isotopic system.

Both lithologies contain an ESE plunging stretching lineation. Shear criteria suggest both a first top WNW shear and a later, semiductile ESE displacement.

**Stop 2-6: Bridge Postmeister Alm. Primary base of the Stangalm Mesozoic sequence.**

Location: N46° 56' 48.6" E13° 43' 58.9"; ÖK 50, sheet 183, Radenthein; road exposure along the Nockalm road in the Heiligenbach valley, E of bridge E PostmeisterAlm.

The outcrop exposes the primary contact between the basement (micaschist) and the transgressively overlying Quartzite (Lower Triassic, previous "Skythian" stage; Fig. 36). The basement micaschist displays open folds, which are discordantly overlain by quartzites of suggested Lower Triassic age. The quartzite represents the basal formation of the Stangalm Mesozoic sequence. Hangingwall sectors of the quartzite are well foliated and display an E-dipping foliation. New sericite is grown on the foliation plane. A new  $^{40}\text{Ar}$ - $^{39}\text{Ar}$  age of a concentrate of a few grains yielded a plateau age of ca.  $89.0 \pm 0.6$  Ma.

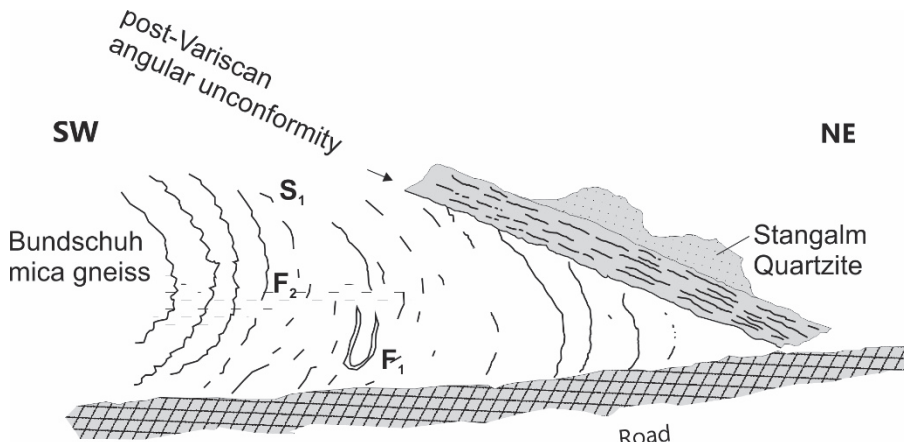


Fig. 36: Sketch showing the structural relationships between folded micaschists the Buntschuh basement and thin quartzites at the base of the Stangalm Group.

**Stop 2-7: Ductile low angle normal fault at the tectonic boundary between the Stangalm and Pfannock Permo-Mesozoic sequences and the Gurktal thrust system.**

Location: N46° 56' 33.2" E13° 45' 40.3" and N46° 56' 07.3" E13° 45' 32.8"; ÖK 50, sheet 183, Radenthein; Nockalm road. Park your car at the Eisentalhöhe parking place.

Follow the path to the Eisentalhöhe (exposure of Hauptdolomite and Kössen Formation of the Pfannock slice of the Gurktal Nappe Complex). Follow ridge from the Eisentalhöhe to the west, which exposes the phyllonite zone and the underlying dolomite marble of the Stangalm unit. A plateau age of  $89.0 \pm 0.6$  Ma was found for newly grown white mica in the basal Lower Triassic Stangalm Quartzite exposed at the base of the Mesozoic cover succession on the Buntschuh basement.

The dolomite marbles of the Stangalm Mesozoic sequence are in part strongly foliated and lineated. The lineation plunges E and ESE. Dolomite microfabrics of the metamorphic Stangalm Mesozoic comprise symmetric as well as asymmetric fabrics indicating a mixture of coaxial and non-coaxial deformation regimes implying partitioning of shear strain. Calcite-dolomite thermometry gives a

bimodal distribution of temperatures with maxima at approx. 360°C and approx. 450°C, while a white mica concentrate gives an Ar-Ar plateau age of 96.2 ± 0.4 Ma.

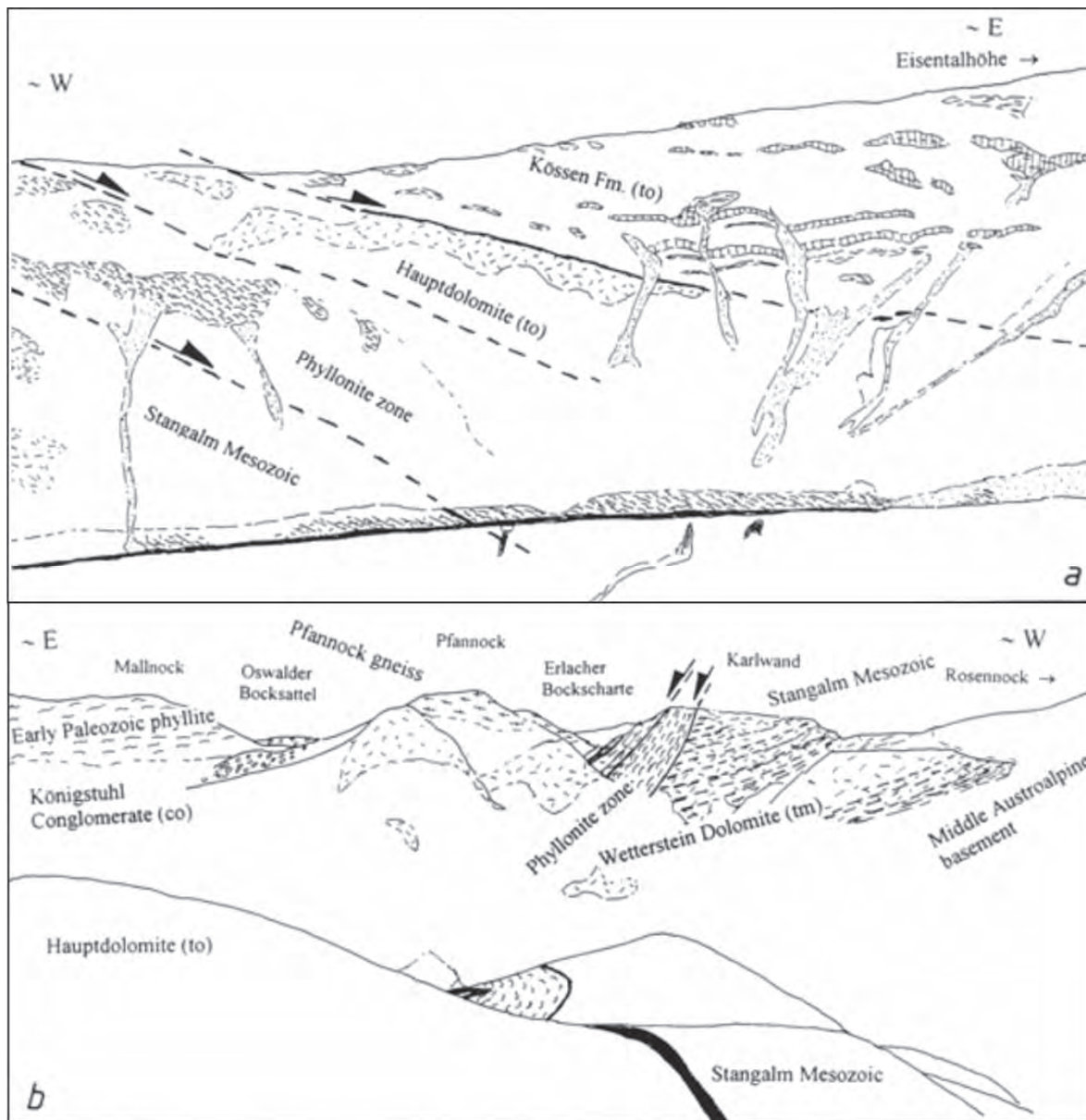


Fig. 37: View from the parking place "Eisentalhöhe" towards N displaying the low-angle normal fault contact between Middle and Upper Austroalpine structural units. a - View from the parking place "Eisentalhöhe" towards . b –View to the south displaying a high-angle normal fault contact between Middle and Upper Austroalpine structural units.

The marbles are overlain by a several tens of metres thick phyllonite, which exhibits a clearly visible extensional crenulation cleavage fabric. Sense of displacement is top to the E/ESE. The phyllonite was interpreted as Carnian Raibl Formation. But the inclusion of chlorite schists exclude this stratigraphic interpretation. This level is now interpreted as part of the Murau Nappe of the Gurktal Nappe Complex because lithological composition and continuous exposure to true Murau Nappe along the structural base of the Gurktal nappe complex.

For the first time, a plateau age of  $85.78 \pm 0.33$  Ma demonstrates the pervasive Late Cretaceous metamorphic overprint on the Murau nappe in the footwall of the regional, ESE-directed ductile detachment fault. This age is interpreted to date cooling after the throughout recrystallization of rocks composing the Murau nappe. A further white mica concentrate gives an Ar-Ar plateau age of  $87.1 \pm 0.5$  Ma (age of ductile shearing), whereas another sample gives a mixed Ar-Ar age of  $204.3 \pm 0.5$  Ma suggesting the polymetamorphic nature of the Phyllonite zone. White micas of the first sample shows a more phengitic composition than that one with the older age.

Views from the parking place to the N (Fig. 37a) and to the S show the structural contacts between various structural units (Fig. 37b).

In the hangingwall, dark Upper Triassic limestones of the Kössen Fm., which belong to the cover of the Pfannock Nappe of the Gurktal Nappe Complex, are exposed. According to Holdhaus (1921 and Kristan-Tollmann and Tollmann (1964), these limestones include in part rich faunas (e.g., *Thamnasteria rectilamellosa*, *Isoclinus bavaricus*, *Cardita austriaca*).

## 5 The “Carboniferous of Nötsch” and the pre-Alpine Gailtal basement: Significance for Alpine-Carpathian tectonics and palaeogeography

**Aim:** The aim for looking to the pre-Alpine Gailtal basement and the Carboniferous of Nötsch in the southernmost Austroalpine region is to discuss the significance of the peculiar tectonostratigraphy of tectonic units in the wider Nötsch area, which is similar to the Grauwackenzone succession of the northern Austroalpine units south of Northern Calcareous Alps. From there, these units extend also to the eastern part of Western Carpathians. These relationships to the Nötsch area show that these units were potentially rooted in that area close to the Periadriatic fault and were then thrusted towards NW or N.

### 5.1 Regional geology

Among all distinct Austroalpine tectonic basement units of Eastern Alps and Western Carpathians, the Nötsch-Veitsch-Ochtina (NVO) unit is particularly interesting because of two reasons: (1) It comprises elsewhere unknown Lower Carboniferous clastic shallow water formations overlain by Upper Carboniferous terrestrial conglomerates and sandstones, which are interpreted to represent deep to shallow marine molasse deposits following initial stages of the early Late Carboniferous Variscan orogeny (Schönlau, 1985; Krainer, 1992); and (2) the Veitsch (Eastern Alps) (Ratschbacher, 1984) and Ochtina/North Gemicic unit (Western Carpathians) (Vozárová et al., 2013) nappes containing similar strata are overlain by a pre-Variscan amphibolite-grade metamorphic basement unit and a Lower Paleozoic phyllitic basement (Kaintaleck basement; Neubauer et al., 1994, 2002), all representing tectonic units in the footwall of the Late Jurassic/Early Cretaceous oceanic Meliata suture similar as in West Carpathians.

The Nötsch area is located between the Periadriatic and the Bleiberg fault (Fig. 38), the latter being part of a major regional strike-slip fault (Drau Range South Margin fault) in the southernmost part of the Austroalpine domain (Bartel et al., 2014) subparallel to the Periadriatic fault. To the north of the the Bleiberg fault, the Drauzug s. str. (Drau Range) containing there Pb-Zn mineralizations is exposed. The Nötsch area comprises, from base to top, similar three tectonic units as the Grauwackenzone (incl. the NVO unit) in the northern part of the Austroalpine nappe complex (Figs. 38, 39): (1) the unmetamorphic Carboniferous Nötsch Group (Schönlau, 1985), (2) the retrogressed amphibolite

facies-grade metamorphic Nötsch crystalline basement ("Granite of Nötsch" of Exner, 1985), and (3) the rarely fossil-bearing (Silurian-Devonian) greenschist facies-grade metamorphic Gailtal crystalline basement (Schönlau, 1979).

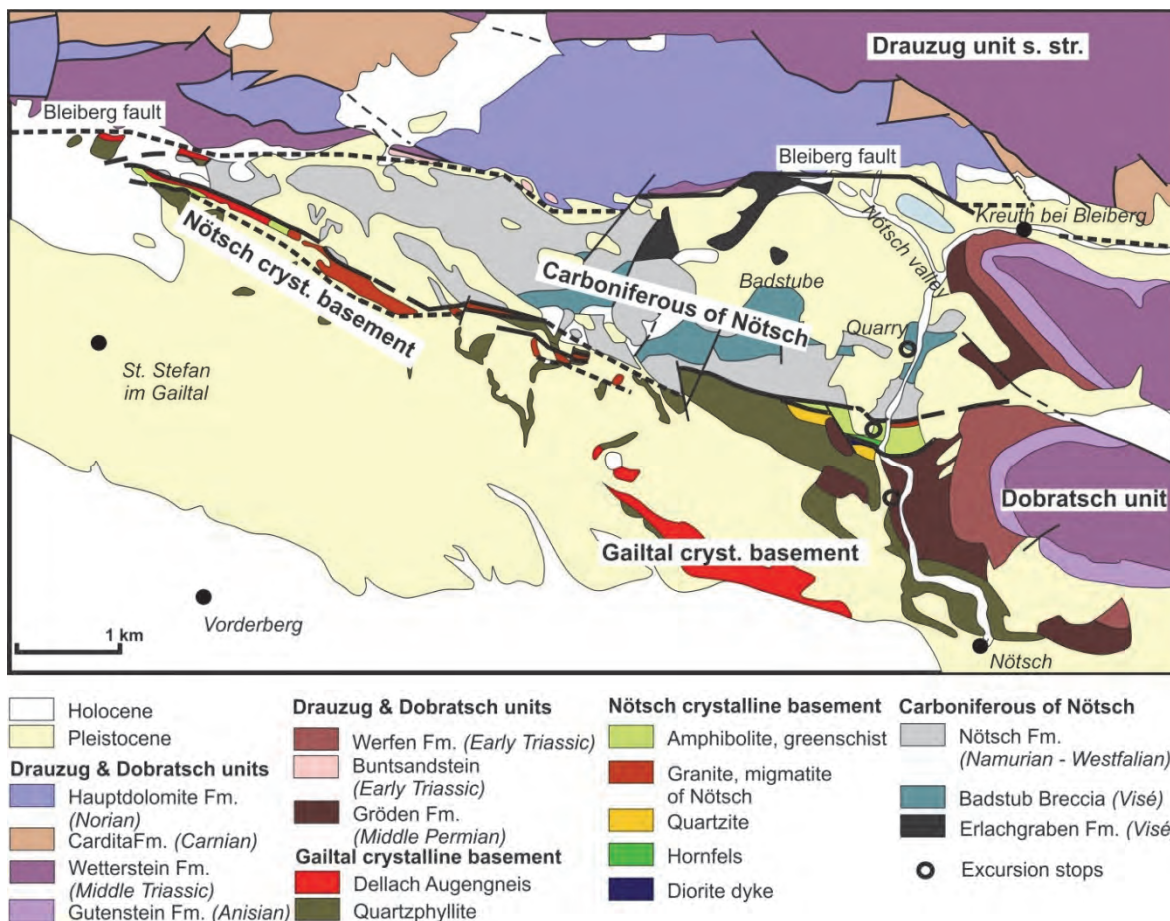


Fig. 38: Geological map of the Nötsch area (after Anderle, 1977 and Schönlau, 1989).

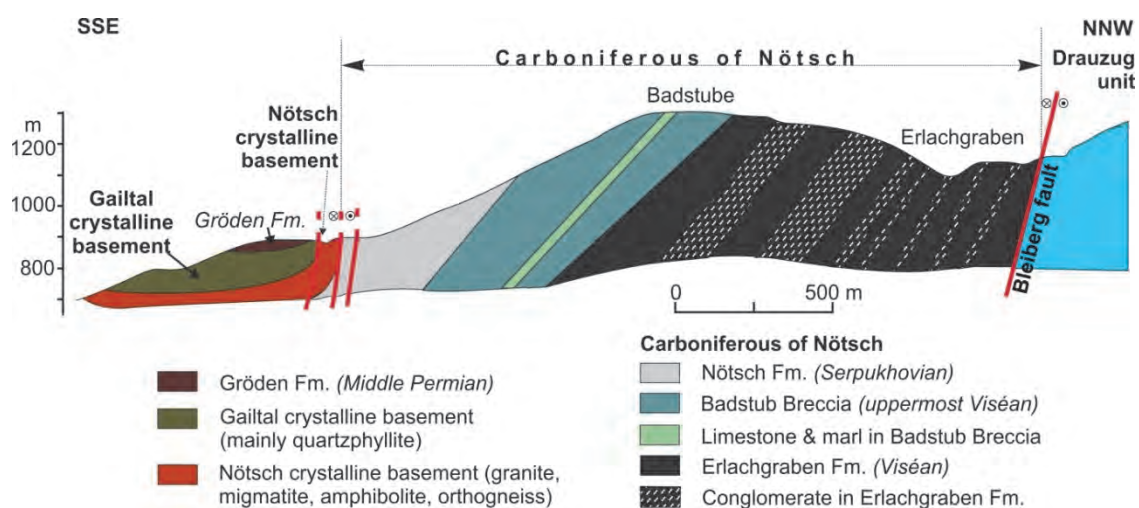


Fig. 39: Section along the western ridge of the Nötsch valley (modified after Schönlau, 1985).

The eastern Gailtal crystalline basement consists mostly of quartz-phyllite, within which Silurian conodonts were found in a marble horizon (Schönlau, 1979). According to own unpublished data, the Dellach augengneiss with the U-Pb zircon age of  $441.6 \pm 6.7$  Ma is a tectonic lens within the Gailtal basement and represents a Silurian magmatic rock overprinted by Carboniferous metamorphism (Ar-Ar sericite ages of  $321 \pm 1$  Ma to  $345 \pm 1$  Ma) and a second thermal stage with a maximum age of  $265 \pm 3$  Ma. Ductile shearing can be recognized (Fig. 40b) and we tentatively relate the Permian age to this event.

By an angular unconformity (Fig. 40f), the Gailtal crystalline basement is covered by the Gröden Fm. at the base of the Upper Permian to Upper Triassic cover of the Dobratsch. Consequently, the Gailtal crystalline basement is part of the Dobratsch unit. The cover has some distinct features, e.g. Middle Triassic volcanics and some pelagic Upper Triassic limestones making it distinct from the Drauzug s. str. north of the Bleiberg fault.

The eastern Gailtal crystalline basement consists mostly of quartz-phyllite, within which Silurian conodonts were found in a marble horizon (Schönlau, 1979). According to own unpublished data, the Dellach augengneiss with the U-Pb zircon age of  $441.6 \pm 6.7$  Ma is a tectonic lens within the Gailtal basement and represents a Silurian magmatic rock overprinted by Carboniferous metamorphism (Ar-Ar sericite ages of  $321 \pm 1$  Ma to  $345 \pm 1$  Ma) and a second thermal stage with a maximum age of  $265 \pm 3$  Ma. Ductile shearing can be recognized (Fig. 40b) and we tentatively relate the Permian age to this event.

By an angular unconformity (Fig. 40f), the Gailtal crystalline basement is covered by the Gröden Fm. at the base of the Upper Permian to Upper Triassic cover of the Dobratsch. Consequently, the Gailtal crystalline basement is part of the Dobratsch unit. The cover has some distinct features, e.g. Middle Triassic volcanics and some pelagic Upper Triassic limestones making it distinct from the Drauzug s. str. north of the Bleiberg fault.

In the underlying amphibolite-grade Nötsch crystalline basement (Figs. 38, 39, 40a), U-Pb zircon ages of  $480.3 \pm 9.4$  Ma and  $442.5 \pm 1.7$  Ma from mylonitic orthogneisses indicate a similar age of intrusion of granitoids as the Dellach augen-gneiss. However, Ar-Ar white mica ages range from  $408 \pm 2$  Ma to maximum  $430 \pm 2$  Ma constraining cooling after a pre-Variscan stage of amphibolite-grade metamorphism. Biotite and K-feldspar plateau ages are at  $344 \pm 2$  Ma to  $337 \pm 2$  Ma are overprinted by a younger event between  $213 \pm 1$  Ma and  $198 \pm 1$  Ma interpreted to result from an advanced stage of Alpine rifting. The lower boundary of the Nötsch crystalline basement is a cataclastic shear zone (Fig. 40c).

The Carboniferous of Nötsch is a famous fossil-rich very-low grade to unmetamorphic Lower Carboniferous succession with the Erlachgraben Fm. at the base, the Badstube Breccia (Fig. 40d) in middle part of the section and the Nötschgraben Fm. at the top. The nature of the contact to the overlying Permian Gröden Fm., sedimentary or tectonic, is unknown. Rich flora (van Amerom and Schönlau, 1992) and faunas (e.g., Schraut, 1999) proof an age from latest Viséan to early Bashkirian (Schönlau in Hubmann et al., 2014) of the Carboniferous of Nötsch. Recently, Vachard et al. (2018) described limestone clasts within the Badstube Breccia, reworked from a carbonate shelf, indicating that they are older than the Badstube Fm. Microfacies and fossil assemblages with abundant algae indicate that a shallow marine carbonate shelf was developed at the northern margin of the deep-sea basin of Nötsch.

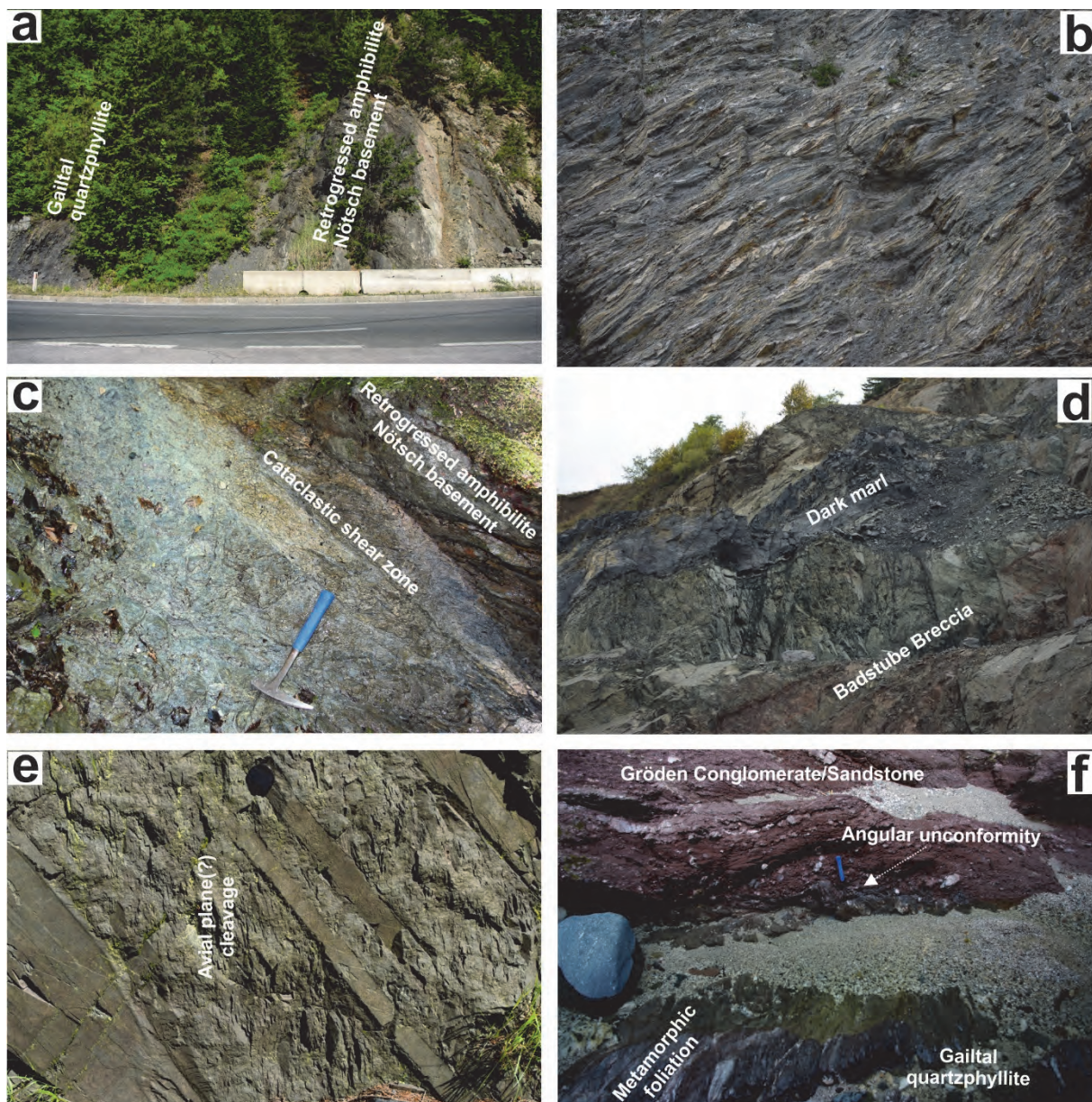


Fig. 40: Field photographs of various rocks of the retrogressed Nötsch basement, the Gailtal crystalline basement and of the Carboniferous of Nötsch.

Own data, white mica Ar-Ar ages from orthogneiss boulders (Exner, 1983a) of the Pölland area at the western margin of the Nötschgraben Fm. (Fig. 38), show plateau ages ranging from  $343 \pm 4$  Ma to  $380 \pm 2$  Ma and are affected by a post-depositional very low-grade metamorphic overprint, which is also reflected in rare axial plane cleavage (Fig. 40e).

The new data has significance for the Variscan history. We assume that an early Variscan amphibolite-grade metamorphic unit was exhumed along a thrust fault and shed clasts into the molasse-type basin in the footwall (Fig. 42 for a model). This metamorphic unit was not the Nötsch crystalline basement, which has a different age pattern.

The new data demonstrate, beside its significance for the Variscan history, that the tectonic succession of the Nötsch area at the southernmost part of the Austroalpine unit has a strong similarity to the nappe stack (including the NVO unit) of the northern Austroalpine sectors (Grauwacken zone and Ochtina/North Gemic unit in western Carpathians; see Fig. 43 for details of correlation). We consider,

therefore, these three units of the Nötsch area as a remnant of the root zone of the basement and cover nappes in the footwall of the Meliata suture. The structural relationships demonstrate >150–200 km large-scale nappe transport of the Meliata suture remnants in the Eastern Alps and the involvement of large, hitherto undetected Cenozoic strike-slip faults within the Austroalpine nappe structure.

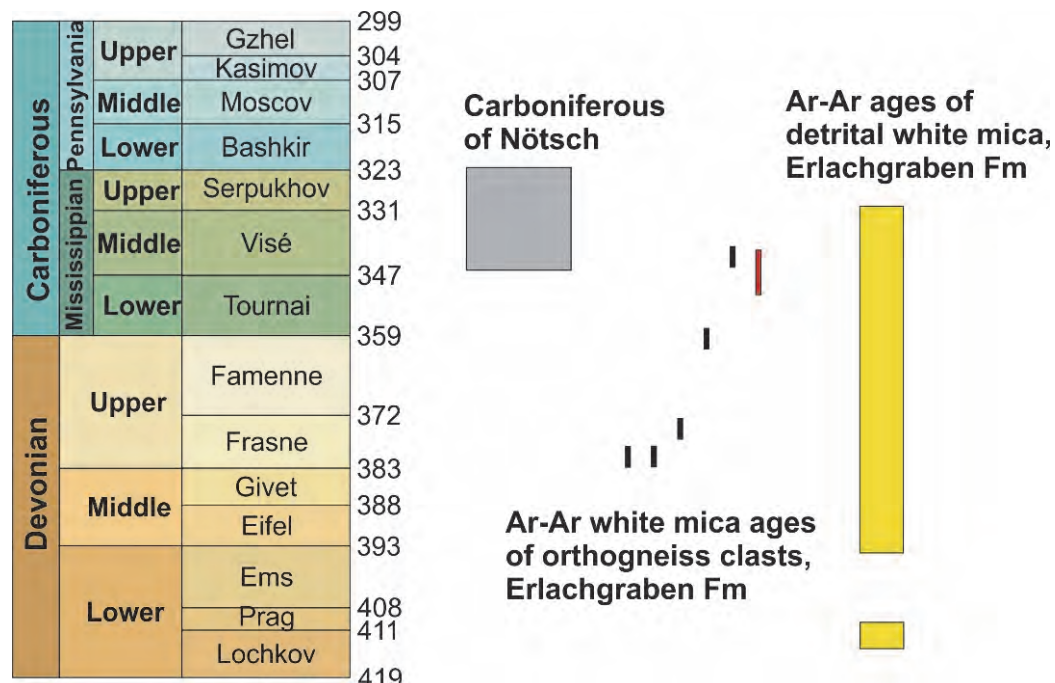


Fig. 41: Detrital white mica ages in comparison to the depositional age of the Carboniferous of Nötsch.

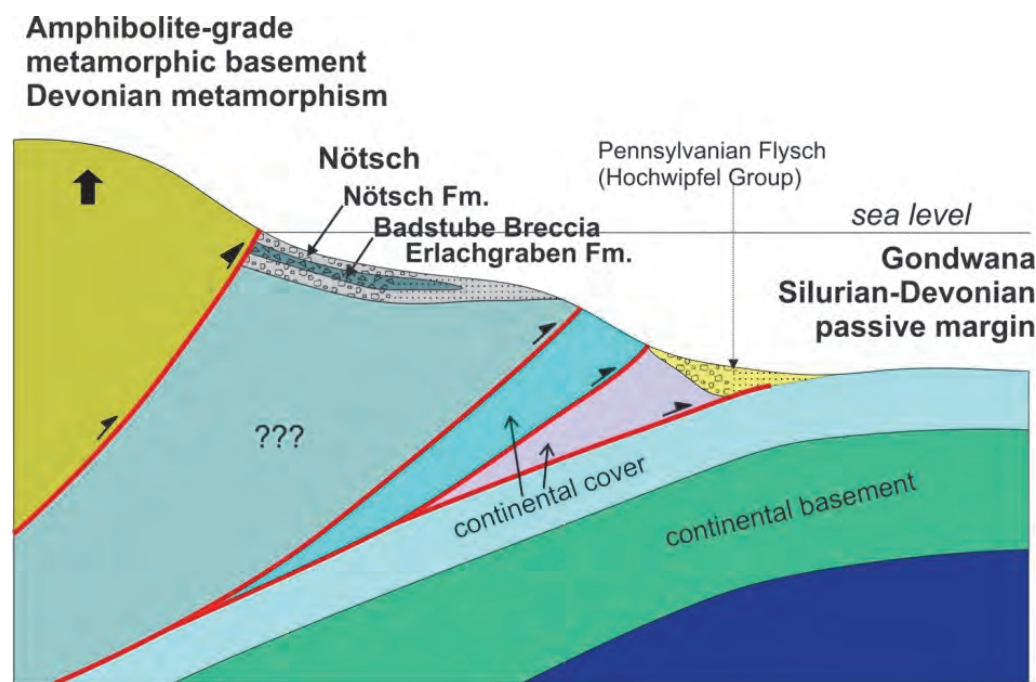


Fig. 42: Tectonic model of the Carboniferous of Nötsch.

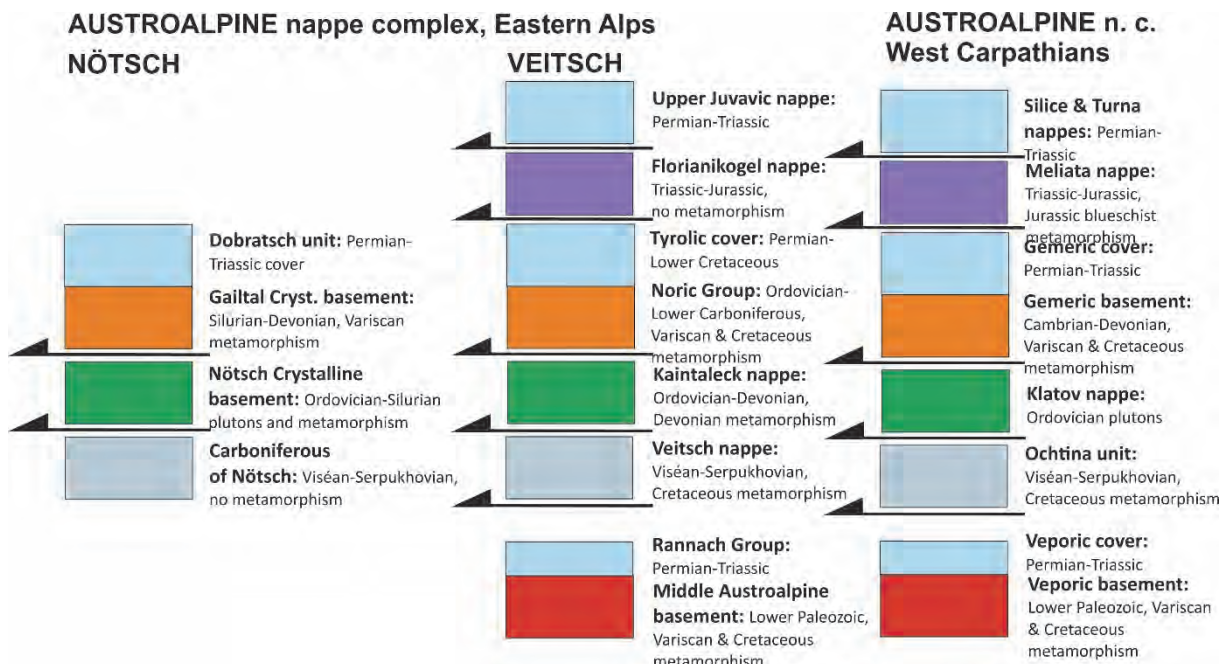


Fig. 43: Comparison of the tectonostratigraphy of the Nötsch area with that of the northeastern Austroalpine nappe complex and with Western Carpathians. Note that the age of thrusting in the Nötsch area is uncertain, whereas in the other areas the age of thrusting was during Cretaceous.

## 5.2 Stops

### Stop 3-1: Nötschgraben quarry with Badstub Breccia

Location: N46° 37' 01.9" E13° 36' 52.0"; ÖK 50, sheet 200 Arnoldstein; Jakomini quarry.

The quarry exposes mainly the Badstub Breccia overlying the Erlachgraben Fm. and underlying the Nötsch Fm. According to Krainer and Mogessie (1991), the Upper Visean Badstub Fm. consists of amphibolite breccias and conglomerates with intercalated sandstones, siltstones and shales. In the upper part of the sequence, these sedimentary rocks contain some fossils, e.g., brachiopod shells. Based on structural, textural and compositional features, these authors suggested that these sediments represent submarine resedimented deposits formed by sediment gravity flows on a proximal fan or slope (fan delta, slope apron) along an active strike-slip fault zone parallel to a continental margin. We interpret this fault as a thrust. Major and minor element chemistry of the amphibolite clasts argue for metamorphosed tholeiitic ocean floor basalts of the amphibolite clasts.

### Stop 3-2: Nötsch Valley: Road cut with Nötsch crystalline basement, boundary to Gaital Phyllite

Location: N46° 36' 35.7" E13° 36' 35.1"; ÖK 50, sheet 200 Arnoldstein.

This road cut exposes the boundary of retrogressed amphibolites of the pre-Variscan Nötsch crystalline basement to the overlying Variscan Gaital Quartzphyllite (Fig. 40a). The boundary shows ductile fabrics overprinted by late stage cataclastic fabrics. The Gaital Quartzphyllite is ductilely deformed and exhibits boudinage (Fig. 40b). Depending on the state of vegetation, the boundary of the retrogressed Nötsch crystalline basement to the Nötsch Formation of the Carboniferous of Nötsch can be seen, too.

**Stop 3-3: Nötschgraben – Angular unconformity at base of Dobratsch unit**

Location: N46° 36' 29.3" E13° 36' 35.5"; ÖK 50, sheet 200 Arnoldstein.

The outcrop in the Nötsch Valley exposes the angular unconformity between the Variscan Gailtal Quartzphyllite with a Variscan age of greenschist facies metamorphism and red overlying conglomerate and sandstone of the Permian Gröden Fm. of the Dobratsch unit. This proves that the Gailtal crystalline basement is part of the Dobratsch unit.

**6 Periadriatic fault and the Eastern Carnic Alps and Karawanken**

FRANZ NEUBAUER, JOHANN GENSER, ANDREAS ETZEL & BIANCA HEBERER

**Aim:** The aims of this part of the excursion are:

- (1) to examine the Southalpine unit, particularly regarding the differences of the Permian to Middle Triassic successions in comparison to the Austroalpine domain,
- (2) to investigate the complexities of the Periadriatic fault and the Late Miocene and Pliocene formation of the Klagenfurt basin and its overriding by the North Karawanken, and
- (3) to assess the significance of exhumed tectonic basements units exposed along the Periadriatic fault in the Eisenkappel area.

**6.1 Periadriatic fault system**

The Periadriatic fault is the longest and most important strike-slip fault system of the Alpine mountain belt and separates the Southalpine units in the south from the Penninic units in its western part and Austroalpine units in its eastern part. The eastern PAF is considered as southern confining fault of the Late Oligocene to Early Miocene extruding wedge (Neubauer, 1988; Neubauer and Genser, 1990; Ratschbacher et al., 1989, 1991a, 1991b; Schmidt et al., 1991). Several distinct connotations are generally associated with the Periadriatic fault: (1) A major dextral strike fault with an offset between 150 to 400 km, (2) a separation of vergency: to the north north of the fault, to the south in the Southalpine unit, (3) a metamorphic boundary, (4) Eocene to Oligocene slab break-off magmatism along its trace. Although distinct reviews exist for major portions of the Periadriatic fault (Schmid et al., 1989; Rosenberg, 2004), not much attention has been paid to its eastern part.

This contribution is aimed to fill this gap and discusses important issues on the eastern part of the Periadriatic fault from the Lesach Valley to the eastern Karawanken Mountains. The Periadriatic fault is the most important strike-slip fault in the Alps and separates the Southalpine unit in the south, with top to-the-south motion from the Austroalpine and Penninic units with a top-north or northwest transport in the north (e.g., Schmid et al., 1989, 2004; Fodor et al., 1998). The Periadriatic fault can be traced from the Po Plain west of Torino to the Pannonian basin. It extends for approximately 700 km from NW Italy to NE Slovenia, where it disappears beneath Neogene sediments of the Pannonian basin (Fodor et al., 1998). The Periadriatic fault (PAF) (Figs 1, 3, 7, ) strikes largely E–W parallel to the Alps, except for its central segment, the NW–SE striking Giudicarie fault (Pomella et al., 2012 and references therein).

The eastern segments of the PAF are called Gailtal and Pustertal faults and the eastern extension in the Karawanken Mts. has no special name. It represents a fault system composed of several distinct faults, which are from west to east: the eastern segment between Mules and Pannonian basin, which

is also often called Gail Valley fault, which is cross-cut by two NW-trending faults, the Möll Valley and the Lavant Valley faults. The eastern PAF exposes a flower structure (Polinski and Eisbacher, 1992). These allow a further distinction of three segments of the eastern PAF because of their peculiar structure: (1) The segment between Mules and Hochstuhl fault is straight and separates mainly basement (Brixen Quartzphyllite unit; Lower Palaeozoic to Lower Carboniferous Variscan basement of the Southalpine unit in the south and mostly basement rocks, the Gailtal basement in the eastern segment and the Defereggel quartzphyllite unit in the north. (2) The segment between Hochstuhl and Lavant Valley faults is characterized by the juxtaposition of Permomesozoic strata of the Southalpine unit to the North Karawanken unit, which overrode the Neogene Klagenfurt basin. Furthermore, in contrast to the western segment of the Southalpine unit, the Lower Palaeozoic to Lower Carboniferous basement only occurs in inliers within anticlines. (3) The eastern segment is poorly exposed and separates the Pohorje basement from Neogene sediments in the south.

In the Eastern Alps, the PAF separates the Southalpine units from the Austroalpine units. The units on either side of the PAF show differences in tectonic style, paleogeography, facies and degree and age of metamorphism (e.g. Schmid et al., 1989; Tollmann, 1977). During Alpine collision, the Austroalpine units underwent a complex tectonic and metamorphic evolution, whereas the Southalpine unit largely escaped Alpine metamorphism (e.g., Bistacchi et al., 2010). The eastern PAF also represents a boundary of metamorphic overprint separating the largely unmetamorphic Southalpine unit (with the exception of the small Eder unit – a strike-slip duplex with greenschist facies metamorphic overprint: Läufer et al., 1997), from Austroalpine units with Cretaceous-age low-grade metamorphic conditions (e.g., Müller et al., 2001, 2002). The PAF consists of bundles of kinematically linked large-scale faults. Fault rocks along the PAF comprise a several kilometer wide mylonitic belt for deeper crustal levels and a few tens of meters wide cataclasitic zone at shallower levels (Rosenberg, 2004). The TRANSALP transect near Bruneck proved the subvertical trend of the PAF near the surface and a continuous bend to the S up to ~60° dip near the upper/lower crustal boundary (Bleibinhaus and Groschup, 2008; Bleibinhaus et al., 2009).

The transpressional PAF shows, with exception of the Giudicarie fault segment, a dextral displacement, whereas estimations of the lateral offset range from 150 km to 450 km (e.g. Haas et al., 1995). Rare evidence for local sinistral displacements and reactivation is reported, too (Mancktelow et al., 2001; Nemes, 1997; Rathore and Becke, 1980), which verifies polyphase activation of the fault. Along the PAF, a vertical offset of several kilometers occurs locally (Läufer et al., 1997; Nemes, 1997; Schmid et al., 1989; von Blanckenburg et al., 1998; Heberer et al., 2017).

Along the eastern part of the Periadriatic fault, a number of small lamellae of basement and cover rock successions as well as generally Oligocene tonalites are exposed. These include:

- (1) The Lesach lamella with Permian Gröden Sandstone in the Lesach Valley (western extension of the Gail Valley) (Sassi et al., 1974; Zanferrari, 1976; Nemes, 1997). Note that further west, additional lamellae are known, including the Winnebach-Bruneck and Mauls-Pens lamellae, which are not discussed here;
- (2) the Eisenkappel crystalline basement in the surrounding;
- (3) the Eisenkappel Paleozoic unit, and
- (4) Oligocene tonalites.

## 6.2 Lesach lamella

The Lesach lamella with its Permian Gröden Sandstone is located c. 3 km south of similar lithologies within the Drau Range and is separated from this unit by the Gailtal crystalline basement. The Dobrautsch is the only location within the DR, where Permian redbeds (Gröden Fm.) are located nearby the PAF (Anderle, 1977). We suggest as the most appropriate origin of the Lesach lamella the southern Dobrautsch and its eastern extension. This implies a dextral strike-slip duplication of Permian strata compared to the base of the DR strata in the north and a minimum dextral offset of 50 – 60 km of the Lesach lamella along the PAF.

## 6.3 Eisenkappel crystalline basement

The Eisenkappel area in the eastern Karawanken Mountains in Austria and Slovenia exposes north to the Periadriatic fault, metamorphic and plutonic units, which include a deformed tonalite lamella, the Eisenkappel crystalline basement with the Eisenkappel pluton and the Eisenkappel Paleozoic units. The Eisenkappel pluton intruded into amphibolite-facies rocks ("Altkristallin") to the south (Exner, 1972; Faninger and Štruc, 1978; for a map, see Bauer et al., 1981). It is composed of mainly granites and diorites and minor gabbro, monzonite, and granodiorite (Visonà and Zanferrari, 2000; Bole et al., 2001). According to Miller et al. (2011), contact metamorphism of the Eisenkappel granite to the Eisenkappel Paleozoic unit implies an emplacement pressure of  $\leq 350$  MPa (Exner, 1972, 1976). Based on mineral age date done in the mid-70s, an early Triassic intrusion age was postulated (e.g., Cliff et al., 1975; Scharbert, 1975). In order to improve on these data, Genser and Liu (2010) dated zircons from seven samples and titanite from one sample by U/Pb LA-ICP-MS at Xi'an and amphiboles and biotites from four samples, and K-feldspars from five samples by the Ar-Ar method at Salzburg University. According to their data, one diorite sample (with very small zircon grains) from Slovenia gave U/Pb ages between 450 and 500 Ma. Zircons from the main rocks of the Karawanken pluton (biotite-granite, granodiorite, amphibole-granite) often show a spread of data points along the concordia with a maximum between 280 and 300 Ma and a smaller cluster at about 240-250 Ma. The titanite gave ages of about 245 Ma. Ar-Ar dating yielded ages between 245 and 260 Ma for amphiboles from granitic rocks and an age of 235 Ma for a K-rich amphibole from a gabbro. Biotites gave ages of 245 Ma, 242 Ma, and 232 Ma for granitic rocks, and 228 Ma for biotite from the gabbro. K-feldspars show patterns with increasing ages with high-temperature gas release steps. The ages reach (pseudo)plateaus of about 170-180 Ma, reliable low-temperature release steps are at about 70-80 Ma. Genser and Liu (2010) draw the following main conclusions from their ages:

- (1) There is an Ordovician magmatic event preserved in the Karawanken belt.
- (2) The time of intrusion of the main Eisenkappel granitoids is between 280 and 300 Ma, i.e. of early Permian age.
- (3) The spread of U/Pb zircon ages along the concordia down to about 245 Ma points to elevated temperatures up to the end of the Permian. This is also supported by the U/Pb titanite age and Ar-Ar amphibole ages; the latter confirming cooling below ca. 550 °C between 260 and 245 Ma.
- (4) Cooling below 300 °C (biotite ages) occurred in the Middle Triassic.
- (5) K-feldspar Ar-Ar ages indicate cooling below ca. 250 °C in mid-Jurassic time and probably some reheating in the Cretaceous.

Miller et al. (2011) reported mineral-whole rock Sm–Nd analyses of two cumulate gabbros of  $249 \pm 8.4$  Ma and  $250 \pm 26$  Ma ( $\epsilon_{\text{Nd}}$ : +3.6) from an alkaline gabbro body with within-plate geochemical characteristics. Garnet-whole rock Sm–Nd analyses of two associated silicic samples yielded well-constrained ages of  $238.4 \pm 1.9$  Ma and  $242.1 \pm 2.1$  Ma ( $\epsilon_{\text{Nd}}$ : -2.6) indicating Triassic magmatism.

#### 6.4 Eisenkappel Paleozoic unit

The very low-grade metamorphic Eisenkappel Paleozoic unit consists of slates, greywackes and includes a prominent pillow diabase horizon, which shows mildly alkaline geochemical characteristics (Loeschke, 1970). The age of the Eisenkappel Paleozoic unit is still uncertain and is interpreted either as Ordovician or Early Carboniferous (Loeschke and Schnepf, 1987). The Eisenkappel Paleozoic unit is welded with contact metamorphism with Eisenkappel crystalline basement (Exner, 1972, 1976).

#### 6.5 Oligocene tonalites

The eastern Periadriatic fault includes Oligocene tonalites, which intruded during initial fault motion at uncertain depths (>15 km) and which were later exhumed to the surface (Pomella et al., 2011; Neubauer et al., 2018). The pressure estimates for the depth of intrusion are as follows: 6.2 to 7.5 kbar for the Mauls tonalite, 3.5 to 4 kbar (Finkenstein; Diener, 2002), 4.1 to 5.5 kbar for the Karawanken (=Eisenkappel) tonalite (Elias, 1998; Table 1). This results in intrusion depth of 23 to 29 km for Mauls, 9 – 13 km for Finkenstein and 15 – 20 km for the Eisenkappel tonalite (Elias, 1998; Diener, 2002).

The main displacement initiated during the intrusion of tonalites, which ranges in age from  $32.9 \pm 0.2$  to  $29.00 \pm 0.97$  Ma, although in this segment, reliable ages are still scarce (Rosenberg, 2004 for data compilation). The tonalite intrusion is considered to result from slab-break-off (von Blanckenburg and Davies, 1995), which resulted in rheological weakening and mechanical decoupling of the Southalpine unit from the Austroalpine/Penninic units (von Gosen, 1989b; Handy et al., 2005; Rosenberg, 2004). A wide range of fault rocks is reported ranging from ductile mylonites to fault gouge as some well-exposed sections testify (von Gosen, 1989b; Nemes, 1997; Handy et al., 2005). Mylonites from the Eisenkappel area gave a preliminary Ar-Ar biotite age of  $19.0 \pm 0.3$  Ma (own unpublished age). Activity along the fault started in the mid-Oligocene, coeval with the intrusion of tonalitic and subordinate granodioritic bodies adjacent to the fault (e.g., Rosenberg, 2004; von Blanckenburg and Davies, 1995; von Blanckenburg et al., 1998). Most of the linearly aligned plutons are located north of the fault and magmas ascended along the fault system (Rosenberg, 2004; Schmid et al., 2004). Different models of the transport of the magma up to the plutons are discussed: The initiation is considered by slab breakoff (von Blanckenburg and Davies, 1995; von Blanckenburg et al., 1998), the linearly aligned plutons weakened the crust and triggered the fault, whereas plutons developed from the geometry of the mylonitic foliation (Rosenberg, 2004; von Gosen, 1989b).

Both basaltic and granitic magmatism took place during continental collision between 42 and 25 Ma (von Blanckenburg and Davies, 1995), but most plutons are almost isochronic with ages ranging from 28 to 34 Ma (e.g. Rosenberg, 2004) as e.g. the ~32 Ma old tonalite gneisses along the Gailtal and Pustertal faults (Nemes, 1997; Rosenberg, 2004; Sassi et al., 1974). The chemistry of the basalts proves partially molten metasomatic parts of the lithospheric mantle as the source of the magma feeding (von Blanckenburg et al., 1998).

Location	Rock type	Depth of intrusion (kbar)	Method	Age ± error (Ma)	Reference
Mauls	Tonalite	6.2–7.5	U-Pb Zr	29.00 ± 0.97	Elias, 1998
Mauls	Fault gouge		K-Ar	15.89 ± 0.33	Zwingmann and Mancktelow, 2004
Nampolach	Tonalite gneiss		AFT	25.2 ± 1.9	Hejl, 1997
Finkenstein	Tonalite	3.5–4.0	U-Pb Zr	32.9 ± 0.2	Diener, 2002
Finkenstein	Tonalite		AFT	26 ± 2	Hejl, 1997
Eisenkappel	Tonalite	4.1–5.5	U-Pb Zr	31.4 ± 0.7	Elias, 1998
Eisenkappel	Tonalite		K-Ar Bt	29± 6, 28± 4	Scharbert, 1975
Eisenkappel	Tonalite		AFT	16–20	Nemes, 1997
Eisenkappel	Tonalite		AHe	6.4 – 11.4	Heberer et al., 2017
Pohorje	Granodiorite		U-Pb Zr	18.64 ± 0.11	Fodor et al., 2008

Table 1: Geochronological ages from the eastern segment of the Periadriatic fault. AFT – apatite fission track, Bt – biotite, Zr – zircon.

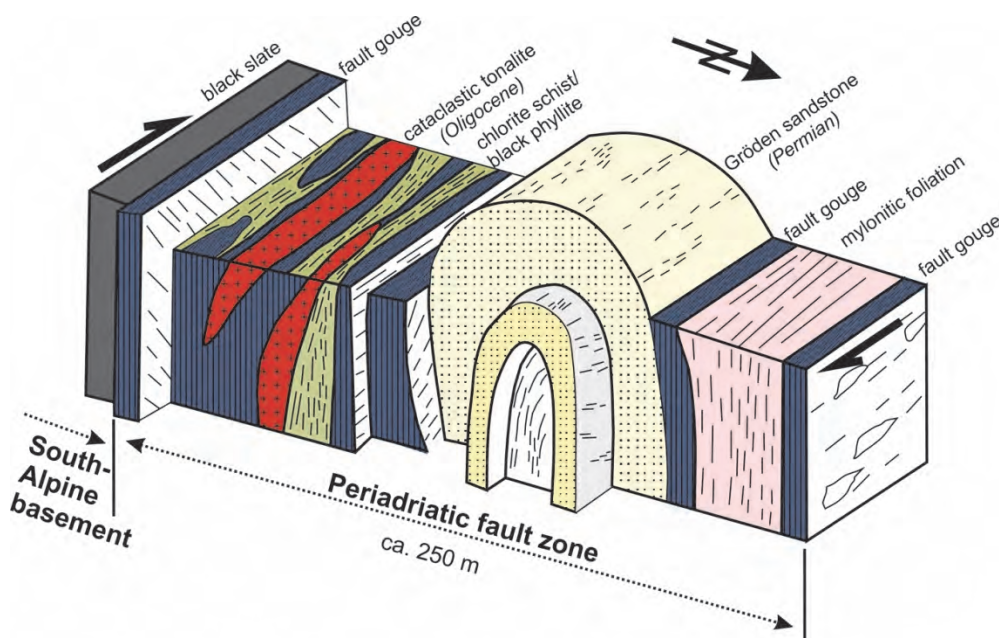


Fig. 44: Cross-section across the Periadriatic fault in the central part of the Periadriatic fault (modified from Nemes, 1997 and Cao and Neubauer, 2016).

## 6.6 Fault rocks along the Periadriatic fault

The tonalites and accompanying shear lenses include a wide variety of fault rocks ranging from mylonite and low-grade phyllonites, pseudotachylites over a wide variety of cataclastic rocks to fault gouge (von Gosen, 1989b; Nemes, 1997). The fault contains many narrow and long tonalite lenses,

which are preserved in many different structural states as undeformed bodies, tonalite gneisses, phyllonites/chlorite schist and cataclastic tonalite (Fig. 44). The tonalites and accompanying shear lenses include a wide variety of fault rocks ranging from mylonite and low-grade phyllonites, pseudotachylytes over a wide variety of cataclastic rocks to fault gouge (von Gosen, 1989b; Nemes, 1997). The fault rocks are considered to have formed by mainly dextral strike-slip and subordinate late-stage top-S reverse faulting (Nemes, 1997).

## 6.7 Stops

The Nassfeld region is a classical area well described by Schönlaub and Forke (2007), which also includes the detailed geological map (Fig. 45).

### **Stop 3-4: Tröpolach: Marble of Eder unit with Alpine ductile fabrics along the Periadriatic fault**

Location: N46° 36' 02.3" E13° 17' 12.0"; ÖK 50, sheet 198 Weißbriach; roadcut on Naßfeld road, ca. 700 metres SSW to Oselitzen near Tröpolach (north bridge at 734 NN).

The outcrop exposes steeply dipping, E-trending mylonitic Eder marble, actually a greenschist-facies-grade mylonite, with a prominent foliation and a subhorizontal stretching lineation. The mylonite is interpreted to represent an expression of Oligocene deformation along the Periadriatic fault. Läufer et al. (1997) and Nemes (1997) describe a polyphase calcite fabric. According to some preliminary Ar-Ar white ages at ca. 30 Ma, this unit was affected by Oligocene ductile shearing during an early stage of motion along the Periadriatic fault.

### **Stop 3-5: Lower Carboniferous Hochwipfel Group**

Location: N46° 35' 58.1" E13° 17' 09.4"; ÖK 50, sheet 198 Weißbriach; east Oselitzen river bed, below curve/bridge of Naßfeld road, ca. 700 metres S to Oselitzen near Tröpolach.

The outcrop exposes greyish to dark siltstones and graywackes of the Hochwipfel Group (Early Carboniferous). The Hochwipfel Group is interpreted to represent the infilling of a synorogenic flysch basin on top of the Devonian carbonate platform. Mader et al. (2007) describe an Early Variscan, early Carboniferous metamorphic source for the Hochwipfel flysch.

### **Stop 3-6: Upper Carboniferous to Middle Triassic of the Southalpine unit. Nassfeld: Walking tour from mountain hut Watschiger Alm to Kammleiten summit**

Location: N46° 33' 54.8", E13° 17' 12.0" to N46° 34' 33.1" E13° 17' 45.9"; ÖK 50, sheet 198 Weißbriach.

A walking tour down from the top station of the cable-car down to Naßfeld saddle allows to study cyclic marine/terrestrial Upper Carboniferous formations of the Auernig Group, various Permian formations including Permian shallow water carbonates and overlying mostly marine Lower and Middle Triassic strata. The details are well described in Schönlaub and Forke (2007). The Middle to Upper Carboniferous Auernig Group monitors marine transgression in a post-Variscan intramontane molasse basin on top of the Variscan nappe structure of Carnic Alps. The marine Upper Carboniferous and Permian sedimentation is distinct from that of the Austroalpine units north of the Periadriatic fault, which is purely terrestrial. The Middle Triassic Muschelkalk Conglomerate is likely a result of extensional tectonics indicating Middle Triassic reorganization of the depositional realm.

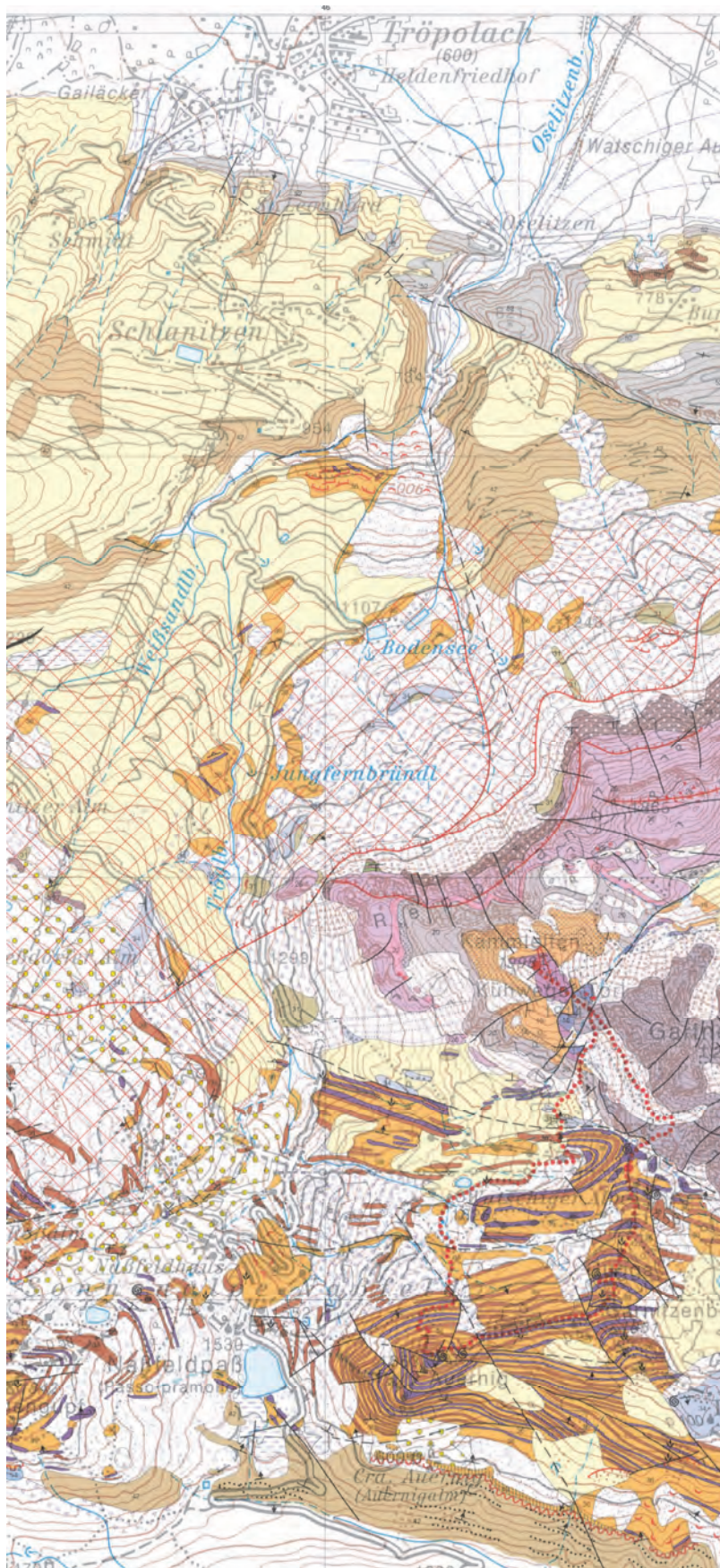


Fig. 45: Detailed geological map of the Nassfeld region (from Schönlaub and Forke, 2007).

 1	Jüngste Flussablagerung, Wildbachschutt Deposito fluviale più recente, deposito torrentizio	 24	Treßdorf-Kalk (Unteres Perm) Calcare di Tressdorf (Permiano Inferiore)
 2	Murenschutt Detrito di debris flow	 25	Trogkofel-Konglomerat, Trogkofelbrekzie (Unteres Perm) Conglomerato di Trogkofel, breccia di Trogkofel (Permiano Inferiore)
 3	Schwemmkegel Cono alluvionale	 26	Trogkofel-Kalk (Unteres Perm), S Spaltenfüllungen Calcare di Trogkofel (Permiano Inferiore), S fissuri
 4	Hangschutt, Schutthalde Detrito di versante, falda di detrito	 27	Zweikofel-Formation (Unteres Perm) Formazione di Zweikofel (Permiano Inferiore)
 5	Blockwerk, Bergsturzmaterial Detrito a grossi blocchi, deposito di frana di crollo	 28	Konglomeratlage darin Livello di conglomerato della Formazione di Zweikofel
 6	Vernässung, Moor Zona palustre, torbiera	 29	hellgrauer, massiger Kalk darin Formazione di Zweikofel (presenza di calcare massiccio grigio chiaro)
 7	Abrisslinie Orlo di distacco di frana	 30	Schieferlage darin Livello di scisti della Formazione di Zweikofel
 8	Zerrspalte Fessura, crepa	 31	Grenzland-Formation (Schiefer, grauer und grüner Sandstein; Unteres Perm) Formazione di Grenzland (scisti, arenarie grigie e verdi; Permiano Inferiore)
 9	Stark bewegter, aufgelockerter Bereich Zona mobile ed instabile	 32	Kalklage darin Livello di calcare della Formazione di Grenzland
 10	Große Wanderblöcke N Tressdorfer Höhe Massi erratici N Tressdorfer Höhe	 33	Konglomeratlage darin Livello di conglomerato della Formazione di Grenzland
 11	Moränenstreu Morenico sparso	 34	Schulterkofel-Formation (Ober-Karbon) Formazione di Schulterkofel (Carbonifero Superiore)
 12	Localmoräne mit groben Blockwerk, Wall Morena locale con grandi massi, con diga naturale	 35	Schiefer-, Konglomeratlage darin Formazione di Schulterkofel (presenza di strati scistosi)
 13	(Grund-)Moräne Morena basale	 36	Auernig-Formation (graubrauner Siltschiefer und Sandstein; Ober-Karbon) Formazione di Auernig (scisti argillosi grigi-bruni e arenarie; Carbonifero Superiore)
 14	Schlern-Dolomit (Ladinium) Dolomia dello Sciliar (Ladinico)	 37	Kalklage darin Livello di calcare della Formazione di Auernig
 15	Kalk darin Dolomia dello Sciliar (relitti di calcare)	 38	Quarzitischer Sandstein, Quarzkonglomeratlage darin Livello di arenarie quarzoso, conglomerato della Formazione di Auernig
 16	Muschelkalk (Anisium) Muschelkalk (Anisico)	 39	Trögl-Kalk (Echinodermenschutt- und Fusilinenkalk; Ober-Karbon) Calcare di Creta di Rio Secco (Calcare massiccio a echinoderme e fusilinidi; Carbonifero Superiore)
 17	Tuff- und Agglomerat darin Tufi ed agglomerati del Muschelkalk	 40	Auernigalm-Kalkbrekzie (Ober-Karbon) Brecchia calcarea di Casera Auernig (Carbonifero Superiore)
 18	Muschelkalk-Konglomerat (Anisium) Conglomerato di Muschelkalk (Anisico)	 41	Postvariszische Transgressionsbildungen (Lyditbrekzie, Konglomerat bis Geröllschiefer, Schiefer, Malinier-Fm.; Ober-Karbon-Kasimov-Stufe) Sedimenti trasgressivi post ercinica (brecchia lìdica, conglomerati e scisti di detrito, scisti, calcari; Carbonifero Superiore - Kasimoviano Inferiore)
 19	Werfen-Formation (Kalke und Schiefer, tieferer Teil dolomitisiert; "Skyth") Formazione di Werfen (calcari e scisti; parte inferiore dolomitizzata, Scitico)	 42	Hochwipfel-Formation (Schiefer, Sandstein, Grauwacke; Unter- bis Mittel-Karbon) Formazione di Hochwipfel (scisti, arenarie, grovacche; Carbonifero Inferiore-Medio)
 20	Bellerophon-Formation (Oberes Perm) Formazione a Bellerophon (Permiano Superiore)	 43	Lyditbrekzien-Lage darin Strato di brecchia lìdica della Formazione di Hochwipfel
 21	Bellerophon-Formation, dunkelgrauer Mergel und Schiefer an der Basis (Oberes Perm) Marne grigie scure e scisti alla base della Formazione a Bellerophon (Permiano Superiore)	 44	Debritlegge (mit Kalkgeröll) darin Strato di con ciottoli calcarei della Formazione di Hochwipfel
 22	Gröden-Formation (Mittleres Perm); S Spaltenfüllung in Trogkofel-Kalk (Trogkofel, Zweikofel Ost, Obere Garnitenklamm) Formazione di Val Gardena (Permiano Medio); S = riempimento di fessura nel calcare del Trogkofel/Creta di Aip, Zweikofel orientale, alta gola di Garnitz)		
 23	Gröden-Formation mit Tarvis-Brekzie an Basis (Dolomit- und Kalkbrekzie mit violetter und brauner Matrix; Unteres Perm) Formazione di Val Gardena con breccia di Tarvisio alla base (breccia di calcare e dolomia con matrice viola e marrone-rossiccia; Permiano Inferiore)		

Fig. 45 continued. Legend to the detailed geological map of the Nassfeld region (from Schönlaub and Forke, 2007).

**Stop 3-7: Bärental Valley Bärental Conglomerate (Pliocene) and North Karawanken thrust**

Location: N46° 29' 44.0" E14° 09' 44.0"; ÖK 50, sheet 211 Windisch Bleiberg; Bärental/Feistritzbach.

The group of outcrops along the road exposes the North Karawanken thrust over the Miocene to Pliocene Bärental Conglomerate, which is part of the Klagenfurt basin (Nemes et al., 1997). Close to the thrust surface, the conglomerate is well affected by brittle deformation with slickensides and striae showing a two-stage kinematics, oblique shortening and dextral strike-slip (Etzel, 2013). This group of outcrops is situated close to the western termination of the North Karawanken thrust, but east of Hochstuhl fault, which transects the Periadriatic fault. The Hochstuhl fault was active during Late Miocene to Pliocene times and is potentially active as some earthquake hypocenters indicate (Reinecker and Lenhardt, 1999).

The formation of the flexural Klagenfurt basin and the interaction with the North Karawanken thrust and Hochstuhl fault is shown in Figure 46 according to a recent MSc thesis (Etzel, 2013 resp. manuscript in preparation).

**Stop 3-8: Viewpoint Schaidasattel: Trace of the Periadriatic fault east of Zellpfarre and of the northern parallel fault of pre-Alpine basement**

Location: N46° 28' 44.2" E14° 28' 02.7"; ÖK 50, sheet 212 Vellach; Schaidasattel, parking place.

The viewpoint from the Schaidasattel (drainage divide between rivers following the Periadriatic fault system) is along the northern boundary fault between North Karawanken cover rocks and the Eisenkappel Paleozoic unit. To the SW, the Koschuta Mts. with its subvertical northern slope can be seen. With its impressive steep northern wall formed by Dachstein reef limestone belonging to the Southalpine unit, and the trace of the PAF follows the E-W valleys north of it. The North Karawanken unit belongs, in terms of Triassic facies, to the Drau Range unit, and is different in facies. The Northern Karawanken including the crystalline rocks north of the Periadriatic fault are exhumed during Late Miocene tectonic processes as (U-Th)/He data testify (Heberer et al., 2017; Fig. 47).

**Stop 3-9: Eisenkappel granite**

Location: N46° 27' 01.3" E14° 28' 27.6"; ÖK 50, sheet 212 Vellach.

Along this roadcut, a prophyric variety of the Eisenkappel granite, dated as Permian, is exposed. The granite has an intrusional contact to paragneisses of Eisenkappel crystalline basement (Exner, 1972, 1976).

**Stop 3-10: Eisenkappel, Ebriach gorge: Diabase pillow basalt**

Location: N46° 28' 39.3" E14° 33' 24.4"; ÖK 50, sheet 212 Vellach; abandoned quarry W Eisenkappel

The gorge well exposes subvertical pillow basalts with a fine-grained plagioclase center and greenish, chlorite-rich rims. Younging is towards south. Best examples of pillows are in the river bed as well as in an abandoned quarry. The age of the pillow basalts is uncertain, interpreted either as Ordovician in comparison with the Magdalensberg Group of the Stolzalpe nappe within the Gurktal nappe complex, or Early Carboniferous (Loeschke and Schnepf, 1987).

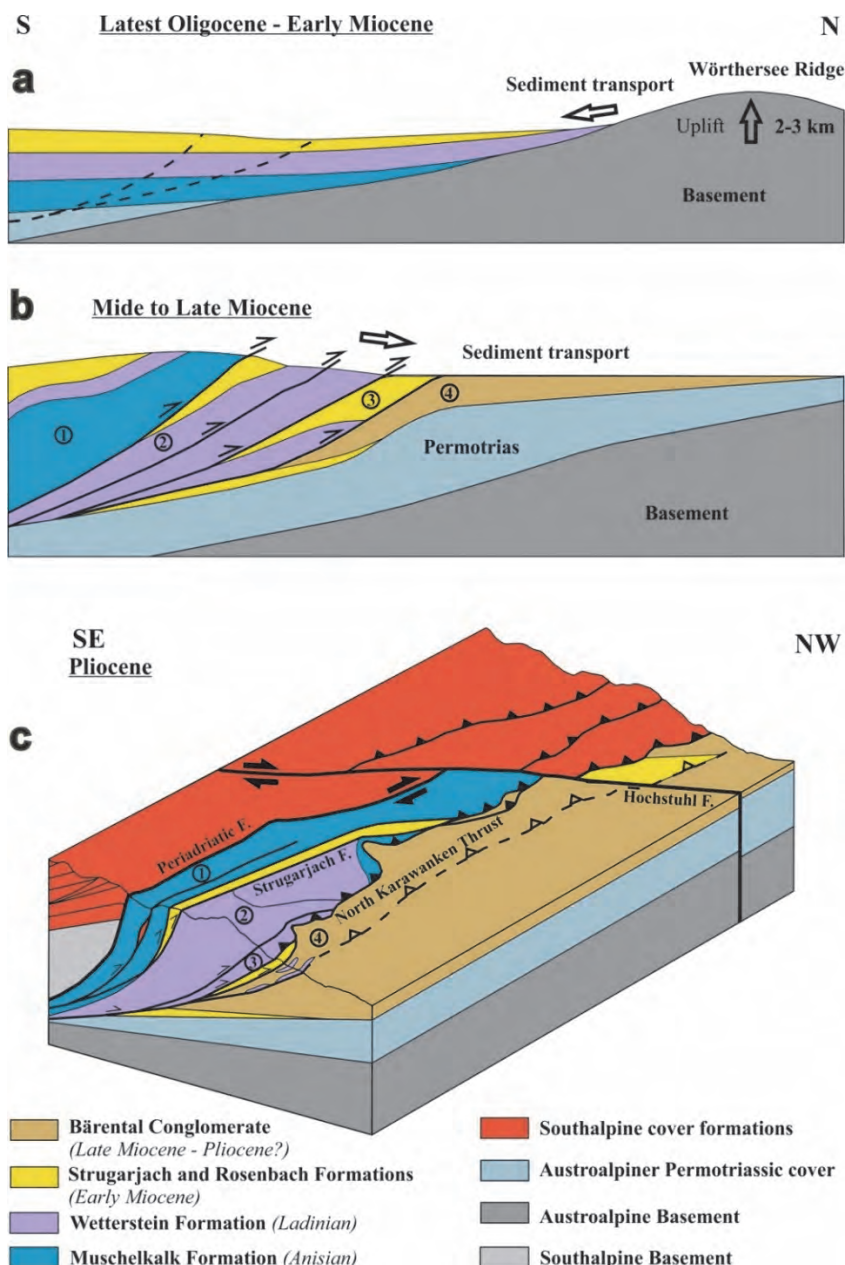


Fig. 46: Tectonic model of the evolution of the flexural Klagenfurt basin and the interaction with the North Karawanken thrust and Hochstuhl fault in three steps (modified from Etzel, 2013; resp. manuscript in preparation).

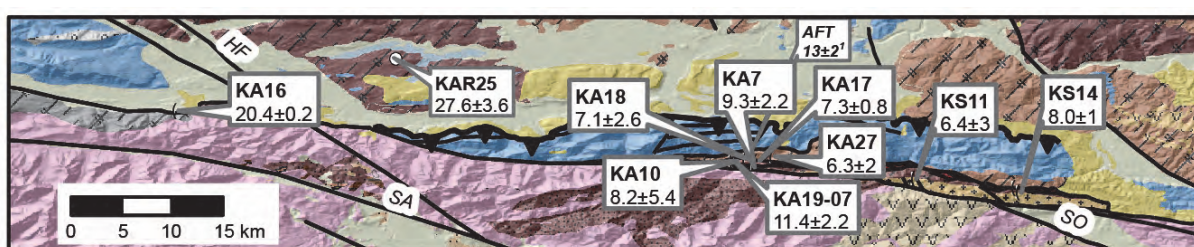


Fig. 47: Map showing apatite (U-Th)/He ages from plutonic rocks in the Karawanken exposed north of the Periadriatic fault. The young ages ranging from 6 to 11 Ma imply significant exhumation during Late Miocene to Pliocene times associated with thrusting of the North Karawanken unit onto the Klagenfurt basin. From Heberer et al. (2017).

**Stop 4-1 (first stop of excursion day 4): S of Hagenegg castle SW Eisenkappel: Permian/Triassic gabbro and diorite**

Location: N46° 28' 31.76", E14° 35' 22.5", ÖK 50, sheet 213 Eisenkappel; dell immediately SW Eisenkappel, near tennis court.

This exposure shows the mutual relationship mainly between cumulate gabbro, gabbro and diorite. The cumulates are composed of olivine, plagioclase, clinopyroxene, brown amphibole and phlogopite. Olivine is the most abundant mafic phase, and is included in poikilitic plagioclase or clinopyroxene (Miller et al., 2011). Miller et al. (2011) found that the Eisenkappel gabbro formed at  $1000 \pm 20$  °C and 0.38–0.47 GPa. Mineral-whole rock Sm–Nd analyses of two cumulate gabbros yielded ages of  $249 \pm 8.4$  Ma and  $250 \pm 26$  Ma implying intrusion at ca. the Permian-Triassic boundary.

**Stop 4-2: Kupitz gorge: Eisenkappel tonalite**

Location: N46° 28' 01.2" E14° 36' 55.1"; ÖK 50, sheet 213 Eisenkappel; Kupitz gorge south of Remscheniggraben.

The Kupitz gorge is a confluent to the Remschenig valley and exposes ductilely deformed Oligocene tonalite juxtaposed to Middle Triassic successions of the Southalpine unit with a phyllonitic contact to the Eisenkappel crystalline basement. Elias (1998) reported a U-Pb zircon age of the Eisenkappel tonalite of  $31.4 \pm 0.7$  and a pressure, based on Al-in-hornblende barometry of 4.1–5.5 kbar. Heberer et al. (2017) found (U-Th)/He ages of  $6.3 \pm 2$  to  $11.4 \pm 2.2$  Ma for tonalite and metamorphic basement implying a Late Miocene to Pliocene age of rock exhumation interpreted to relate to emplacement of the North Karawanken thrust wedge.

**Stop 4-3: Eisenkappel basement, Rapakiwi granodiorite**

Location: N46° 28' 28.9" E14° 35' 37.7"; ÖK 50, sheet 213 Eisenkappel; path east river Vellach south of Remschenigbach confluence.

Within the Karawanken pluton, Exner (1972, 1976) described a granodiorite with Rapakiwi-type K-feldspar mantled by oligoclase. It forms a ca. 10 m thick dyke, which can be followed over 100s of meters.

## **7 Cretaceous and Miocene extension processes at the eastern edge of the Gurktal nappe complex**

FRANZ NEUBAUER, BIANCA HEBERER & JOHANN GENSER

**Aim:** The aims of visiting the Saualpe-Krappfeld area, which is part of the Austroalpine nappe complex, are two-fold:

- (1) The close relationship of exhumation of Cretaceous-aged eclogites with the rapidly subsiding Krappfeld basin, which represents a Late Cretaceous collapse basin, shows the Late Cretaceous age of ca. ESE-WSW extension following subduction and collision of the Eclogite-Gneiss unit. The area with the rapidly subsiding basin represents the counterpart of the Nock detachment (visited during the excursion) at the western margin Gurktal extensional allochthon.
- (2) The area exposes a succession of superimposed sedimentary units in the wider Krappfeld basin, which reactivated the brittle Görtschitz Valley fault during Miocene times. The Görtschitz Valley fault is a dextral transtensional fault with an apparent vertical throw of ca. 3 to 5 km, representing

one of the largest Miocene faults of Eastern Alps, but hitherto forgotten in most compilations. Transtension reflects the eastward lateral rafting on the Miocene Katschberg normal shear zone towards the Pannonian basin.

### 7.1 Introduction

In terms of tectonostratigraphic units (Figs. 48, 49, 50), the Saualpe block comprises at the base, the Koriden Gneiss-Eclogite complex, a continental unit that suffered Cretaceous-aged eclogite metamorphism during A-type subduction (e.g., Miller et al., 2005; Wiesinger et al., 2006 and references therein). An ESE-directed ductile low-angle normal fault separates the Koriden Eclogite-Gneiss complex from the overlying Micaschist complexes (Wiesinger et al., 2006), which underwent Cretaceous-aged amphibolite to upper greenschist facies-grade metamorphism. The Micaschist complexes are exposed along the southern Saualpe block due to the Saualpe South Margin Flexure and within the Friesach half window (Fig. 33). Another ductile low-angle normal fault separates the Micaschist complexes from the overlying Phyllite unit, which is conventionally considered as a part of the lower (Murau) nappe of the large Gurktal nappe complex. The upper nappe (Stolzalpe nappe) of the Gurktal nappe complex comprises very low-grade Ordovician to Lower Carboniferous fossil-rich volcanosedimentary successions of the Magdalensberg Group exposed along the margins of the Krappfeld basin area (e.g., Thiedig et al., 1999). Above the post-Variscan unconformity and metamorphic hiatus, Permian to Triassic cover units with clastics and dolomites (Eberstein Permotriassic) are exposed in the southern Krappfeld area. The Eberstein Permotriias is tilted towards north (Figs. 48, 49) and is also affected by internal thrusts and normal faults (Appold and Pesch, 1984; Ratschbacher and Neubauer, 1989) predating the deposition of the Krappfeld Gosau Group above an erosional contact and angular unconformity (Hermann and Wascher, 1972).

In the central axis of the Austroalpine units in the Eastern Alps, the Upper Cretaceous Gosau Group is exposed in collapse basins on top of the Lower Cretaceous Austroalpine nappe stack formed during Early Cretaceous plate collision. The Krappfeld Group comprises, from base to top, the St. Florian Fm. with basal dolomite conglomerate and shallow water limestones, the turbiditic Wietersdorf Fm. with thick olistostromes and breccia layers (Fig. 50), and the Pemberg Fm. with orbitoid-bearing turbidites and marls (Thiedig, 1975; Leggewie and Thiedig, 1977; Zetter and Dimter, 1992; Thiedig et al., 1999), together ranging from Santonian to earliest Late Maastrichtian (Fig. 50) (van Hinte, 1963; Thiedig and Wiedmann, 1975; Neumann, 1989). Beside, intraformational olistostromes of reef detritus (Thiedig, 1975), the Wietersdorf Fm. includes numerous angular siliciclastic clasts from the Magdalensberg Group mainly demonstrating the erosion of this shallow basement level. The large olistostromes were sourced from the east, likely from reefs at the top of the future Saualpe block (Thiedig, 1975; Neumann, 1989; Sanders et al., 2004), which is taken as evidence for a Late Cretaceous precursor fault of the Miocene Görtschitz Valley fault system.

Above a Paleocene hiatus, a latest Paleocene to Eocene succession is exposed in three separate areas unconformably postdating the Krappfeld Gosau (Figs. 48, 49, 50). It includes: the Holzer Fm. at the base, with red clay, coal, sandstone, dark marls (Zetter and Hofmann, 2001; Drobne et al., 2011) and the Dobranberg Fm. with marine nummulite-rich shallow water limestones and marls (Fig. 51c) (Wilkins, 1989a, 1989b; Kázmér et al., 2003 and references therein; Drobne et al., 2011). The reddish bauxite-like red clay of the Guttaring area is now considered as latest Paleocene in age and as part of the Holzer Formation (Kuhlemann et al., 2008). A few remnants of large blocks of Eocene limestone overly the Phyllite Group exposed to the north of the Guttaring fault, which indicates a widening of

the Eocene land surface west of the Görtschitz Valley fault (Fig. 49). Vitrinite reflectance studies of the coal from the Holzer Fm. exhibit low values ( $R < 0.4$ ) implying only a thin overburden (Sachsenhofer, 1992). There are also some unconsolidated mudstones with coaly layers of uncertain Paleogene to early Miocene age south of Guttaring here considered as Dachberg Fm. (Figs. 49, 50; Appold et al., 1986).

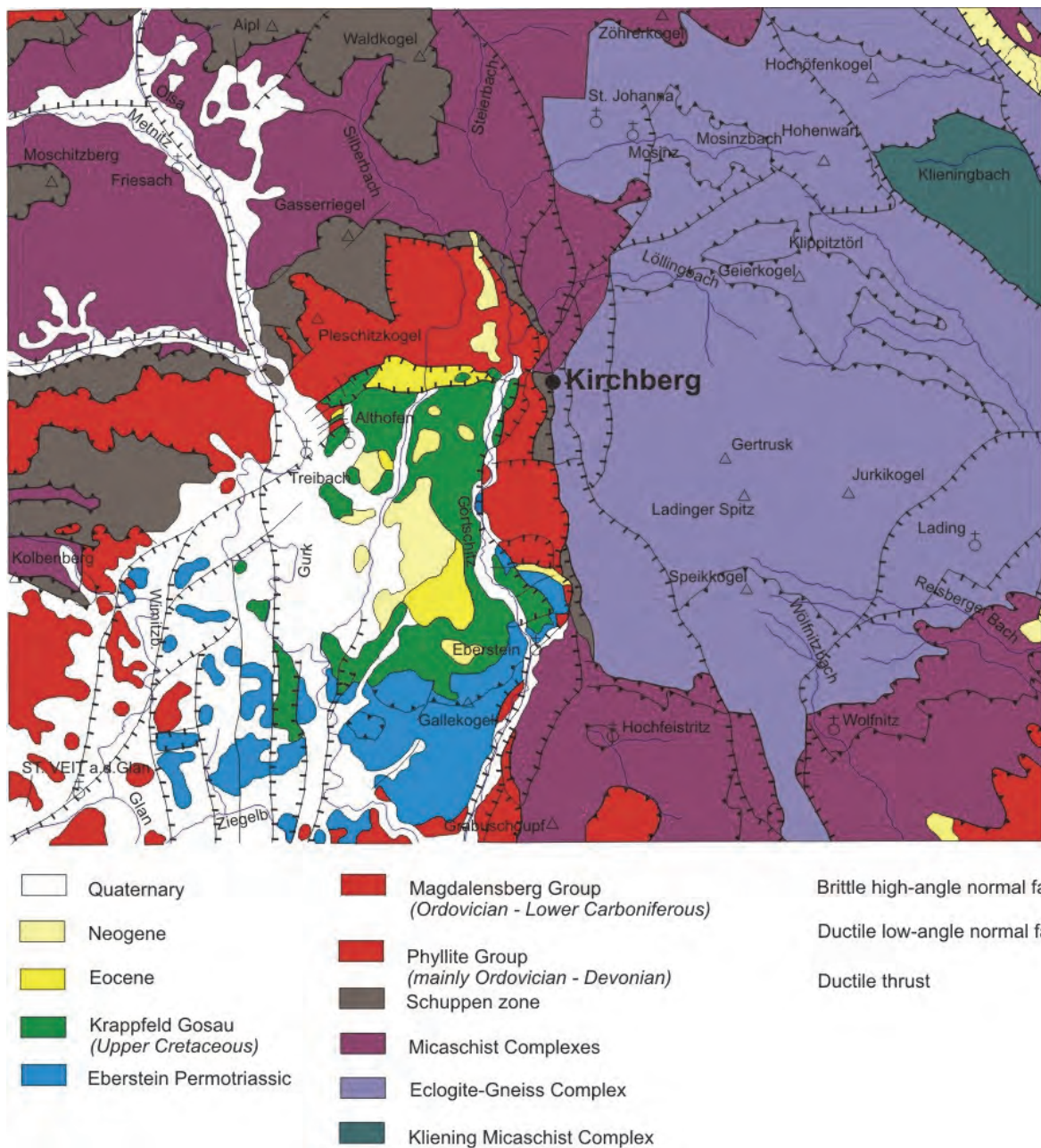


Fig. 48: Simplified geological map of the Krappfeld basin and the Saualpe area (modified after Thiedig et al., 1999 and Weissenbach and Pistotnik, 2000).

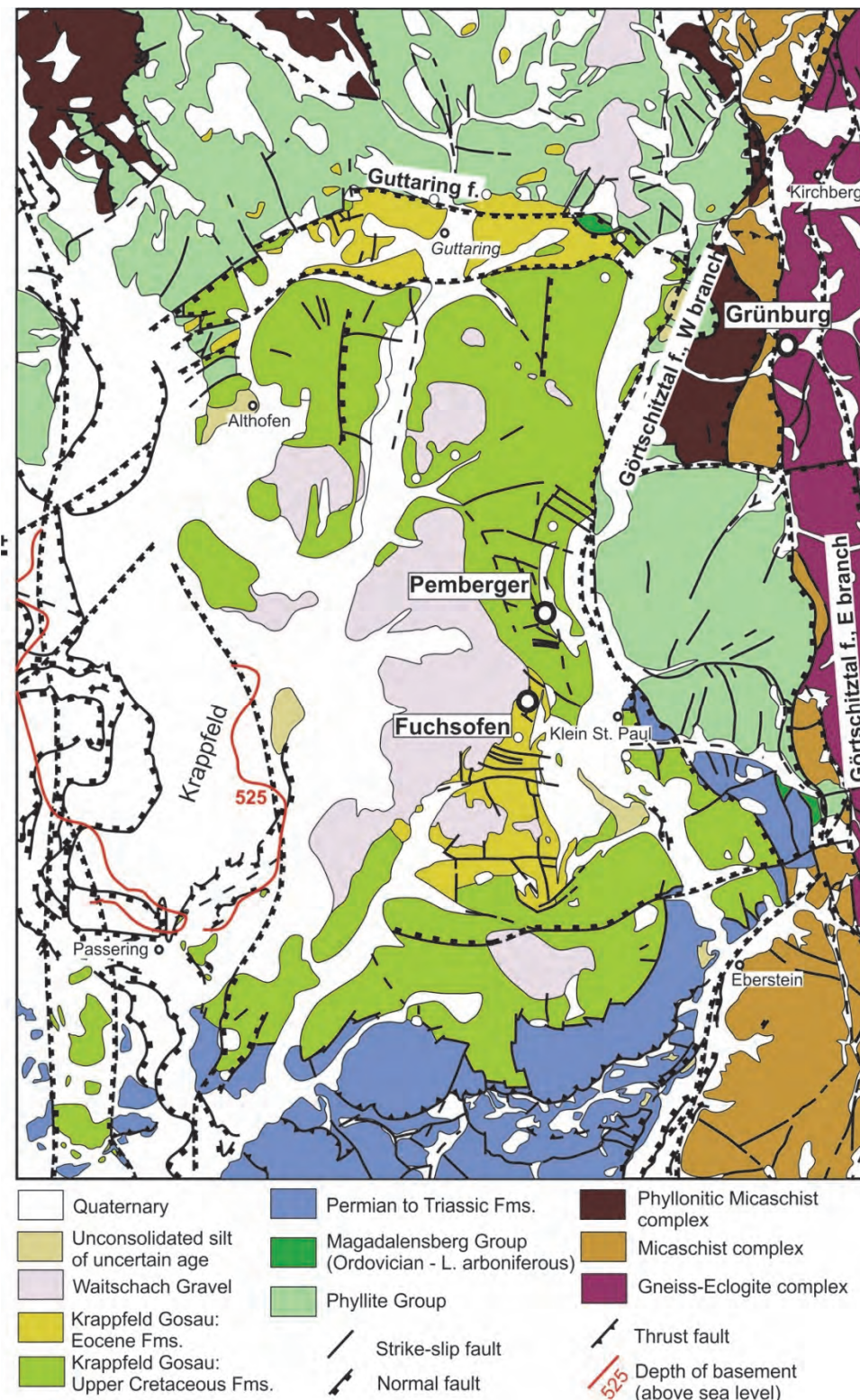
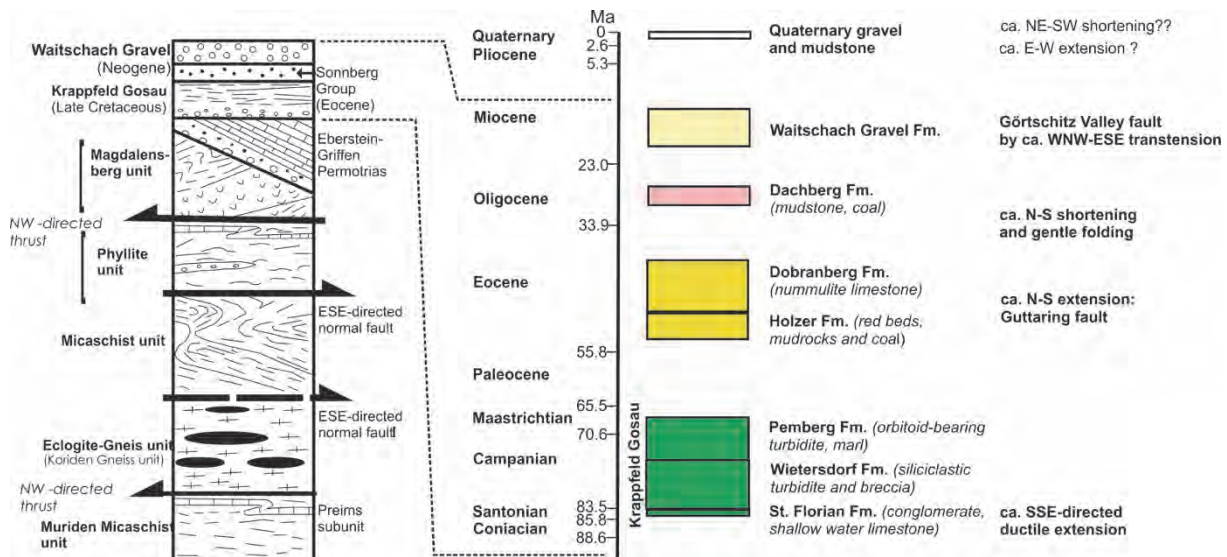


Fig. 49: Detailed geological map of the Krappfeld basin and Saualpe area (modified after Thiedig et al., 1999).

The Miocene Waitschach Gravels are overlying both the Phyllite Group north of the E-W trending Guttaring fault and the former Krappfeld basin west of the Görtschitz valley. Small remnants of Waitschach Gravel on Phyllite Group are exposed west of the Krappfeld basin (Fig. 49) (van Husen, 1976, 1989; Thiedig et al., 1999). The Waitschach Gravels in the eastern part of the Krappfeld basin

comprise abundant large, meter-sized boulders of pegmatite gneiss, paragneiss, quartzite, vein quartz as well as rare eclogite typical for the Koriden Gneiss-Eclogite unit exposed to the east of the Görtschitz Valley (Fritsch, 1962; van Husen, 1989). Consequently, previous researchers argued since Fritsch (1962) that the present-day N-S Görtschitz Valley was not in existence during deposition of the Waitschach Gravels.



*Fig. 50: Left side: Simplified tectonostratigraphy of the Saualpe and Krappfeld region (modified from Wiesinger et al., 2006). Right side shows sedimentary strata of the Krappfeld basin fill and supposed tectonic events affecting that area since Late Cretaceous.*

The present-day Krappfeld itself is a small Quaternary basin with a flat morphology (Fig. 49). It was not glaciated, at least not during the last (Würmian) glaciation (Hiller, 1973; van Husen, 1989). Fluvial gravels and lacustrine silts form the basin fill. According to geophysical investigations, the basin is ca. 150 – 180 meter deep (van Husen, 1989; Walach, 1989). A c. 100 m deep outlet was found at the southern edge by geophysical methods.

The Görtschitz valley fault with ca. 15 – 20 km apparent dextral and ca. 3 to 5 km apparent vertical displacement is the most prominent fault within the central Eastern Alps. The Görtschitz valley follows the western branch of the ca. NNW-trending Görtschitz valley fault, which separates, between Mösel and Eberstein (Fig. 49), the Upper Cretaceous Krappfeld basin fill from Phyllite unit, the Magdalensberg Group and fault-bounded slices of the Eberstein Permotrias. The Görtschitz Valley was not glaciated during the Würmian glaciation (Schillig, 1966; van Husen, 1989). The valley itself includes a few gravel terraces believed to be of Holocene age. Two river terraces are prominent: the upper one at ca. at 670 to 680 m elevation, ca. 110 meters above the present-day valley (e.g. at 565 m elevation at Mösel), and the lower one at ca. 580–590 m elevation, ca. 25–35 m above the present-day valley floor.

## 7.2 Tectonics and geomorphology

The morphology and the post-collisional evolution of the Eastern Alps were heavily affected by eastward-directed lateral extrusion during Late Oligocene to Early Miocene times and intra-orogenic raft tectonics (Neubauer and Genser, 1990; Ratschbacher et al., 1991a; Keil and Neubauer, 2015; . We explain this stage as driven by eastward floating raft tectonics of upper crustal blocks along the basal Katschberg ductile low-angle normal fault away from the Tauern window. The extrusional and rafting

stage was overprinted by south-directed flexure forming the Late Miocene-Pliocene Klagenfurt basin in front of the North Karawanken thrust (Nemes et al., 1997). This refined tectonic model of the interior of the East Alpine extrusional wedge is based on new structural field data and a reassessment of the existing, but hitherto overlooked geological record from the ca. NNW-trending dextral transtensional Götschitz Valley fault system. As discussed before, this fault system with ca. 3 to 5 km apparent vertical displacement is one of the most prominent faults within the central Eastern Alps (Thiedig and Weißenbach, 1975) and juxtaposes the Krappfeld basin with superimposed Upper Cretaceous, uppermost Paleocene–Middle Eocene, Lower Miocene and Quaternary successions to the uplifted Saualpe basement block with its Cretaceous-aged eclogite to greenschist facies grade rocks in the east (Fig. 48). The geometry of and kinematics affecting the Krappfeld basin fill allow defining the superimposed Late Cretaceous to Recent succession of basin-forming tectonic events of the eastern part of central Eastern Alps (Fig. 52): (1) Following Cretaceous continental subduction, exhumation of previously subducted Cretaceous eclogites occurred along an array of ductile low-angle normal faults during Late Cretaceous times and the upper block subsided below sea level forming the collapse-type Krappfeld basin due to extreme ESE–WNW extension (Willingshofer et al., 1999a). (2) After a period of Paleocene non-deposition and deep subtropical weathering (Thiedig, 1970; Kuhlemann et al., 2008), an Eocene marine transgression occurred due to N–S extension forming the Krappfeld basin. (3) Subsequent N–S shortening resulted in gentle Oligocene folding of the Upper Cretaceous-Eocene basin fill. (4) This stage is followed by NE–SW extension consistent with activation of the transtensional Götschitz Valley fault system and at least ca. 2.5 to 3 km apparent vertical offset as part of a raft system of the eastward extruding ALCAPA block (Keil and Neubauer, 2015), in which the Götschitz Valley fault system represents an antithetic transtensional fault to the ductile Katschberg low-angle normal fault at the eastern margin of the Tauern window. The fluvial Waitschach Gravel of likely Karpatian age (Early Miocene) was deposited along the western branch of the Götschitz valley fault system and received detritus from the uppermost units of the Saualpe block in the east (e.g., Fritsch, 1962). Incision of the Götschitz Valley along the western branch of the Götschitz Valley fault started in post-Karpatian times most likely during the Late Miocene-Pliocene flexure of the Klagenfurt basin in the south (Nemes et al., 1997) and resulted in a modified regional drainage system, which reoriented the drainage pattern from east-directed respectively W-directed to a south-directed one.

### 7.3. Stops

#### **Stop 4-4: Wietersdorf, Gosau quarry “Pemberger Riegel”**

Location: N46° 50' 44.1" E14° 31' 40.6"; ÖK 50, sheet 186 St. Veit an der Glan; quarry Pemberger Riegel W Wietersdorf.

The quarry exposes grey calcareous turbidites intercalated with grey marls, which generally dip steeply to the west. The graded turbidite beds include abundant very low-grade angular volcano-sedimentary clasts of the Magdalensberg Group as well as intraformational marly limestone clasts with grain sizes of 6 – 8 cm. The transport direction is supposed to have been from a nearby source located in the east receiving shallow water carbonates. The basin indicates significant subsidence and topography during Late Cretaceous extension. The marly rich succession is partly folded and even axial surface foliation has been documented (von Gosen and Thiedig, 1980).

**Stop 4-5: Wietersdorf, Gosau quarry “Fuchsofen”, Eocene limestone quarry**

Location: N46° 50' 17.2" E14° 31' 33.6"; ÖK 50, sheet 186 St. Veit an der Glan; quarry Fuchsofen W Wietersdorf.

The quarry exposes Eocene limestones of the Dobranberg Fm. with light-colored yellowish marine nummulite-rich shallow water limestones and rare marls (Fig. 51c). These are overlain, above an erosional unconformity, by Miocene unconsolidated gravels of the Waitschach Fm. on top of the Fuchsofen hill. The facies and fossils are described in Kázmér et al. (2003 and references therein) and Drobne et al. (2011). Biostratigraphy indicate a lower to middle Cuisian to Lutetian age (Drobne et al., 2011 and references therein). The limestones dip gently to SW and are transected by ca. N-S trending dextral strike-slip faults (Fig. 51c).

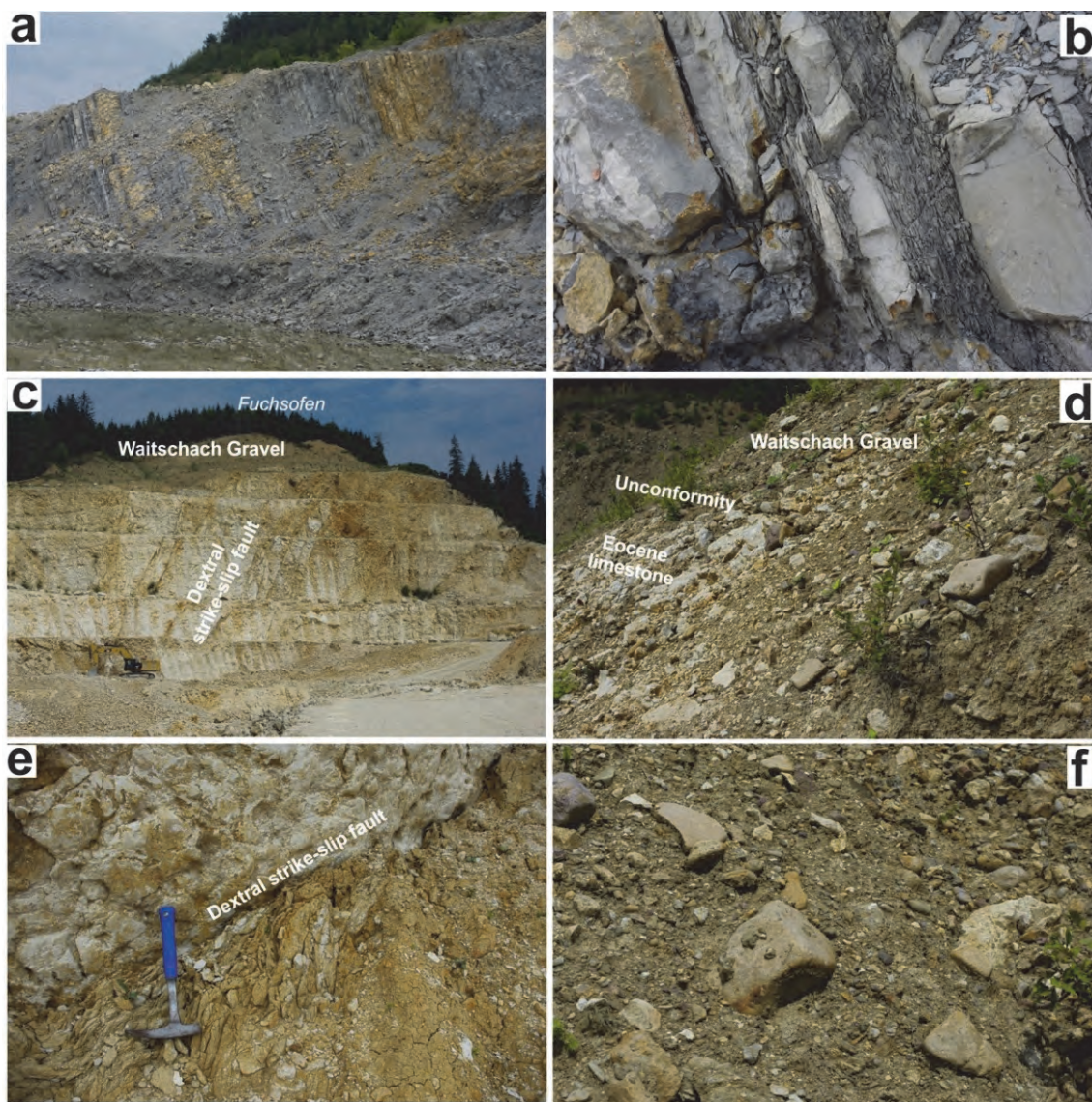


Fig. 51: (a) Late Cretaceous (Santonian) marly turbidites. (b) Detail of turbidites with graded bedding. The left bed shows angular marly limestone clasts. Thickness of the bed: ca. 25 cm. (a) and (b) are from the Pemberger Riegel quarry. (c) Northern slope of the Fuchsofen quarry with massive Eocene limestone overlain by the Miocene Waitschach Gravel at top. (d) Unconformity between Eocene limestone and Miocene Waitschach Gravel. (e) Dextral strike-slip fault transecting the Eocene limestone. (f) Variety of clasts in the Waitschach Gravel at Fuchsofen top.

The Waitschach Gravel at top of Fuchsofen exhibits clasts mostly reworked from the immediate Eocene underground, from the Eberstein Permotrias (e.g. red sandstone of the Gröden Fm.), volcanosedimentary material from the Magdalensberg Group and rare vein quartz and some eclogite from the Saualpe. The occurrence at the top of the Fuchsofen shows the post-depositional post-Miocene uplift of the Krappfeld basin and incision of the Görtschitz Valley.

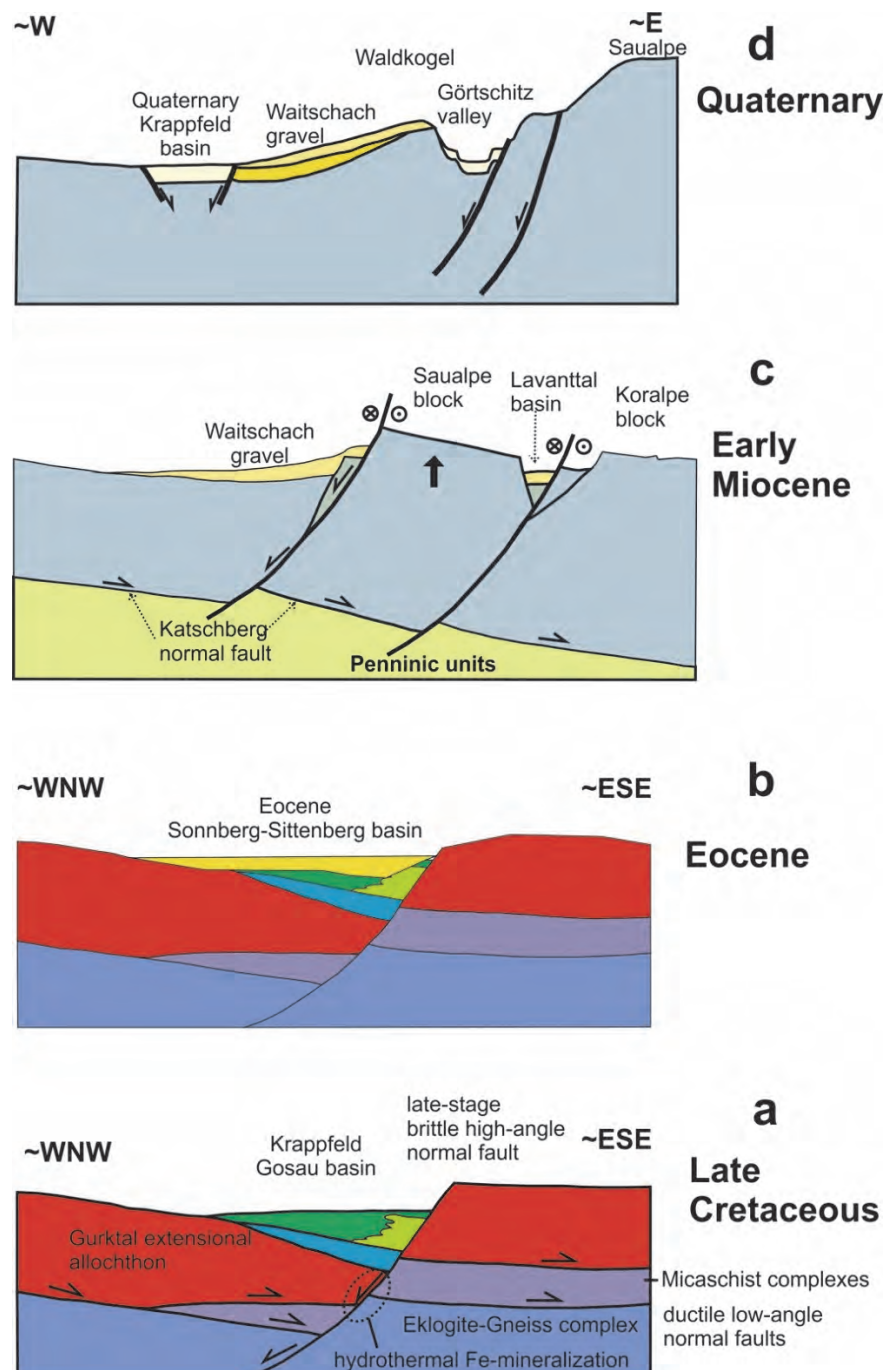


Fig. 52: Tectonic evolution of the Krappfeld basin area in comparison with the basement units exposed to the east. (a) Late Cretaceous extension and formation of the Krappfeld Gosau basin. (b) Eocene shallow water limestone deposition during a tectonically rather quiet period. (c) Early Miocene eastward rafting along the ductile Katschberg normal fault and transtensional reactivation of the Görtschitz Valley fault. (d) Quaternary surface uplift and erosion and incision of the Görtschitz Valley during waning stages along the transtensional Görtschitz Valley fault.

### **Stop 4-6: Grünburg, Cretaceous eclogite**

Location: N46° 51' 23.3" E14° 34' 25.3"; ÖK 50, sheet 186 Sankt Veit an der Glan; Grünburger Bach, slope west/southwest R. Grünburg.

The description of the petrology of this outcrop follows Miller et al. (2005). This outcrop is part of an eclogite lens with a length of about 1500 m and about 150 m wide, intercalated with country rock mica-schists and gneisses. Near the base of the outcrop a pegmatoid dyke containing muscovite, plagioclase and quartz intruded this eclogite parallel to the foliation. The fine- to medium-grained eclogites are of the Fe- and quartz-rich "metabasaltic" variety and consist of garnet + omphacite + quartz + rutile + apatite ± amphibole ± phengite ± clinozoisite ± zircon ± pyrite. Garnet is slightly zoned with rim compositions of  $\text{Prp}_{35-37}\text{Alm}_{39-40}\text{Grs}_{22-24}\text{Sps}_{0.5-0.6}$  and contains inclusions of rutile, quartz, clinozoisite, apatite and zircon. Omphacite is unzoned with 0.34–0.35 mol% jadeite and, together with clinozoisite, defines the foliation and mineral lineation. Subcalcic magnesiohornblende is present as texturally late poikiloblastic grains overgrowing garnet, clinozoisite, quartz and rutile.

The geochemistry of the quartz-rich eclogite from the Grünburger Graben, Saualpe is close to N-MOR basalt, particularly based on a flat chondrite-normalized rare earth element pattern. Heede (1997) attempted to date zircon (multigrain) separates from this eclogite, but without success due to their extremely low U contents (3.6-4.6 ppm) and Pb contamination problems. Sm-Nd studies are in progress (Miller et al., 2005) but were not published yet. The Rb-Sr age of the muscovite from the pegmatoid is  $81.1 \pm 1.5$  Ma, with an initial Sr isotope ratio of  $0.71127 \pm 8$  (Heede, 1997).

**Acknowledgements:** The authors gratefully acknowledge discussions with many persons including Wolfgang Frisch, Robert Handler, Walter Kurz and the TRANSALP Working Group. Work has been supported by grants (nos. P8652, P9918, P14028, P22110, P22728) of the Austrian Science Fund (FWF).

### **References**

- ANDERLE, N., 1977. Geologische Karte der Republik Österreich 1 : 50 000, 200 Arnoldstein. Geologische Bundesanstalt, Wien.
- APPOLD, T. & PESCH, P., 1984. Die Tektonik der postvariskischen Transgressionsserie im Krappfeld (Kärnten/Österreich). Carinthia II, 174/94, 319–337.
- APPOLD, T., THIEDIG, F., VOLLMER, T. & WILKENS, E., 1986. Ein neues Alttertiärvorkommen am Dachberg südlich Guttaring/Kärnten (Österreich). Carinthia II, 176/96, 303–310.
- BARTEL, E.M., NEUBAUER, F., HEBERER, B. & GENSER, J., 2014. States of paleostress north and south of the Periadriatic fault: Comparison of the Drau Range and the Friuli Southalpine wedge. Tectonophysics, 637, 305–327.
- BARTOSCH, T., STÜWE, K. & ROBL, J., 2017. Topographic evolution of the Eastern Alps: The influence of strike-slip faulting activity. 9, 384–398.
- BAUER, F.K., BUCKENBERGER, U., SCHULZE, R., EXNER, C., KUPSCHE, F., LÖSCHKE, J., ROLSER, J., SUETTE, G., TESSENHOHN, F., VAN HUSEN, D. & WALTZ, W., 1981. Geologische Karte der Karawanken 1:25.000, Ostteil (2 sheets), Wien (Geologische Bundesanstalt).
- BECKER, B., 1993. The Structural Evolution of the Radstadt Thrust System, Eastern Alps, Austria - Kinematics, Thrust Geometries, Strain Analysis, Diss., Univ. Tübingen, 76 p., 1993.
- BEHRMANN, J.H., 1990. Zur Kinematik der Kontinentkollision in den Ostalpen, Geotekt.Forsch., 76, 1-180, 1990.

- BELINIĆ, T., STIPČEVIĆ, J., ŽIVČIĆ, M. & ALP-ARRAYWORKING GROUP, 2018. Lithospheric thickness under the Dinarides. *Earth Planet. Sci. Lett.*, 484, 229–240.
- BERTRAND, A., ROSENBERG, C. L. & GARCIA, S., 2015. Fault slip analysis and late exhumation of the Tauern Window, Eastern Alps. *Tectonophysics*, 649, 1–17.
- BERTRAND, A., ROSENBERG, C., RABAUTE, A., HERMAN, F. & FÜGENSCHUH, B., 2017. Exhumation mechanisms of the Tauern Window (Eastern Alps) inferred from apatite and zircon fission track thermochronology, *Tectonics*, 36, <https://doi.org/10.1002/2016TC004133>.
- BIANCHI, I. & BOKELMANN, G., 2014. Seismic signature of the Alpine indentation, evidence from the Eastern Alps. *J. Geodyn.*, 82, 69–77.
- BISTACCHI, A., MASSIRONI, M. & MENEGON, L., 2010. Three-dimensional characterization of a crustal-scale fault zone: The Pusteria and Sprechenstein fault system (Eastern Alps). *J. Struct. Geol.*, 32, 2022–2041.
- BLEIBINHAUS, F. & GROSCHUP, R., 2008. Structure of the Periadriatic Fault in the Eastern Alps from reflection seismic imaging, AGU, San Francisco.
- BLEIBINHAUS, F., LINCK, R., GROSCHUP, R. & GEBRANDE, H., 2009. Seismic structure of the Eastern Alps – TRANSALP revisited, EGU, Wien.
- BÖHM, F., 1992. Mikrofazies und Ablagerungsmilieu des Lias und Dogger der Nordöstlichen Kalkalpen. *Erlanger Geologische Abhandlungen*, 121, 55–217.
- BOLE, M., DOLENEC, T., ZUPANIČ, N. & ČINČ-JUHANT, B., 2001. The Karavanke Granitic Belt (Slovenia)—a bimodal Triassic alkaline plutonic complex. *Schweiz. Mineral. Petrograph. Mitt.*, 81, 23–38.
- BRÜCKL, E., BEHM, M., DECKER, K., GRAD, M., GUTERCH, A., KELLER, G. R. & THYBO, H., 2010. Crustal structure and active tectonics in the Eastern Alps. *Tectonics*, 29, TC2011, <https://doi.org/10.1029/2009TC002491>.
- CAO, S. & NEUBAUER, F., 2016. Deep crustal expressions of exhumed strike-slip fault systems: Shear zone initiation on rheological boundaries. *Earth Sciences Reviews*, 162, 155–176.
- CAPORALI, A., NEUBAUER, F., STANGL, G. ZULIANI, D., 2013. Modeling surface GPS velocities in the Southern and Eastern Alps by finite dislocations at crustal depths. *Tectonophysics*, 590, 136–150.
- CASTELLARIN, A., VAI, G.B. & CANTELLI, L., 2006. The Alpine evolution of the Southern Alps around the Giudicarie faults: A Late Cretaceous to early Eocene transfer zone: *Tectonophysics*, 414, 203–223.
- CHELONI, D., D'AGOSTINO, N. & SELVAGGI, G., 2014. Interseismic coupling, seismic potential, and earthquake recurrence on the southern front of the Eastern Alps (NE Italy). *J. Geophys. Res.: Solid Earth*, 119, 4448–4468.
- CHEMENDA, A.I., MATTAUER, M. & BOKUN, A.N., 1995. Continental subduction and a mechanism for exhumation of high pressure metamorphic rocks: new modelling and field data from Oman. *Earth Planet. Sci. Lett.*, 143, 173–182.
- CLAR, E., 1965. Zum Bewegungsbild des Gebirgsbaues der Ostalpen. *Zeitschr.ift der Deutschen Geologischen Gesellschaft*, 116, 267–291.
- CLIFF, R., HOLZER, H. & REX, D., 1975. The age of the Eisenkappel granite, Carinthia and the history of the Periadriatic lineament. *Verh. Geol. Bundesanst*, 1975, 347–350.
- CLIFF, R.A & COHEN, A., 1980. Uranium-lead isotope systematics in a regionally metamorphosed tonalite from the Eastern Alps. *Earth Planet. Sci. Lett.*, 50, 211–218.
- CLIFF, R.A., DROOP, G.T.R. & REX, D.C., 1985. Alpine metamorphism in the south-east Tauern Window, Austria 2: Rates of heating, cooling and uplift. *J. Metam. Geol.*, 3, 403–415.
- CLIFF, R.A., NORRIS, R.J., OXBURGH, E.R. & WRIGHT, R.C., 1971. Structural, Metamorphic and Geochronological Studies in the Reißeck and the Southern Ankogel Groups, the Eastern Alps. *Jahrb. Geol. Bundesanst.*, 114, 121–272.
- COHEN, K.M., FINNEY, S.C., GIBBARD, P.L. & FAN, J.-X., 2013. The ICS International Chronostratigraphic Chart. *Episodes*, 36, 199–204.

- DALLMEYER R.D., NEUBAUER F., HANDLER R., FRITZ H., MÜLLER W., PANA D. & PUTIS M., 1996. Tectonothermal evolution of the internal Alps and Carpathians: Evidence from  $^{40}\text{Ar}/^{39}\text{Ar}$  mineral and whole rock data. *Eclogae Geologie Helvetica*, 89, 203–227.
- DALLMEYER, R.D., HANDLER, R., NEUBAUER, F. & FRITZ, H., 1998. Sequence of thrusting within a thick-skinned tectonic wedge: Evidence from  $^{40}\text{Ar}/^{39}\text{Ar}$  ages from the Austroalpine nappe complex of the Eastern Alps. *J. Geology*, 106, 71–86.
- DIENER, R., 2002. Die siliziklastischen Sedimente der synorogenen Hochwipfel-Formation im Karbon der Westkarawanken (Österreich/Slowenien/Italien): Sedimentologie, Geochemie und Provenienz. PhD Dissertation, Univ. Stuttgart, p. 366.
- DINGELDEY, CH., DALLMEYER, R.D., KOLLER, F. & MASSONNE, H.-J., 1997. P-T-t history of the Lower Austroalpine Nappe Complex in the "Tarntaler Berge" NW of the Tauern Window: implications for the geotectonic evolution of the central Eastern Alps: Contributions to Mineralogy and Petrology, 129, 1–19.
- DORNER, R., HÖFLING, R. & LOBITZER, H., with contributions of FEITZINGER, G., SVOBODOVÁ, M. & ŠVABENICKÁ, L., 2009. Nördliche Kalkalpen in der Umgebung Salzburgs (Exkursion H am 17. April 2009). Jahresberichte und Mitteilungen des Oberrheinischen Geologischen Vereines, Neue Folge, 91, 317–366.
- DROBNE, K., EGGER, H., HOFMANN, C., MOHAMED, O., OTTNER, F., RÖGL, F., 2011. Stop A3/6 - Pemberger and Fuchsofen quarries to the west of Klein St. Paul. Berichte der Geologischen Bundesanstalt, 85, 111–117.
- ELIAS, J., 1998. The Thermal History of the Ötztal-Stubai Complex (Tyrol, Austria/Italy) in the Light of the Lateral Extrusion Model. *Tübinger Geowiss. Arb. Reihe A* 42, 1–169
- ELSNER, R., 1991. Geologie des Tauern-Südostrandes und geotektonische Konsequenzen, Jahrb. Geol. BUNDESANST., 134, 561–645.
- ETZEL, A., 2013. The Hochstuhl Fault and its relation to the Periadriatic Fault and the North Karawanken Thrust. Master thesis Faculty of Sciences, University of Salzburg, pp. V + 83.
- EXNER, C., 1985. Petrographie und Tektonik des Granitzuges von Nötsch (Kärnten). *Jahrb. Geol. Bundesanst.*, 127, 557–570.
- EXNER, C., 1971. Geologie der peripheren Hafnergruppe (Hohe Tauern). *Jb. Geol. Bundesanst.*, 114, 1–119.
- EXNER, C., 1972. Geologie der Karawankenplutone östlich Eisenkappel, Kärnten. *Mitteilungen der Geologischen Gesellschaft Wien* 64, 1–108.
- EXNER, C., 1976. Die geologische Position der Magmatite des periadriatischen Lineamentes. *Verhandlungen der Geologischen Bundesanstalt* 1976 (2), 3–64.
- EXNER, C., 1980a. Das Kristallin östlich der Katschbergzone, Mitt. Österr. Geol. Ges., 71/72, 167–189.
- EXNER, C., 1980b. Geologie der Hohen Tauern bei Gmünd in Kärnten. *Jahrb. Geol. Bundesanst.*, 123, 343–410.
- EXNER, C., 1982. Geologie der zentralen Hafnergruppe (Hohe Tauern). *Jahrb. Geol. Bundesanst.*, 125, 51–154.
- EXNER, C., 1983a. Zur Petrographie von Gneisgerölle im Karbon von Nötsch (Kärnten). *Jahrb. Geol. Bundesanst.*, 126, 215–217.
- EXNER, C., 1983b. Geologische Karte der Hafnergruppe 1 : 25.000, mit Erläuterungen, Mitt. Ges. Geol. Bergbaustud. Österr., 29, 41–74.
- EXNER, C., 1984. Der Südrand des Tauernfensters bei Spittal an der Drau, *Jb. Geol. Bundesanst.*, 127, 349–367.
- EXNER, C., 1989. Geologie des mittleren Lungaus, *Jahrb. Geol. Bundesanst.*, 132, 7–103.
- EXNER, C., 1990. Erläuterungen zur Geologischen Karte des mittleren Lungaus, Mitt. Ges. Geol. Bergbaustud. Österr., 36, 1–38.
- FANINGER, E. & ŠTRUCL, I., 1978. Plutonic emplacement in the eastern Karavanke Alps. *Gelogija*, 21, 81–87.
- FANTONI, R. & FRANCIOSI, R., 2010. Tectono-sedimentary setting of the Po Plain and Adriatic foreland. *Rend. Fis. Acc. Lincei*, 21 (Suppl 1), S197–S209.

- FAUPL, P. & TOLLMANN, A., 1978. Die Roßfeldschichten: Ein Beispiel für Sedimentation im Bereich einer tektonisch aktiven Tiefseerinne aus der kalkalpinen Unterkreide. *Geologische Rundschau*, 68, 93–120.
- FAUPL, P. & WAGREICH, M., 2000. Late Jurassic to Eocene Paleogeography and Geodynamic Evolution of the Eastern Alps. *Mitteilungen der Österreichischen Geologischen Gesellschaft* 92, 79–94.
- FAVARO, S., SCHUSTER, R., HANDY, M. R., SCHARF, A. & PESTAL, G., 2015. Transition from orogen-perpendicular to orogen-parallel exhumation and cooling during crustal indentation – key constraints from  $^{147}\text{Sm}/^{144}\text{Nd}$  and  $^{87}\text{Rb}/^{87}\text{Sr}$  geochronology (Tauern Window, Alps). *Tectonophysics*, 665, 1–16.
- FINGER, F., G. FRASL, B. HAUNSCHMID, H. LETTNER, A. VON QUADT, A. SCHERMAIER, A. O. SCHINDLMAYR, & STEYRER, H.-P., 1993. The Zentralgneise of the Tauern Window (Eastern Alps): Insight into an intra-Alpine Variscan batholith. In: RAUMER, J.F. VON & NEUBAUER, F., eds., *Pre-Mesozoic geology in the Alps*. pp. 375–391, Springer-Verlag, Berlin Heidelberg New York.
- FODOR, L., GERDES, A., DUNKL, I., KOROKNAI, B., PÉCSKAY, Z., TRAJANOVA, M., HORVÁTH, P., VRABEC, M., BALOGH, K., JELEN, B. & FRISCH, W. 2008. Miocene emplacement and rapid cooling of the Pohorje pluton at the Alpine-Pannonian-Dinaric junction: a Geochronological and structural study. *Swiss J. Geosci.*, 101 Supplement 1, S255–S271.
- FODOR, L., JELEN, B., MÁRTON, E., SKABERNE, D., CAR, J. & VRABEC, M., 1998. Miocene-Pliocene tectonic evolution of the Slovenian Periadriatic fault: Implications for Alpine-Carpathian extrusion models. *Tectonics* 17, 690–709.
- FRANK, W. & SCHLAGER, W., 2006. Jurassic strike slip versus subduction in the Eastern Alps. *International Journal of Earth Sciences* 95, 431–450.
- FRANK, W., 1987. Evolution of the Austroalpine elements in the Cretaceous. In: FLÜGEL, H.W. & FAUPL, P., eds., *Geodynamics of the Eastern Alps*. Deuticke, Wien, pp. 379–406.
- FRANK, W., KRALIK, M., SCHARBERT, S. & THÖNI, M., 1987a. Geochronological data from the Eastern Alps. In: Flügel, H. W. & P. Faupl, P., eds., *Geodynamics of the Eastern Alps*. pp. 272–281, Deuticke, Vienna, 1987.
- FRANK, W., HÖCK, V. & MILLER, C., 1987b. Metamorphic and tectonic history of the central Tauern Window. In: FLÜGEL, H.W. & FAUPL, P., eds., *Geodynamics of the Eastern Alps*. pp. 34–54, Deuticke, Vienna.
- FRANK, W., LELKES-FELVÁRI G. & DUNKL I., 1996. Thermal history of Austroalpine basement rocks of the borehole Fertörákos-1004, Western Hungary.: Advances in Austrian-Hungarian Joint Geological Research, Budapest, 1996, 177–195.
- FREY, M., DESMONS, J. & NEUBAUER, F., 1999. The new metamorphic maps of the Alps: Introduction: *Schweizerische Mineralogische und Petrographische Mitteilungen*, 79, 1–4.
- FRIMMEL, H., 1986. Isotopengeologische Hinweise für die paläogeographische Nachbarschaft von Gurktaler Decke (Oberostalpin) und dem Altkristallin östlich der Hohen Tauern (Österreich). *Schweizerische Mineralogische und Petrographische Mitteilungen*, 66, 193–208.
- FRIMMEL, H., 1988. Metagranitoide am Westrand der Gurktaler Decke (Oberostalpin) – Genese und paläotektonische Interpretation. *Jahrbuch der Geologischen Bundesanstalt*, 131, 575–592.
- FRISCH, W., 1979. Tectonic progradation and plate tectonic evolution of the Alps. *Tectonophysics*, 60, 121–139.
- FRISCH, W., DUNKL, I. & KUHLEMANN, J., 2000a. Post-collisional orogen-parallel large-scale extension in the Eastern Alps. *Tectonophysics*, 327, 239–265.
- FRISCH, W., G. VAVRA & M. WINKLER, 1993. Evolution of the Penninic basement of the Eastern Alps, in *Pre-Mesozoic geology in the Alps*, edited by J. F. von Raumer, and F. Neubauer, pp. 349–360, Springer-Verlag, Berlin Heidelberg New York.
- FRISCH, W., GOMMERINGER, K., KELM, U. & POPP, F., 1987. The Upper Bündner Schiefer of the Tauern Window—a key to understanding Eoalpine Orogenic processes in the Eastern Alps. In: FLÜGEL, H.W. & FAUPL, P., eds., *Geodynamics of the Eastern Alps*. pp. 55–69, Deuticke, Vienna.

- FRISCH, W., KUHLEMANN, J., DUNKL, I., & SZÉKELY, B., 2001. The Dachstein paleosurface and the Augenstein Formation in the Northern Calcareous Alps—a mosaic stone in the geomorphological evolution of the Eastern Alps. *Internal Journal of Earth Sciences*, 90, 500–518.
- FRISCH, W., SZÉKELY, B., KUHLEMANN, J. & DUNKL, I., 2000b. Geomorphological evolution of the Eastern Alps in response to Miocene tectonics. *Z. Geomorph. N. F.*, 44, (1), 103–138.
- FRITSCH, W., 1962. Geröllfunde vom Fuchsofen bei Klein St. Paul im Görtschitztal. *Carinthia II*, 72, 75–78.
- FRITZ, A., BOERSMA, M. & KRAINER, K., 1990. Steinkohlenzeitliche Pflanzenfossilien aus Kärnten. *Carinthia II*, Sonderheft, 49, 1–189.
- FROITZHEIM, N., SCHMID, S. M. & FREY, M., 1996. Mesozoic paleogeography and the timing of eclogite-facies metamorphism in the Alps: A working hypothesis. *Eclogae geol. Helv.*, 89, 81–110.
- FROITZHEIM, N., PLASIENKA, D. & SCHUSTER, R., 2008. Alpine Tectonics of the Alps and Western Carpathians. Mesozoic and Cenozoic. In: McCann, T., ed., *The Geology of Central Europe, Volume 2*. Geological Society, London, pp. 1141–1232.
- FÜGENSCHUH, B., MANCKTELOW, N. & SEWARD, D., 2000. Cretaceous to Neogene cooling and exhumation history of the Oetztal-Stubai basement complex, eastern Alps: A structural and fission track study. *Tectonics*, 19, 905–918.
- GAIIDES, F., ABART, R., DE CAPITANI, C., SCHUSTER, R., CONNOLLY, J.A.D. & REUSSER, E., 2006. Characterization of polymetamorphism in the Austroalpine basement east of the Tauern Window using garnet isopleth thermobarometry. *Journal of metamorphic Geology*, 24, 451–475.
- GAWLICK, H.-J., FRISCH, W., VECSEI, A., STEIGER, T. & BÖHM, F., 1999. The change from rifting to thrusting in the Northern Calcareous Alps as recorded in Jurassic sediments. *Geologische Rundschau*, 87, 644–657.
- GENSER, J. & LIU, X., 2010. On the age of the Eisenkappel granites. *Journal of Alpine Geology*, 52, 121–122 (PanGeo Austria 2010, Abstract volume).
- GENSER, J. & NEUBAUER, F., 1989. Low angle normal faults at the eastern margin of the Tauern window (Eastern Alps). *Mitt. Österr. Geol. Ges.*, 81(1988), 233–248.
- GENSER, J., 1992. Struktur- Gefüge- und Metamorphoseentwicklung einer kollisionalen Plattengrenze: Das Beispiel des Tauernstrandes (Kärnten/Österreich). Unpubl. Diss. Univ. Graz, 379 pp.
- GENSER, J., CLOETINGH, S. & NEUBAUER, F., 2007. Late orogenic rebound and oblique Alpine convergence: New constraints from subsidence analysis of the Austrian Molasse basin. *Global Planet. Change* 58, 214–223.
- GENSER, J., J.D. VAN WEES, S. CLOETINGH, S. & NEUBAUER, F., 1996. Eastern Alpine tectono-metamorphic evolution: constraints from two-dimensional P-T-t modelling. *Tectonics*, 13, 584–604.
- GIESE, U., 1988. Lower Paleozoic volcanic evolution at the northwestern border of the Gurktal nappe Upper Austroalpine, eastern Alps. *Schweizerische Mineralogische und Petrographische Mitteilungen*, 68, 381–396.
- GRENERCZY, G. & KENYERES, A., 2006. Crustal deformation between Adria and the European platform from space geodesy. In: PINTER, N. ET AL., EDs., *The Adria Microplate: GPS Geodesy, Tectonics and Hazards*, NATO Sci. Ser. IV, vol. 61, , pp. 321–334, Springer, Dordrecht, Netherlands, [https://doi.org/10.1007/1-4020-4235-3\\_22](https://doi.org/10.1007/1-4020-4235-3_22).
- HAAS, J., KOVACS, S., KRYSTYN, L. & LEIN, R., 1995. Significance of Late Permian Triassic facies zones in terrane reconstructions in the Alpine North Pannonian domain. *Tectonophysics* 242, 19–40.
- HANDY, M.R., BABIST, J., WAGNER, R., ROSENBERG, C. & KONRAD, M., 2005. Decoupling and its relation to strain partitioning in continental lithosphere: insight from the Periadriatic fault system (European Alps). *Geol. Soc. Lond. Spec. Publ.*, 243, 249–276.
- HANDY, M.R., USTASZEWSKI, K., KISSLING, E., 2015. Reconstructing the Alps–Carpathians–Dinarides as a key to understanding switches in subduction polarity, slab gaps and surface motion. *Int. J. Earth Sci.*, 104, 1–26.

- HANDY, R., SCHMID, S.M., BOUSQUET, R., KISSLING, E. & BERNOULLI, D., 2010. Reconciling plate-tectonic reconstructions of Alpine Tethys with the geological-geophysical record of spreading and subduction in the Alps. *Earth Sci. Rev.*, 102, 121–158.
- HÄUSLER, H., 1988. Unterostalpine Jurabreccien in Österreich. Versuch einer sedimentologischen und paläogeographischen Analyse nachtriadischer Breccienserien im Unterostalpinen Rahmen des Tauernfensters (Salzburg – Tirol). *Jahrb. Geol. Bundesanst.*, 131, 21–125.
- HAWKESWORTH, C.J., 1976. Rb/Sr Geochronology in the Eastern Alps. *Contrib. Mineral. Petrol.*, 54, 225–244.
- HAWKESWORTH, C.J., WATERS, D.J. & BICKLE, M.J., 1975. Plate tectonics in the Eastern Alps. *Earth Planet. Sci. Lett.*, 24, 405–413.
- HEBERER, B., REVERMAN, R. L., FELLIN, M. G., NEUBAUER, F., DUNKL, I., ZATTIN, M., SEWARD, D., GENSER, J. & BRACK, P. 2017. Postcollisional cooling history of the Eastern and Southern Alps and its linkage to Adria indentation. *Int. J. Earth Sci.*, 106, 1557–1580.
- HEEDE, H. U., 1997. Isotopengeologische Untersuchungen an Gesteinen des ostalpinen Saualpenkristallins, Kärnten-Österreich. - Münstersche Forschungen zur Geologie und Paläontologie 81, 168 pp.
- HEIDORN, R., NEUBAUER, F., GENSER, J. & HANDLER, R., 2003.  $^{40}\text{Ar}/^{39}\text{Ar}$  mica age constraints for the tectonic evolution of the Lower Austroalpine to Penninic nappe boundary, Austria: TRANSALP Conference, Extended abstract of oral and poster presentations, Trieste, 10 – 12 February 2003, *Mem. Sci. Geol. (Padova)*, 54, 217–220.
- HEJL, E., 1997. ‘Cold spots’ during the Cenozoic evolution of the Eastern Alps: thermochronological interpretation of apatite fission-track data: *Tectonophysics*, 272, 159–172.
- HERMANN, P. & WASCHER, W., 1972. Basiskonglomerate der Krappfeldgau bei Rottenstein/Kärnten. *Verhandlungen der Geologischen Bundesanstalt (Wien)*, 1972, 299–308.
- HETÉNYI, G., PLOMEROVÁ, J., BIANCHI, J., KAMPFOVÁ EXNEROVÁ, H., BOKELMANN, G., MARK R. HANDY, M., BABUŠKA, V., ALPARRAY-EASI WORKING GROUP, 2018. From mountain summits to roots: Crustal structure of the Eastern Alps and Bohemian Massif along longitude 13.3°E. *Tectonophysics* 744, 239–255.
- HILLER, O. K., 1973. Zur Morphogenese des Krappfeldbeckens in Kärnten. *Mitt. Österr. Geogr. Ges.* 115, 86–105.
- HÖCK, V., & MILLER, C., 1987. Mesozoic ophiolitic sequences and non-ophiolitic metabasites in the Hohe Tauern. In: FLÜGEL, H.W. & FAUPL, P., eds., *in Geodynamics of the Eastern Alps*. pp. 16–33, Deuticke, Vienna, 1987.
- HÖCK, V., KOLLER, F., 1989. Magmatic evolution of the Mesozoic ophiolites in Austria. *Chem. Geol.*, 77, 209–227.
- HOINKES, G., KOLLER, F., RANTITSCH, G., DACHS, E., HÖCK, V., NEUBAUER F. & SCHUSTER, R., 1999. Alpine metamorphism of the Eastern Alps: Schweizerische Mineralogische und Petrographische Mitteilungen, 79, 155–181.
- HOLDHAUS, K., 1921. Über die Auffindung von Trias im Königstuhlgebietes in Kärnten. *Anzeiger der Akademie für Wissenschaften Wien mathematisch-naturwissenschaftliche Klasse*, 58, 19–21.
- HOLUB, B. & MARSCHALLINGER, R., 1989. Die Zentralgneise im Hochalm-Ankogel-Massiv (östliches Tauernfenster). Teil I: Petrographische Gliederung und Intrusionsabfolge, *Mitt. Österr. Geol. Ges.*, 81, 5–31, 1989.
- HUBMANN, B., EBNER, F., FERRETTI, A., KIDO, E., KRAINER, K., NEUBAUER, F., SCHÖNLAUB, H.P. & SUTTNER, T. J., 2014. The Paleozoic Era(the) Abhandlungen der Geologischen Bundesanstalt, 66 (Sec. Ed.), 9–135.
- JANÁK, M., FROITZHEIM, N., K. YOSHIDA, K., SASINKOVÁ, V., NOSKO, M., KOBAYASHI, HIRAJIMA, T., VRABEC, M., 2015. Diamond in metasedimentary crustal rocks from Pohorje, Eastern Alps: a window to deep continental subduction. *Journal of Metamorphic Geology*, 33,
- JÁNAK, M., FROITZHEIM, N., LUPTÁK, B., VRBEC, M. & KROGH RAVNA, E.J., 2005. First evidence for ultrahigh-pressure metamorphism of eclogites in Pohorje, Slovenia: tracing deep continental subduction in the Eastern Alps. *Tectonics*, 23, TC5014, <https://doi.org/10.1029/2004TC001641>.
- KÁZMÉR, M., DUNKL, I., FRISCH, W., KUHLEMANN, J. & OZSVÁRT, P., 2003. The Palaeogene forearc basin of the Eastern Alps and Western Carpathians: subduction erosion and basin evolution. *J. Geol. Soc.*, 160, 413–428.

- KEIL, M. & NEUBAUER, F., 2015. Orogen-parallel extension and topographic gradients east of the Tauern window: a possible indication of intra-orogenic raft tectonics? *Austrian Journal of Earth Sciences*, 108, 1, 6–17.
- KOROKNAI, B., NEUBAUER, F., GENSER, J. & TOPA, D., 1999. Metamorphic and tectonic evolution of the Austroalpine units at the western margin of the Gurktal nappe complex, Eastern Alps. *Schweizerische Mineralogische und Petrographische Mitteilungen*, 79, 277–295.
- KOZUR, H. & MOSTLER, H. 1992. Erster paläontologischer Nachweis von Meliaticum und Süd-Rudabanyaicum in den Nördlichen Kalkalpen (Österreich) und ihre Beziehung zu den Abfolgen der Westkarpaten. *Geologisch-Paläontologische Mitteilungen der Universität Innsbruck*, 18, 87–129.
- KOZUR, H., 1991. The Evolution of the Meliata-Hallstatt ocean and its significance for the early evolution of the Eastern Alps and Western Carpathians. *Palaeogeography, Palaeoclimatology, Palaeoecology* 87, 109–135.
- KRAINER, K. & MOGESSIE, A., 1991. Composition and Significance of Resedimented Amphibolite Breccias and Conglomerates (Badstub Formation) in the Carboniferous of Nötsch (Eastern Alps, Carinthia, Austria). *Jahrbuch der Geologischen Bundesanstalt*, 134, 65–81.
- KRAINER, K., 1984. Sedimentologische Untersuchungen an permischen und untertriadischen Sedimenten des Stangalm-Mesozoikums (Kämten/Österreich). *Jahrbuch der Geologischen Bundesanstalt*, 127,
- KRAINER, K., 1987. Das Perm der Gurktaler Decke: eine sedimentologische Analyse Carinthia II, 177/97, 49–92.
- KRAINER, K., 1989. Molassesedimentation im Oberkarbon der Ostalpen am Beispiel der Stangnock Formation am NW-Rand der Gurktaler Decke (Österreich). *Zentralblatt für Geologie und Paläontologie Teil 1*, 1988, H. 7/8, 807–820.
- KRAINER, K., 1992. Fazies Sedimentationsprozesse und Paläogeographie im Karbon der Ost- und Südalpen. *Jahrbuch der Geologischen Bundesanstalt*, 135, 99–193.
- KRISCHE, O. & GAWLICK, H.-J., 2015. Age and significance of Lower Cretaceous mass flows: Ischler Breccia revisited (Rossfeld Formation, Northern Calcareous Alps, Austria). *Austrian Journal of Earth Sciences*, 108, 128–150.
- KRISCHE, O., GORIČAN, S. & GAWLICK, H.-J., 2014. Erosion of a Jurassic ophiolitic nappe-stack as indicated by exotic components in the Lower Cretaceous Rossfeld Formation of the Northern Calcareous Alps (Austria). *Geologica Carpathica*, 65, 3–24.
- KRISTAN-TOLLMANN, E. & TOLLMANN, A., 1964. Das mittelostalpine Standardprofil aus dem Stangalm-Mesozoikum (Kärnten). *Mitteilungen der Geologischen Gesellschaft Wien*, 56(1963), 539–589.
- KROHE, A., 1987. Kinematics of Cretaceous nappe tectonics in the Austroalpine basement of the Koralpe region (eastern Austria): *Tectonophysics*, 136, 171–196.
- KRUHL, J.H., 1993. The P-T-d development at the basement-cover boundary in the north-east Tauern Window (Eastern Alps): Alpine continental collision, *J. metamorphic Geol.*, 11, 31–47.
- KUHLEMANN, J., TAUBOLD, H., VENNEMANN, T., DUNKL, I. & FRISCH, W., 2008. Clay mineral and geochemical composition of Cenozoic paleosol in the Eastern Alps (Austria). *Austrian J. Earth Sci.*, 108, 60–69.
- KURZ W & FRITZ H., 2003. Tectonometamorphic Evolution of the Austroalpine nappe complex in the Central Eastern Alps—Consequences for the Eo-Alpine Evolution of the Eastern Alps. *Int. Geol. Rev.*, 45, 1100–1127.
- KURZ, W. & NEUBAUER, F., 1996. Deformation partitioning and shear localization during the updoming of the Sonnblick area in the Tauern Window (Eastern Alps, Austria), *J. Struct. Geol.*, 18, 1327–1343, 1996.
- KURZ, W., F. NEUBAUER, H. GENSER. H. & HORNER, H., 1994. Sequence of Tertiary brittle deformations in the eastern Tauern Window (Eastern Alps). *Mitt. Österr. Geol. Ges.*, 86 (1993), 153–164.
- KURZ, W., NEUBAUER, F. & GENSER, J., 1996. Kinematics of Penninic nappes (Glockner Nappe and basement-cover nappes) in the Tauern Window (Eastern Alps, Austria) during subduction and Penninic-Austroalpine collision, *Ecl. geol. Helv.*, 89, 573–605.
- KURZ, W., NEUBAUER, F., GENSER, J. & DACHS, E., 1998. Alpine geodynamic evolution of passive and active continental margin sequences in the Tauern Window (Eastern Alps, Austria, Italy): a review. *Geol. Rundsch.* 87, 225–242.

- KURZ, W., NEUBAUER, F., GENSER, J., UNZOG, W. & DACHS, E., 2001. Tectonic Evolution of Penninic Units in the Tauern Window during the Paleogene: Constraints from Structural and Metamorphic Geology. In: PILLER W.E. & RASSER M.W. (eds.), Paleogene of the Eastern Alps, Österr. Akademie der Wissenschaften, Schriftenreihe der Erdwissenschaftlichen Kommissionen, 14, 347–375.
- LAMMERER, B. & WEGER, M., 1998. Footwall uplift in an orogenic wedge: the Tauern Window in the Eastern Alps of Europe. *Tectonophysics*, 285, 213–230.
- LÄUFER, A.L., FRISCH, W., STEINITZ, G. & LOESCHKE, J., 1997. Exhumed fault-bounded Alpine blocks along the Periadriatic lineament: the Eder unit (Carnic Alps, Austria). *Geologische Rundschau*, 86, 612–626.
- LEGGEWIE, R. & THIEDIG, F., 1977. Oberkreidesedimente am Ostrand des Krappfeldes (Kärnten, Österreich). *Mitteilungen des Geologisch-Paläontologischen Institutes der Universität Hamburg* 47, 229–246.
- LEGRAIN, N., STÜWE, K. & WÖLFER, A., 2014. Incised relict landscapes in the eastern Alps: Geomorphology, 221, 124–138.
- LEIN, R., 1987. Evolution of the Northern Calcareous Alps during Triassic times. In: FLÜGEL, H.W. & FAUPL, P., eds., *Geodynamics of the Eastern Alps*. Deuticke, Vienna, pp. 85–102.
- LINZER, H.G., MOSER, F., NEMES, F., RATSBACHER, L. & SPERNER, B., 1997. Build-up and dismembering of the eastern Northern Calcareous Alps. *Tectonophysics*, 272, 97–124.
- LINZER, H.-G., RATSBACHER, L. & FRISCH, W., 1995. Transpressional collision structures in the upper crust: the fold-thrust belt of the Northern Calcareous Alps. *Tectonophysics*, 242, 41–61.
- LIPPITSCH, R., KISSLING, E. & ANSORGE, J., 2003. Upper mantle structure beneath the Alpine orogen from high-resolution teleseismic tomography. *J. Geophys. Res.*, 108, 2376. <https://doi.org/10.1029/2002JB002016>.
- LIU, Y., GENSER, J., HANDLER, R., FRIEDL, G. & NEUBAUER, F., 2001.  $^{40}\text{Ar}/^{39}\text{Ar}$  muscovite ages from the Penninic/Austroalpine plate boundary, Eastern Alps. *Tectonics*, 20, 528–547.
- LOESCHKE, J. & SCHNEPF, H., 1987. Zur Geologie des Diabaszuges östlich Eisenkappel (Kärnten/Österreich). *N. Jb. Geol.-Paläont. Abh.*, 174, 303–329.
- LOESCHKE, J., 1970. Zur Geologie und Pétrographie des Diabaszuges westlich Eisenkappel (Ebriachtal/Karawanken/Österreich). *Oberrhein. geol. Abh.*, 19, 73–100.
- LÜSCHEN, A., BORRINI, D., GEBRANDE, H., LAMMERER, B., MILLAHN, K., NEUBAUER, F., NICOLICH, R., TRANSALP WORKING GROUP, 2005. TRANSALP – deep crustal Vibroseis and explosive seismic profiling in the Eastern Alps. *Tectonophysics*, 414, 9–38.
- LUTH, S.W. & WILLINGSHOFER E., 2008. Mapping of the post-collisional cooling history of the Eastern Alps. *Swiss J. Geosci.*, 101:207–223.
- MADER, D., NEUBAUER, F. & HANDLER, R., 2007:  $^{40}\text{Ar}/^{39}\text{Ar}$  dating of detrital white mica of Late Palaeozoic sandstones in the Carnic Alps (Austria): implications to provenance and tectonic setting of sedimentary basins. *Geologica Carpathica*, 58 (2), 133–144.
- MANCKTELOW, N.S., STÖCKLI, D. F., GROLLIMUND, B., MÜLLER, W., FÜGENSCHUH, B. & VIOLA, G., 2001. The DAV and the Periadriatic fault system in the Eastern Alps south of the Tauern window. *Int. J. Earth Sci.*, 90, 593–622.
- MANDL, G. W., 2000. The Alpine sector of the Tethyan shelf – Examples pf Triassic to Jurassic sedimentation and deformation from the Northern Calcareous Alps: *Mitt. Österr. Geol. Ges.*, 92(1999), 61–77.
- ANDL, G. W. & ONDREJKOVA, A., 1991. Über eine triadische Tiefwasserfazies (Radiolarite, Tonschiefer) in den Nördlichen Kalkalpen – ein Vorbericht: *Jahrbuch der Geologischen Bundesanstalt (Wien)*, 134, 309–318.
- MARSCHALLINGER, R. & HOLUB, B., 1991. Die Zentralgneise im Hochalm-Ankogel-Massiv (östliches Tauernfenster) Teil II: Geochemische und zirkontypologische Charakteristik. *Mitt. Österr. Geol. Ges.*, 82, 19–48.
- MÁRTON, E., DROBNE, K., COSOVIC, & MORO, A., 2003. Paleomagnetic evidence for Tertiary counterclockwise rotation of Adria. *Tectonophysics*, 377, 143–166.

- MILLER, C., THÖNI, M., GOESSLER, W. & TESSADRI, R., 2011. Origin and age of the Eisenkappel gabbro to granite suite (Carinthia, SE Austrian Alps). *Lithos* 125, 434–448.
- MILLER, C., THÖNI, M., KONZETT, J., KURZ, W. & SCHUSTER, R., 2005. Eclogites from the Koralpe and Saualpe type-localities, Eastern Alps, Austria: Mitteilungen der Österr. Mineralogischen Gesellschaft, 150, 227–263.
- MISSONI, S. & GAWLICK, H.-J., 2011. Evidence for Jurassic subduction from the Northern Calcareous Alps (Berchtesgaden; Austroalpine, Germany). *International Journal of Earth Sciences (Geologische Rundschau)* 100, 1605–1631.
- MÜLLER, W., DALLMEYER, R.D., NEUBAUER, F. & THÖNI, M. 1999. Deformation-induced resetting of Rb/Sr and  $^{40}\text{Ar}/^{39}\text{Ar}$  mineral systems in a low-grade, polymetamorphic terrane (eastern Alps, Austria). *Journal of the Geological Society (London)*, 156, 261–278.
- MÜLLER, W., KELLEY, S. P. & VILLA, I. M., 2002. Dating fault-generated pseudotachylytes: comparison of Ar-40/Ar-39 stepwise-heating, laser-ablation and Rb-Sr microsampling analyses. *Contrib. Mineral. Petrol.* 144, 57–77.
- MÜLLER, W., PROSSER, G., MANCKTELOW, N., VILLA, I., KELLEY, S., VIOLA, G. & OBERLI, F., 2001. Geochronological constraints on the evolution of the Periadriatic Fault System (Alps). *Int. J. Earth Sci.*, 90, 623–653.
- MUTTONI, G., KENT, D.V. & CHANNELL, J.E.T., 1996. Evolution of Pangea: Paleomagnetic constraints from the southern Alps, Italy: *Earth and Planetary Science Letters*, 140, 97–112.
- NEMES, F., 1997. Kinematics of the Periadriatic Fault in the Eastern Alps - Evidence from structural analysis, fission track dating and basin modelling. Doctoral Thesis Faculty of Sciences, University of Salzburg, pp. 225.
- NEMES, F., NEUBAUER., F., CLOETINGH, S. & GENSER, J., 1997. The Klagenfurt Basin in the Eastern Alps: a decoupled intra-orogenic flexural basin? *Tectonophysics*, 282, 189–204.
- NEUBAUER, F., 1987. The Gurktal Thrust System within the Austroalpine region – some structural and geometrical aspects. In: FLÜGEL, H.W. & FAUPL, P., eds., *Geodynamics of the Eastern Alps*. Deuticke, Wien, pp. 226–236.
- NEUBAUER, F., 1988. Bau und Entwicklungsgeschichte des Rennfeld-Mugel- und des Gleinalmkristallins (Ostalpen). *Abh. Geol. Bundesanst.*, 42: 1–137.
- NEUBAUER, F., 2014. The structure of the Eastern Alps: from Eduard Suess to present-day knowledge. *Austrian Journal of Earth Sciences*, 107/1, 83–93.
- NEUBAUER, F., 2016. Formation of an intra-orogenic transtensional basin: the Neogene Wagrain basin in the Eastern Alps. *Swiss Journal of Geosciences*, 109, 37–56.
- NEUBAUER, F. & GENSER, J., 1990. Architektur und Kinematik der östlichen Zentralalpen – eine Übersicht. *Mitteilungen des Naturwissenschaftlichen Vereines für Steiermark*, 120, 203–219.
- NEUBAUER, F. & PISTOTNIK., J., 1984. Das Altpaläozoikum und Unterkarbon des Gurktaler Deckensystems (Ostalpen) und ihre paläogeographischen Beziehungen. *Geologische Rundschau*, 73, 149–174.
- NEUBAUER, F., DALLMEYER, R.D., DUNKL I. & SCHIRNIK, D., 1995. Late Cretaceous exhumation of the metamorphic Gleinalm dome, Eastern Alps: kinematics, cooling history and sedimentary response in a sinistral wrench corridor: *Tectonophysics*, 242, 79–89.
- NEUBAUER, F., FRISCH, W. & HANSEN, B.T., 2002. Early Palaeozoic tectonothermal events in basement complexes of the eastern Graywacke Zone (Eastern Alps. evidence from U-Pb zircon data. *International Journal of Earth Sciences*, 91, 775–786.
- NEUBAUER, F., GENSER, J. & HANDLER, R., 2000. The Eastern Alps: result of a two-stage collision process. *Mitteilungen der Österr. Geologischen Gesellschaft*, 92, 117–134.
- NEUBAUER, F., HANDLER, R., HERMANN, S. & PAULUS, G., 1994. Tectonostratigraphy and structure of the eastern Graywacke Zone, Eastern Alps. *Mitt. Österr. Geol. Ges. (ALCAPA issue)*, 87: 61–74.
- NEUBAUER, F., HOINKES, G., SASSI, F.P., HANDLER, R., HöCK, V., KOLLER, F. & FRANK, W., 1999. Pre-Alpine metamorphism of the Eastern Alps. *Schweizerische Mineralogische und Petrographische Mitteilungen*, 79. p. 41–62.

- NEUBAUER, F., BERNROIDER, M., LEITNER, C., SCHORN, A., ZIEGLER, T. & GENSER, J., 2017. Die Evaporite des Haselgebirges als metamorphe Gesteine: Bildung, Umwandlung, Gefüge, Alter und Konsequenzen für die Struktur der Nördlichen Kalkalpen. Arbeitstagung „Angewandte Geowissenschaften an der GBA“, Bad Ischl, Hallstatt, Gmunden, p. 29–37, Geologische Bundesanstalt, Wien.
- NEUBAUER, F., HEBERER, B., DUNKL, I., LIU, S., BERNROIDER, M., DONG, Y., 2018. The Oligocene Reifnitz tonalite (Austria) and its host rocks: implications for Cretaceous and Oligocene-Neogene tectonics of southeastern Eastern Alps. *Geologica Carpathica*, 69, 237–253.
- NEUMANN, H.-H., 1989. Die Oberkreide des Krappfeldes. Arbeitstagung Geologische Bundesanstalt, 1989, 70–79.
- OBERHÄNSLI, R., BOUSQUET, R., ENGI, M., GOFFÉ, B., GOSSO, G., HANDY, M., HÖCK, V., KOLLER, F., LARDEAUX, J. M., POLINO, R., ROSSI, P.L., SCHUSTER, R., SCHWARTZ, S., SPALLA, I., 2004. Metamorphic structure of the Alps 1: 100000000. Paris, Commission for the Geological Map of the World.
- ORTNER, H., REITER, F. & BRANDNER, R., 2006. Kinematics of the Inntal shear zone–sub-Tauern ramp fault system and the interpretation of the TRANSALP seismic section, Eastern Alps, Austria. *Tectonophysics*, 414, 241–258.
- PISTOTNIK, J., 1973/74. Zur Geologie des NW-Randes der Gurktaler Masse (Stangalm-Mesozoikum, Österreich). *Mitteilungen der Österreichischen Geologischen Gesellschaft*, 66/67, 127–142.
- PISTOTNIK, J., 1976. Ein Transgressionskontakt des Stangalm-Mesozoikums (Gurktaler Alpen, Kärnten/Österreich). *Carinthia II*, 166/86, 127–131.
- PISTOTNIK, J., 1996. Geologische Karte der Republik Österreich 1 : 50.000, Blatt 183 Radenthein. Geologische Bundesanstalt, Wien.
- PLAŠIENKA, D., 2018. Continuity and episodicity in the early Alpine tectonic evolution of the Western Carpathians: How large-scale processes are expressed by the orogenic architecture and rock record data. *Tectonics*, 37, 2029–2079. <https://doi.org/10.1029/20792017TC004779>.
- PLÖCHINGER, B., 1983. Salzburger Kalkalpen. Sammlung geol. Führer 73, 144 p., Borntraeger, Berlin., Stuttgart.
- POLINSKI, R.K. & EISBACHER, G.H., 1992. Deformation partitioning during polyphase oblique convergence in the Karawanken Mountains, southeastern Alps. *Journal of Structural Geology* 14, 1203–1213.
- POMELLA, H., FLÖSS, D., SPECKBACHER, R., TROPPER, P., FÜGENSCHUH, B., 2015. The western end of the Eoalpine High-Pressure Belt (Texel unit, South Tyrol / Italy). *Terra Nova*, 28, 60–69.
- POMELLA, H., KLÖTZLI, U., SCHOLGER, R., STIPP, M. & FÜGENSCHUH, B., 2011. The Northern Giudicarie and the Meran-Mauls fault (Alps, Northern Italy) in the light of new paleomagnetic and geochronological data from boudinaged Eo-/Oligocene tonalites. *International Journal of Earth Sciences*, 100, 1827–1850.
- POMELLA, H., STIPP, M. & FÜGENSCHUH, B., 2012. Thermochronological record of thrusting and strike-slip faulting along the Giudicarie fault system (Alps, Northern Italy). *Tectonophysics*, 579, 118–130.
- RANTITSCH, G., 1997. Thermal history of the Carnic Alps (Southern Alps, Austria) and its palaeogeographic implications: *Tectonophysics*, 272, 213–232.
- RANTITSCH, G. & RUSSEGG, B., 2000. Thrust-related very low grade metamorphism within the Gurktal nappe complex (Eastern Alps). *Jahrbuch der Geologischen Bundesanstalt*, 142, 219–225.
- RATHORE, J.S. & BECKE, M., 1980. Magnetic fabric analyses in the Gail Galley (Carinthia, Austria) for the determination of the sense of movements along this region of the Periadriatic Line. *Tectonophysics* 69, 349–368.
- RATSCHBACHER, L., 1984. Beitrag zur Neugliederung der Veitscher Decke (Grauwackenzone) in ihrem Westabschnitt (Obersteiermark Österreich). *Jahrbuch der Geologischen Bundesanstalt* 127, 423–453.
- RATSCHBACHER, L., 1986. Kinematics of Austro-Alpine cover nappes: changing translation path due to transpression: *Tectonophysics*, 125, 335–356

- RATSCHBACHER, L. & NEUBAUER, F., 1989. West-directed decollement of Austro-Alpine cover nappes in the eastern Alps: geometrical and rheological considerations. In: COWARD, M.P., DIETRICH, D. & PARK, R.G., Eds., Alpine Tectonics. Geological Society [London] Special Publication, 45, 243–262.
- RATSCHBACHER, L., FRISCH, W., NEUBAUER, F., SCHMID, S.M. & NEUGEBAUER, J., 1989. Extension in compressional orogenic belts: The eastern Alps. *Geology*, 17, 404–407.
- RATSCHBACHER, L., FRISCH, W., LINZER, H.G. & MERLE, O., 1991a. Lateral extrusion in the Eastern Alps, part 2: Structural analysis: *Tectonics*, 10, 257–271
- RATSCHBACHER, L., MERLE, O., DAVY, P. & COBBOLD, P., 1991b. Lateral extrusion in the Eastern Alps, part 1. boundary-conditions and experiments scaled for gravity. *Tectonics*, 10, 245–256, <https://doi.org/10.1029/90tc02622>.
- REINECKER, J. & LENHARDT, W.A., 1999. Present-day stress field and deformation in eastern Austria. *International Journal of Earth Sciences*, 88, 532–550.
- RING, U., RATSCHBACHER, L., FRISCH, W., BIEHLER, D. & KRALIK, M., 1989. Kinematics of the Alpine plate-margin – structural styles, strain and motion along the Penninic-Australpine boundary in the Swiss-Austrian Alps: *Journal of the Geological Society (London)*, 146, 835–849.
- ROBL, J. & STÜWE, K., 2005. Continental collision with finite indenter strength: 2. European Eastern Alps. *Tectonics* 24, TC4014. <https://dx.doi.org/10.1029/2004TC001741>.
- ROBL, J., HERGARTEN, S. & STÜWE, K., 2008a. Morphological analysis of the drainage system in the Eastern Alps. *Tectonophysics*, 460, 263–277
- ROBL, J., STÜWE, K., HERGARTEN, S., EVANS, L., 2008b. Extension during continental convergence in the Eastern Alps: The influence of orogen-scale strike-slip faults. *Geology* 36, 963–966.
- ROSENBERG, C. L., 2004. Shear zones and magma ascent: A model based on a review of the Tertiary magmatism in the Alps, *Tectonics*, 23, TC3002, <https://dx.doi.org/10.1029/2003TC001526>.
- ROSENBERG, C.L., BERGER, A., BELLAHSEN, N. & BOUSQUET, R., 2015. Relating orogen-width to shortening, erosion, and exhumation during Alpine collision. *Tectonics* 34, 1306–1328. <https://dx.doi.org/10.1002/2014TC003736>.
- ROSENBERG, C.L., BRUN, J.-P., CAGNARD, F. & GAPAIS, D., 2007. Oblique indentation in the Eastern Alps: insights from laboratory experiments. *Tectonics* 26 (TC2003). <https://doi.org/10.1029/2006TC001960>.
- ROSENBERG, C. L., SCHNEIDER, S., SCHARF, S., BERTRAND, A., HAMMERSCHMIDT, K., RABAUTE, A. & BRUN, J.-P., 2018. Relating collisional kinematics to exhumation processes in the Eastern Alps. *Earth-Sci. Rev.*, 176, 311–344.
- ROSSNER, R., 1976. Struktur und Position der Quarzphyllitdecke im Rahmen des Unterostalpins der Radstädter Tauern. *N. Jb. Geol. Paläont. Abh.*, 151, 281–303.
- ROSSNER, R., 1977. N-Vergenz oder S-Vergenz im Schuppenbau der Werfen St. Martiner Zone (Nordkalkalpen, Österreich)? *N. Jb. Geol. Paläont. Mh.*, 419–432.
- ROSSNER, R., 1979. Gebirgsbau und alpidische Tektonik am Nordostrand des Tauernfensterrahmens (Nördliche Radstädter Tauern, Österreich). *Jb. Geol. Bundesanst. Wien*, 122, 251–387.
- SACHSENHOFER, R. F., 1992. Coalification and thermal histories of Tertiary basins in relation to late Alpidic evolution of the Eastern Alps. *Geologische Rundschau*, 81, 291–308.
- SACHSENHOFER, R. F., 2001. Syn- and post-collisional heat flow in the Cenozoic Eastern Alps. *Int. J. Earth Sci.* 90, 579–592.
- SACHSENHOFER, R.F., LANKREIJER, A., CLOETINGH, S. & EBNER, F., 1997. Subsidence analysis and quantitative basin modelling in the Styrian Basin (Pannonian Basin System, Austria). *Tectonophysics*, 272, 175–196.
- SANDERS, D., PONS, J. M., CAUS, E., 2004. Shallow-water limestone clasts in a Campanian deep-water debrite (Krappfeld, Central Alps, Austria): implications for carbonate platform history. *Ann. Naturhist. Mus. Wien*, 106 A, 139–165

- SASSI, F.P., ZANFERRARI, A., ZIRPOLI, G., BORSI, S. & DEL MOO, A., 1974. The Austrides to the south of the Tauern Window and the periadriatic lineament between Mules and Mauthen. *Neues Jahrbuch für Geologie und Paläontologie - Monatshefte*, 421-434.
- SCHARBERT, S., 1975. Radiometrische Altersdaten von Intrusivgesteinen im Raum Eisenkappel (Karawanken, Kärnten). *Verh. Geol. Bundesanst.*, 1975, 301-304.
- SCHARF, A., HANDY, M. R., SCHMID, S. M., FAVARO, S., SUDO, M., SCHUSTER, R., & HAMMERSCHMIDT, K., 2016. Grain-size effects on the closure temperature of white mica in a crustal-scale extensional shear zone—Implications of in-situ  $^{40}\text{Ar}/^{39}\text{Ar}$  laser-ablation of white mica for dating shearing and cooling (Tauern Window, Eastern Alps), *Tectonophysics*, 674, 210–226.
- SCHARF, A., HANDY, M. R., ZIEMANN, M. A. & SCHMID, S. M., 2013. Peak-temperature patterns of polyphase metamorphism resulting from accretion, subduction and collision (eastern Tauern Window, European Alps)—A study with Raman microspectroscopy on carbonaceous material (RSCM). *J. Metamorph. Geol.*, 31, 863–880.
- SCHARF, A., HANDY, M.R., FAVARO, S., SCHMID, S.M. & BERTRAND, A., 2013. Modes of orogen-parallel stretching and extensional exhumation in response to microplate indentation and roll-back subduction (Tauern Window, Eastern Alps). *Int. J. Earth Sci.*, 102, 1627–1654.
- SCHILLIG, D., 1966. Geomorphologische Untersuchungen in der Saualpe (Kärnten). *Tübinger Geogr. Stud.*, 21, 1–81.
- SCHIMANA, R., 1986. Neue Ergebnisse zur Entwicklungsgeschichte des Kristallins um Radenthein (Kärnten, Österreich), *Mitt. Ges. Geol. Bergbaustud. Österr.*, 33, 221–232.
- SCHMID, S.M., AEBLI, H.R., HELLER, F. & ZINGG, A., 1989. The role of the Periadriatic Line in the tectonic evolution of the Alps. In: COWARD, M.P., DIETRICH, D. & PARK, R.G., eds., *Alpine Tectonics*. Geol. Soc. London Spec. Publ., 45, pp. 153–171.
- SCHMID, S.M., FÜGENSCHUH, B., KISSLING, E. & SCHUSTER, R., 2004. Tectonic map and overall architecture of the Alpine orogen. *Eclogae Geologicae Helvetiae*, 97, 93–117.
- SCHMID, S.M., SCHARF, A., HANDY, M.R. & ROSENBERG, C.L., 2013. The Tauern Window (Eastern Alps, Austria): a new tectonic map, with cross-sections and a tectonometamorphic synthesis. *Swiss J. Geosci.*, 106, 1–32.
- SCHMIDT, T., BLAU, J. & KAZMER, M., 1991. Large-scale strike-slip displacement of the Drauzug and the Transdanubian mountains in Early Alpine history - evidence from Permo-Mesozoic facies belts. *Tectonophysics*, 200, 213–232.
- SCHÖNLAUB, H. P., 1979. Das Paläozoikum in Österreich. *Abhandl. Geol. Bundesanst.*, 33, 1–124.
- SCHÖNLAUB, H.P., 1985. Das Karbon von Nötsch und sein Rahmen. *Jahrb. Geol. Bundesanst.*, 127, 673–692.
- SCHÖNLAUB, H.P., 1989. Geologische Karte der Republik Österreich 1 : 50 000, 199 Hermagor. *Geologische Bundesanstalt*, Wien.
- SCHÖNLAUB, H. P. & FORKE, H. C., 2007. Die post-variszische Schichtfolge der Karnischen Alpen – Erläuterungen zur Geologischen Karte des Jungpaläozoikums der Karnischen Alpen 1:12500. *Abhandlungen der Geologischen Bundesanstalt*, 61, 3–157.
- SCHORN, A., NEUBAUER, F., GENSER, J. & BERNROIDER, M., 2013. The Haselgebirge evaporitic mélange in central Northern Calcareous Alps (Austria): part of the Permian to Lower Triassic rift of the Meliata ocean? *Tectonophysics*, 583, 28–48.
- SCHRAUT, G., 1999. Paläofaunistische Untersuchungen aus dem Unterkarbon von Nötsch (Kärnten, Österreich), Teil 2: Cephalopoda (Nautiloidea, Ammonoidea), Crustacea (Phyllocarida) Echinoidea. *Jahrbuch der Geologischen Bundesanstalt*, 141, 503–517.
- SCHUSTER, R. & FRANK, W., 1999. Metamorphic evolution of the Austroalpine units east of the Tauern Window: Indications for Jurassic strike-slip tectonics. *Mitteilungen der Gesellschaft der Geologie- und Bergbaustudenten Österreichs*, 42(1999), 37–58.

- SCHUSTER, R. & STÜWE, K., 2008. Permian metamorphic event in the Alps. *Geology*, 36, 603–606.
- SCHUSTER, R., KOLLER, F., HOECK, V., HOINKES, G. & BOUSQUET, R., 2004. Explanatory notes to the map: Metamorphic structure of the Alps – Metamorphic evolution of the Eastern Alps. *Mitteilungen der Österreichischen Mineralogischen Gesellschaft* 149, 175–199.
- SCHUSTER, R., SCHARBERT, S., ABART, R. & FRANK W., 2001. Permo-Triassic extension and related HAT/LP metamorphism in the Austroalpine–Southalpine realm: *Mitt. Ges. Geol. Bergbaustrud. Österr.* v. 45, 111–141.
- SPÖTL, C., LONGSTAFFE, F.J., RAMSEYER, K., KUNK, R. & WIESHEU, R., 1998. Fluid-rock reactions in an evaporitic mélange, Permian Haselgebirge, Austrian Alps: *Sedimentology*, 45, 1019–1945.
- STAMPFLI, G. M. & MOSAR J., 1999. The making and becoming of Apulia. *Mem. Sci. Geol.*, 51, 141–154.
- STEFANI, C., 2002. Variation in terrigenous supplies in the Upper Pliocene to Recent deposits of the Venice area. *Sedimentary Geology*, 153, 43–55.
- THEINER, U., 1987. Das Kristallin der NW-Nockberge - Eine kristallingeologische Neuuntersuchung, Unveröff. Diss. formal-naturw. Fak. Univ. Wien, pp. 154.
- THIEDIG, F. 1970. Verbreitung, Ausbildung und stratigraphische Einstufung neogener Rotlehme und Grobschotter in Ostkärnten (Österreich). *Mitt. Geol.-Paläont. Inst. Univ. Hamburg*, 38, 97–116.
- THIEDIG, F., 1975. Submarine Brekzien als Folge von Felsstürzen in der Turbidit-Fazies der Oberkreide des Jrappfeldes in Kärnten (Österreich). *Mitt. Geol.-Paläont. Inst. Universität Hamburg* 44, 495–516.
- THIEDIG, F., VAN HUSEN, D. & PISTOTNIK, J., 1999. Geologische Karte der Republik Österreich 1 : 50.000, 186 Sankt Veit an der Glan. *Geologische Bundesanstalt*, Wien.
- THIEDIG, F., WEISSENBACH, N., 1975. Die Junge Bruchtektonik der Saualpe. *Clausthaler Geologische Abhandlungen*, Sonderband, 1, 155–174.
- THIEDIG, F., WIEDMANN, J., 1976. Ammoniten und das Alter der höheren Kreide (Gosau) des Krappfeldes in Kärnten (Österreich). *Mitt. Geol.-Paläont. Inst. Univ. Hamburg*, 45, 9–27.
- THÖNI, M., 1999. A review of geochronological data from the Eastern Alps. *Schweiz. Mineral. Petrogr. Mitt.*, 79, 209–230
- THÖNI, M., 2002. Sm-Nd isotope systematics in garnet from different lithologies (Eastern Alps) – age results, and an evaluation of potential problems for garnet Sm-Nd Chronometry. *Chemical Geology*, 194, 353–379.
- THÖNI, M. & JAGOUTZ, E., 1992. Some new aspects of dating eclogites in orogenic belts: Sm-Nd, Rb-Sr, and Pb-Pb isotope results from the Austroalpine Saulape and Koralpe type-locality (Carinthia/Styria, southeastern Austria): *Geochimica et Cosmochimica Acta*, 56, 347–368.
- TOLLMANN, A., 1975. Die Bedeutung des Stangalm-Mesozoikums in Kärnten für die Neugliederung des Oberostalpins in den Ostalpen. *Neues Jahrbuch für Geologie und Paläontologie Monatshefte*, 150, 19–43.
- TOLLMANN, A., 1977. Die Geologie von Österreich (Band I): Die Zentralalpen. Deuticke, Wien.
- TOLLMANN, A., 1987. The Alpidic Evolution of the Eastern Alps. In: FLÜGEL, H.W. & FAUPL, P., eds., *Geodynamics of the Eastern Alps*. Deuticke, Wien, pp. 361–378.
- TRANSALP Working Group: Gebrände H., Lüschen E., Bopp M., Bleibinhaus F., Lammerer B., Oncken, O., Stiller, M., Kummerow, J., Kind, R., Millahn K., Grassl H., Neubauer, F., Bertelli L., Borrini D., Fantoni R., Pessina C., Sella M., Castellarin A., Nicolich R., Mazzotti A. & Bernabini M., 2002. First deep seismic reflection images of the Eastern Alps reveal giant crustal wedges and transcrustal ramps: *Geophysical Research Letters*, 29/10, 92-1–92-4.
- USTASZEWSKI, K., SCHMID, S.M., FÜGENSCHUH, B., TISCHLER, M., KISSLING, E. & SPAKMAN, W., 2008. A map-view restoration of the Alpine–Carpathian–Dinaridic system for the early Miocene. *Swiss J. Geosci.*, 101, 273–294.
- VACHARD, D., KRAINER, K. & SCHÖNLAUB, H. P., 2018. Lower Serpukhovian (Steshevian) foraminifers and algae from exotic limestone clasts of Nötsch (Eastern Alps, Austria). *Geobios*, 51, 75–100.

- VAN AMEROM, H. W. J. & SCHÖNLAUB, H. P., 1992. Pflanzenfossilien aus dem Karbon von Nötsch und der Hochwipfel-Formation der Karnischen Alpen (Österreich). *Jahrb. Geol. Bundesanst.*, 135, 195–216.
- VAN GELDER, I., WILLINGSHOFER, E., SOKOUTIS, D., CLOETINGH, S.A.P.L., 2017. The interplay between subduction and lateral extrusion: a case study for the European Eastern Alps based on analogue models. *Earth Planet. Sci. Lett.*, 472, 82–94.
- VAN HINTE, J. E., 1963. Zur Stratigraphie und Mikropaläontologie der Oberkreide und des Eozäns des Krappfeldes (Kärnten). *Jb. geol. Bundesanstalt, Sdb.* 8, 1–147.
- VAN HUSEN, D., 1976. Zur quartären Entwicklung des Krappfeldes und des Berglandes um St. Veit an der Glan. *Mitt. Ges. Geol. Bergbaustud. Österreichs*, 23, 55–68.
- VAN HUSEN, D., 1989. Die Entwicklung des Krappfeldes und seiner weiteren Umgebung im Pliozän und Pleistozän. *Arbeitstagung Geologische Bundesanstalt* 1989, 107–119.
- VAVRA, G. & FRISCH, W., 1989. Pre-Variscan back-arc and island arc magmatism in the Tauern Window (Eastern Alps). *Tectonophysics*, 169, 271–280.
- VAVRA, G. & HANSEN, B.T., 1991. Cathodoluminescence studies and U/Pb dating of zircons in pre-Mesozoic gneisses of the Tauern Window: implications for the Penninic basement evolution. *Geol. Rundschau*, 80, 703–715, 1991.
- VAVRA, G., 1989. Die Entwicklung des penninischen Grundgebirges im östlichen und zentralen Tauernfenster der Ostalpen - Geochemie, Zirkontypologie, U/Pb-Radiometrie. *Tüb. Geowiss. Abh. Reihe A*, 6, 1–150.
- VISONÀ, D. & ZANFERRARI, A., 2000. Some constraints on geochemical features in the Triassic mantle of the easternmost Austroalpine–Southalpine domain: evidence from the Karawanken pluton (Carinthia, Austria). *International Journal of Earth Sciences*, 89, 40–51.
- VON BLANCKENBURG, F. & DAVIES, J. H., 1995. Slab breakoff: A model for syncollisional magmatism and tectonics in the Alps. *Tectonics*, 14, 120–131.
- BLANCKENBURG, F., KAGAMI, H., DEUTSCH, A., OBERLI, F., MEIER, M., WIEDENBECK, M., BARTH, S. & FISCHER, H., 1998. The origin of Alpine plutons along the Periadriatic Lineament. *Schweizerische Mineralogische und Petrographische Mitteilungen* 78, 55–66.
- VON GOSEN, W., 1989a. Gefügeentwicklungen, Metamorphosen und Bewegungen der ostalpinen Baueinheiten zwischen Nockgebiet und Karawanken (Österreich). *Geotektonische Forschungen*, 72, 1–247
- VON GOSEN, W., 1989b. Fabric developments and the evolution of the Periadriatic Lineament in southeast Austria. *Geological Magazine*, 126, 55–71.
- VON GOSEN, W., THIEDIG, F., 1980. Erster Nachweis alpidischer Schieferung in postvariszischer Transgressionsserie und Oberkreide des Krappfeldes und der Griffener-St. Pauler Berge (Kärnten/Österreich). *Verhandlungen der Geologischen Bundesanstalt Wien* 1979, 313–335.
- VON GOSEN, W., PISTOTNIK, J. & SCHRAMM, J. M., 1987. Schwache Metamorphose in Gesteinsserien des Nockgebietes und im Postvariszikum des Karawankenvorlandes (Ostalpen, Kärnten). *Jahrbuch der Geologischen Bundesanstalt*, 130, 31–36.
- VOZÁROVÁ, A., LAURINC, D., ŠARINOVÁ, K., LARIONOV, A., PRESNYAKOV, S., RODIONOV, N. & PADERIN, I., 2013. Pb ages of detrital zircons in relation to geodynamic evolution: Paleozoic of the Northern Gmericum (Western Carpathians. Slovakia). *Journal of Sedimentary Research*, 83, 915–927.
- VOZÁROVA, A., VOZÁR, J. & MAYR, M., 1999. High-pressure metamorphism of basalts in the evaporitic sequence of the Haselgebirge: An evidence from Bad Ischl (Austria): *Abhandl. Geol. Bundesanst. (Wien)*, 56, 325–330.
- WAGNER, T., FRITZ, H., STÜWE, K., NESTROY, O., RODNIGHT, H., HELLSTROM, J. & BENISCHKE, R., 2011. Correlations of cave levels, stream terraces and planation surfaces along the River Mur—Timing of landscape evolution along the eastern margin of the Alps. *Geomorphology*, 134, 62–78.
- Wagreich, M. & Decker, K., 2001. Sedimentary tectonics and subsidence modelling of the type Upper Cretaceous Gosau basin (Northern Calcareous Alps, Austria). *Int. J. Earth Sciences*, 90, 714–726.

- WAGREICH, M., 1995. Subduction tectonic erosion and Late Cretaceous subsidence along the northern Austroalpine margin (Eastern Alps, Austria). *Tectonophysics*, 242, 63–78.
- WALACH, G., 1989. Geophysikalische Prospektionsprojekte auf ÖK-Blatt 186 St. Veit/Glan. Arbeitstagung Geologische Bundesanstalt, 1989, 122–125.
- WEISSENBACH, N. & PISTOTNIK, J., 2000. Geologische Karte der Republik Österreich 1 : 50000, 186 Sankt Leonhard im Lavanttal. Geologische Bundesanstalt, Wien.
- WIESINGER, M., NEUBAUER, F. & HANDLER, R., 2006. Exhumation of the Saualpe eclogite unit, Eastern Alps: constraints from  $^{40}\text{Ar}/^{39}\text{Ar}$  ages: Mineralogy and Petrology, 88, 149–180.
- WILKENS, E., 1989a. Paläogene Sedimente des Krappfeldes und seiner Umgebung. Arbeitstagung Geologische Bundesanstalt 1989, 85–99.
- WILKENS, E., 1989b. Entstehung von Großforaminiferen-Akkumulationen, Biofabric-Entwicklung und Bioklastaggregationen im Alttertiär des Sonnberges. Arbeitstagung Geol. Bundesanst., 1989, 100–106.
- WILLINGSHOFER, E. & CLOETINGH, S., 2003. Present-day lithospheric strength of the Eastern Alps and its relationship to neotectonics. *Tectonics* 22, 1075, <https://doi.org/10.1029/2002tc001463>.
- WILLINGSHOFER, E., NEUBAUER, F. & CLOETINGH, S. 1999a. Significance of Gosau basins for the upper Cretaceous geodynamic history of the Alpine—Carpathian belt: Physics and Chemistry of the Earth Part A: Solid Earth and Geodesy, 24, 687–695.
- WILLINGSHOFER, E., WEES, J.D. VAN, CLOETINGH, S. A. P. L. & NEUBAUER, F. 1999b. Thermomechanical evolution of an accretionary wedge: the Austroalpine of the Eastern Alps – indications and implications from 2D-numerical modelling. *Tectonics*, 18, 809–826.
- WÖLFLER, A., KURZ, W., FRITZ, H. & STÜWE, K., 2011. Lateral extrusion in the Eastern Alps revisited: Refining the model by thermochronological, sedimentary, and seismic data. *Tectonics*, 30, TC4006, <https://doi.org/10.1029/2010TC002782>.
- WORTEL, M.J.R. & SPAKMAN, W., 2000. Subduction and slab detachment in the Mediterranean–Carpathian region. *Science*, 290, 1910–1917.
- ZANFERRARI, A., 1976. On the occurrence of a Permo-Scythian syncline outcropping in the middle Lesachtal along the Gailtal line (Carinthia, Austria). *Neues Jahrb. Geologie und Paläontologie - Monatshefte* 2, 109–117
- ZETTER, R., DIMTER, A., 1992. Palynostratigraphische Untersuchungen oberkretazischer Sedimente des Krappfeldes (Kärnten). *Mitt. Gesellschaft der Geologie- und Bergbaustudenten in Österreich*, 38, 175–183.
- ZETTER, R., HOFMANN, C.-C., 2001. New aspects of the palynoflora of the lowermost Eocene (Krappfeld Area, Carinthia). In: Piller, W.E., Rasser, M.W. (eds.), *Paleogene of the Eastern Alps*, Österr. Akad. Wiss. Schriftenr. Erdwiss. Komm. 14, 473–507.
- ZWINGMANN, H. & MANCKTELOW, N., 2004. Timing of Alpine fault gouges. *Earth. Planet. Sci. Lett.* 223, 415–425.